Bipyridine - Porphyrin Conjugates

A thesis presented in partial fulfilment of the requirements for the degree
of Masterate of Science in Chemistry
at Massey University

Jacinda Louise Allwood
1998

Abstract

The research carried out for this thesis comprises an investigation into the synthesis of bipyridyl-bridged porphyrin compounds and their metal complexes.

Chapter One introduces the bipyridine ligand and summarises research carried out on the functionalisation of 2,2'-bipyridine (bpy). A proposal for a novel study involving the connection of porphyrin functionalities to bpy *via* vinylic linking groups is discussed, and the Wittig methodology proposed to achieve this is described.

Chapter Two outlines the synthesis of the 4,4'-diformyl-2,2'-bipyridine ligand necessary for the Wittig reaction to form the primary target compound, a bipyridyl-bridged bisporphyrinyl ligand. Synthesis of the bipyridine dialdehyde ligand had previously been reported *via* a four step procedure from 4,4'-dimethyl-2,2'-bipyridine in reasonable yield, a result which was unable to be reproduced. The methodology involved an oxidation of the dimethyl bipyridine to the corresponding dicarboxylic acid, esterification to the dimethylester, reduction to form the dialcohol, followed by an oxidation to the desired dialdehyde ligand. All attempts at this procedure, using various reagents for the final oxidation step, were either unsuccessful or resulted in very low yields of product. Thus an alternative single step SeO_2 oxidation of 4,4'-dimethyl-2,2'-bipyridine to form the target dialdehyde was explored. Optimisation of this procedure gave an efficient one step synthesis of 4,4'-diformyl-2,2'-bipyridine, **4**.

Chapter Three discusses the synthesis of the porphyrin phosphonium salt, the second precursor required for this work. Tetra-*meso*-substituted porphyrin moieties were used so that the phosphonium salt appendage would be connected through one of the pyrrolic carbon atoms. A *meso*-tetraphenylporphyrin (TPP) phosphonium salt **5**, had been synthesised in these laboratories, thus the synthetic methodology previously developed was repeated to make this Wittig precursor. The synthesis of a second, more soluble *meso*-tetraxylylporphyrin (TXP) phosphonium salt, **13**, was also developed (an eight step synthesis from mesitylene and pyrrole) and optimised so as to improve the solubility of the resulting bpy compounds.

Application of the Wittig reaction using dialdehyde **4**, and the TPP phosphonium salt **13**, is discussed in Chapter Four. Both the monomeric 4-(*trans*-2"-vinyl-TPPyl)-4'-formyl-2,2'-bipyridine, **14**, and the dimeric 4,4'-(*trans*-2"-vinyl-TPPyl)-2,2'-bipyridine, **15**, bipyridine-porphyrin conjugates were successfully synthesised. The bipyridine ligand is connected to

the porphyrin through a vinylic linking group to one of the pyrrolic positions (2-position) of the porphyrin ring. Bisporphyrinyl ligand **15**, as expected, proved to be insoluble in organic solvents. Before continuing with the more soluble TXP phosphonium salt **13**, some test metallation reactions were performed using the soluble monomeric porphyrinyl bipyridine ligand **14**. Zinc was inserted into the porphyrin ring to form 4-[(*trans*-2"-vinyl-TPPato)zinc(II)]-4'-formyl-2,2'-bipyridine, **16**. Coordination of rhenium to the bipyridyl moiety of the monomeric porphyrin ligand, formed the complex 1,1'-$Re(CO)_3Cl$[4-(*trans*-2"-vinyl-TPPyl)-4'-formyl-2,2'-bipyridine], **17**. A subsequent Wittig reaction was carried out to form the complex 1,1'-$Re(CO)_3Cl$[4,4'-(*trans*-2"-vinyl-TPPyl)-2,2'-bipyridine], **18**.

The remainder of Chapter Four reports the methodology developed for an efficient synthesis of the target bipyridyl-bridged dimeric porphyrin ligand 4,4'-(*trans*-2"-vinyl-TXPyl)-2,2'-bipyridine, **20**, using the tetraxylylporphyrin phosphonium salt, TXP-CH_2PPh_3Cl, **13**. Ligand **20** was first synthesised in two steps. Connection of one porphyrin ring to 4,4'-diformyl-2,2'-bipyridine **4**, formed the monomeric porphyrin ligand, 4-(*trans*-2"-vinyl-TXPyl)-4'-formyl-2,2'-bipyridine, **19**. A second Wittig reaction on this ligand resulted in the target bisporphyrinyl compound. A more efficient one step Wittig reaction was then investigated, resulting in a high yielding single step preparation of bisporphyrinyl bipyridine **20**.

Coordination of the metal ions Mo, Re, and Ru, to the bipyridyl moiety of the target bipyridyl-bridged tetraxylylporphyrin dimer **20**, are described in Chapter Five. A monoporphyrinyl molybdenum-bound bipyridine complex, 1,1'-$Mo(CO)_4$[4-(*trans*-2"-vinyl-TXPyl)-4'-formyl-2,2'-bipyridine], **22**, was synthesised *via* a Wittig reaction from the bipyridyl molybdenum complex 1,1'-$Mo(CO)_4$[4,4'-diformyl-2,2'-bipyridine], **21**. The rhenium-bound bisporphyrinyl complex, 1,1'-$Re(CO)_3Cl$[4,4'-(*trans*-2"-vinyl-TXPyl)-2,2'-bipyridine], **23** was synthesised in a single step metallation reaction of the bisporphyrinyl bipyridine **20** with rhenium pentacarbonyl chloride. A bisporphyrinyl ruthenium(II) bipyridine complex 1,1'-$Ru(CO)_2Cl_2$[4,4'-(*trans*-2"-vinyl-TXPyl)-2,2'-bipyridine], **25**, was synthesised in a one step Wittig reaction from the Ru(II)bpy complex 1,1'-$Ru(CO)_2Cl_2$[4,4'-diformyl-2,2'-bipyridine], **24**. The synthesis and characterisation of a tetraporphyrinyl ruthenium(II)bisbipyridine complex is also reported. 1,1'-$RuCl_2$[bis-4,4'-(*trans*-2"-vinyl-TXPyl)-2,2'-bipyridine], **27**, was synthesised *via* a single step metallation reaction between bisporphyrinyl bipyridine **20** and a $RuCl_2(DMSO)_4$ complex.

Chapter Six contains a brief summary of the results obtained throughout this study and future work to be done in this area.

Acknowledgements

I would like to thank the following people for their respective roles throughout the duration of the research for, and completion of, this thesis:

My two supervisors, Dr. Tony Burrell and Dr. David Officer, for their advice and expertise when it comes to porphyrins, bipyridines, and metallating them. As well as their continued enthusiasm throughout the past few years and the generation of funding to keep us all going.

The NMR unit and the mass spectrometry unit for their respective analyses.

My fellow chemistry postgrad's, from the old days of Bob, Wayne, and the Sherburn clan, to the more recent recruits of Kirsty, Warwick, Giovanna, Ben, and Sonya, as well as Rekha and Dr. Dave Harding down the end, for making chemistry-land not a bad place to work. I would especially like to thank Bob and Wayne, for without them I would have dropped out years ago.

Most importantly, I would like to thank Mum and Dad for their constant and unconditional support both financially and emotionally. Who somehow possessed and infinite faith in my ability to complete this thesis, even when I doubted it myself. They are without doubt the coolest parents ever.

And of course Aaron, who has been of constant support throughout the past three years, helped me through those times of panic and put up with my bad moods with little complaint. I cannot thank him enough for his unselfish support and encouragement when he too was enduring the fate of a looming thesis.

Table of Contents

List of Figures

List of Tables

Abbreviations

amu	Atomic mass units
Bpy	2,2'-Bipyridine
CT	Charge transfer
DBU	1,8-Diazabicyclo[5.4.0]undec-7-ene
FAB	Fast Atom Bombardment
h	Hours
^{1}H NMR	Proton Nuclear Magnetic Resonance Spectroscopy
HRMS	High Resolution Mass Spectrometry
LDA	Lithium diisopropylamide
LMCT	Ligand-to-metal charge transfer
mins	Minutes
MLCT	Metal-to-ligand charge transfer
MnP	Manganese peroxidase
NLO	Non-linear optical
RT	Room temperature
tlc	Thin Layer Chromatography
TPP	5,10,15,20-Tetraphenylporphyrin (*meso*-tetraphenylporphyrin)
TXP	5,10,15,20-Tetra(3,5-dimethylphenyl)porphyrin (*meso*-tetraxylylporphyrin)
UV/Vis	Ultraviolet/Visible Spectroscopy
Xy	3,5-Dimethylphenyl (xylyl)

Chapter One

Introduction

The unsustainability of our current petroleum based fuel resources has become increasingly apparent over the past few decades. Consequently, there is a growing interest in the chemical synthesis and study of complexes capable of performing useful light-induced functions for energy generation.[1] One of the most successful approaches to date, exploits the unique photochemical, photophysical and electrochemical properties of transition metal-bound polypyridine complexes.[2]

1.1 Polypyridines

Polypyridine ligands such as 2,2'-bipyridine (bpy), 1,10-phenanthroline (phen), and 2,3-bis(2-pyridyl)pyrazine (2,3-dpp), (Figure 1.1-1), are nitrogen-containing aromatic compounds. These molecules are strong, chelating bidentate ligands thus form a wide variety of metal complexes. The metal ion is bound through interaction with the lone pairs of electrons of the nitrogen atoms.

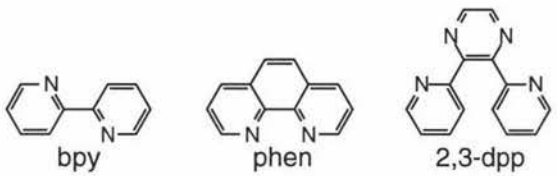

Figure 1.1-1
Polypyridine ligands bpy, phen, and 2,3-dpp.

Throughout the last twenty years, metal polypyridine complexes, particularly those of ruthenium(II), have played a key role in the development of transition metal photochemistry, electrochemistry, and energy and electron transfer studies.[1,3] In particular, the thermal and photochemical stability of $Ru(bpy)_3^{2+}$ and its derivatives, have made them the most extensively studied and widely used metal polypyridyl systems. With their unique combination of excited state reactivity, chemical stability, and redox properties, bipyridine ligands have been key components in many areas of research, from self-assembling double helicates,[4-8] to DNA intercalating agents,[9,10] cation recognition,[11] and anion sensors and receptors[12,13]. Transition metal-bound bipyridine complexes have also become fundamental components in the study of solar energy utilisation.[2,14-17]

1.1.1 Metallated bipyridine complexes

Of the regio-isomers of bipyridine, bpy (Figure 1.1-1) has the most suitable nitrogen atom arrangement for transition metal complex formation. For complexation, the ligand must assume a *cis* conformation with respect to its nitrogen atoms. In this form the lone pairs of electrons are available to interact with the bonding orbitals of the metal (M) ion (Figure 1.1-2).

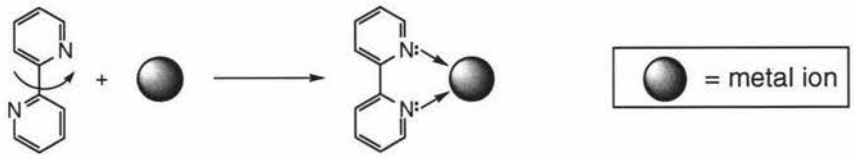

Figure 1.1-2
Conformation of free bpy, and metal-bpy complex.

Often upon coordination, highly coloured M-bpy complexes are formed. In these cases the colour is due to the complex possessing a strong charge transfer (CT) transition in the visible region of the spectrum, a property of the complex as a whole, not of the individual components. In such metal complexes, bipyridines have the capacity to act as either an electron donor (ligand to metal charge transfer, LMCT), or an electron acceptor (metal to ligand charge transfer, MLCT).

Photochemically, many M-bpy systems form a triplet excited state with a relatively long lifetime. As a result, the absorbed energy can be transferred to a suitable acceptor before it is dissipated as heat.[2] This property is crucial in terms of their potential as dyes in solar energy utilisation.

1.1.2 Metal bipyridyl complexes: models for solar cells

The study of photon absorption and energy transfer from photoactivated antenna molecules to energy-accepting units is of intense international interest.[18,19] In the past three years, a significant number of metal complexes with useful photochemical properties have been synthesised and their light harvesting properties studied.

Yamamoto *et al.*[17] synthesised a polymeric photoactive species that consisted of a chain of bpy units connected through their 5 and 5' positions, with intermittent $Ru^{II}(bpy)_3$ units (Figure 1.1-3 below). UV/Vis spectroscopic studies revealed that Yamamoto's polymer contains three times as many bipyridine units (PBpy) as $Ru(bpy)_3^{2+}$-like units. Yet through relative fluorescence intensities it was discovered that following irradiation, emission of light occurs mainly from the $Ru(bpy)_3^{2+}$-like units.

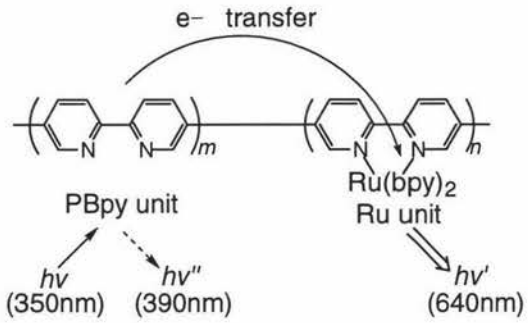

Figure 1.1-3
PBpy-Ru(bpy)$_2$ complex used by Yamamoto *et al.* for fluorescence studies.

This emission from the Ru unit (640nm) arises despite irradiation with light corresponding to the absorption wavelength of the PBpy unit (350nm). This strongly suggests that absorption of light is occurring by way of the photoactive antenna-like PBpy unit. Following absorption, most of the photoactivated energy is transferred to the Ru units from which the light emission occurs. These interesting photoexcited state properties of the PBpy-Ru(bpy)$_3$ polymer confirm the potential of such complexes as photoactive models for the study of synthetic light harvesting devices.

A group of Swedish chemists[16] have based their approach to a synthetic light harvesting system on the initial steps of the process by which chlorophyll P_{680} harvests light energy. On illumination, chlorophyll P_{680}, found in a photoactive enzyme of green plants, transfers an electron to a series of receptors. The oxidised P_{680}^+ is then reduced back to P_{680} by electron transfer from a cluster of manganese ions. Sun *et al.*[16] have developed a synthetic model successfully able to mimic this process. The model (Figure 1.1-4) consists of a core ruthenium(II)trisbipyridyl complex covalently attached to a manganese electron donor unit, and an external electron acceptor.

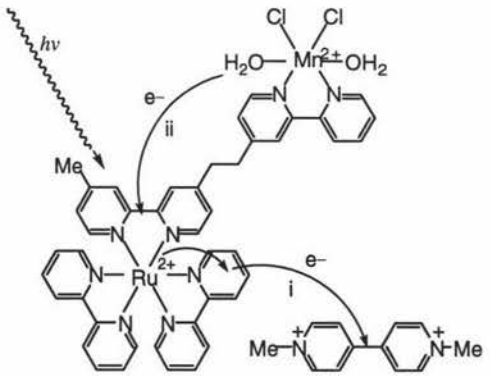

Figure 1.1-4
Model for the electron transfer process in chlorophyll P_{680} showing the proposed pathway of electron transfer following irradiation.

Upon irradiation (*hv*), the ruthenium(II)trisbipyridyl moiety transfers an electron to the external acceptor, methyl viologen (i). The Ru unit then recovers the electron by internal electron transfer from the coordinated manganese ion (ii), thus reducing back the oxidised photoactive unit in order to be able to repeat the process.

These cases indicate that ruthenium-bound bipyridyl complexes possess the ability to absorb photons of light and on doing so, eject an electron, in a similar manner to naturally occurring light harvesting systems. In view of this, the next task for the chemist was to develop the concept of utilising this photoactivated energy, by incorporating such complexes into molecular scale devices, devices that could channel the photoactive energy in such a way that it could be used immediately or stored.

1.1.3 Incorporation into solar cells

Due to the interest in the application of these complexes in molecular photovoltaic devices, adsorption of ruthenium(II)bipyridyl photoactive moieties onto conducting films is a growing area of research. Recent developments have shown a marked increase in the sunlight-to-electricity conversion efficiencies of solar cells based on such materials.[20] Some of the most efficient cells of this kind, have been based on the covalent attachment of a ruthenium(II)polypyridyl complex to nanocrystalline TiO_2. In the past, the connection has generally been through a carboxylic acid functionality of the complex reacting with surface hydroxyl groups of the film.[20-23]

Michael Grätzel and his research team in Lausanne, Switzerland, are studying the conversion of light to electricity using nanocrystalline TiO_2.[15] Their approach involved the synthesis of the ruthenium polypyridyl complex $[Ru(4,4'\text{-dimethyl-}2,2'\text{-bpy})(4'\text{-}PO_3H\text{-terpy})(NCS)]^+$, shown in Figure 1.1-5.

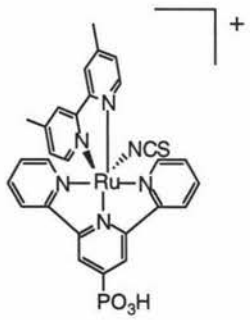

Figure 1.1-5
Ruthenium polypyridyl photoactive complex, which adsorbs onto nanocrystalline TiO_2 through its phosphonate group.

A monolayer of this photoactive complex is strongly adsorbed, through its phosphonate appendage onto a TiO_2 surface backed by a layer of conducting glass. This phosphonate

link enables electronic coupling between the complex and the oxide, allowing efficient light-induced charge separation. Grätzel *et al.* discovered that upon irradiation, the adsorbed complex performs as a charge transfer sensitizer. Following metal-to-ligand charge transfer photo-excitation, the complex injects electrons into the conduction band of the TiO_2 film. It produces a maximum incident photon-to-current conversion efficiency (IPCE), at a wavelength of 510nm, which exceeds 70% (Figure 1.1-6).

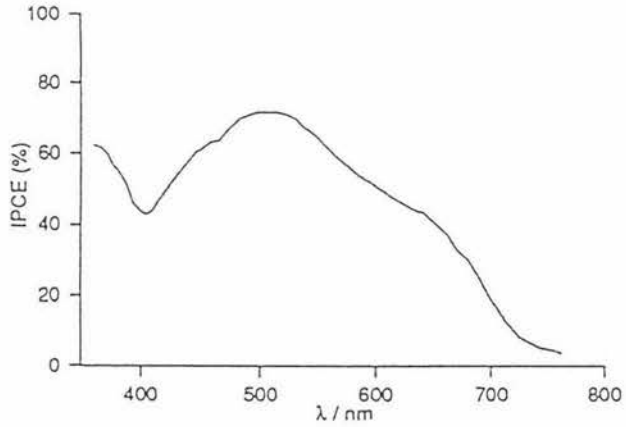

Figure 1.1-6
Photocurrent action spectrum obtained with a nanocrystalline TiO_2 film supported onto a conducting glass sheet, and derivatised with a monomolecular layer of Grätzel's ruthenium(II)bipyridyl complex. The IPCE is plotted as a function of wavelength in the visible region of the spectrum.

Considering photon loss through both absorption and scattering by the conducting glass, this conversion yield of photons to electric current at 510 nm is practically quantitative. However, the radiation reaching the earth's surface consists of light of varying wavelengths, not only that of 510nm. Thus, although this work by Grätzel is a very significant development in the production of non-silicon solar cells, a photovoltaics expert claims that it is still not as efficient as the silicon-based analogues which cover a wider spectrum.[24] Yet Grätzel believes that due to the relative low cost of production of his cell, it could have important implications as a potential power source for less wealthy, sunny climate countries.

It is becoming more evident that transition metal-bound bipyridine complexes have huge potential in the area of solar energy utilisation. However, from Grätzel's findings, their capacity as the light harvesting component for solar cells, may be limited due to their narrow range of efficient molar absorptivity. To more efficiently utilise solar energy, the light harvesting component should be capable of absorbing photons of wavelengths across the solar spectrum, through both the visible and high energy infrared regions of the electromagnetic spectrum. One way biological systems overcome this problem is by using a wide variety of pigments in each light harvesting system. For example, the chloroplasts of green plants contain five different key chromophores, each of which absorb photons of light

at varying wavelengths (Figure 1.1-7).[25] As a result, their combined electronic absorption spectra adequately cover the range of the solar spectrum.

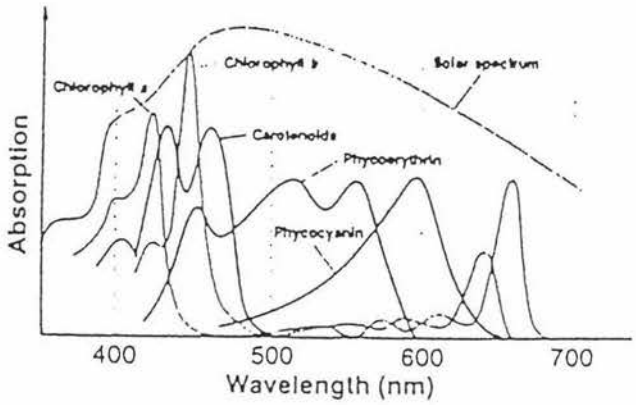

Figure 1.1-7
The electronic absorption spectra of the photosynthetic pigments in green plants, and the solar spectrum.

So how can the properties of transition metal bound bipyridyl complexes be altered, in order to produce more efficient solar cells? This may be possible by taking advantage of the ease in functionalising the bipyridine ligand. Functionalisation can occur either before or after coordination to a metal ion, making it possible to fine tune the properties of a desired complex through both the choice of appendage, and the method of connection.

1.2 Functionalised bipyridines

2,2'-Bipyridine ligands are readily able to be functionalised through one or both of the 3-positions,[26] 4-positions,[13,27] 5-positions,[28,29] or 6-positions,[30,31] either before or after complexation to a metal ion. Once formed, the complex can be further functionalised through ligand attachment to the metal ion.[32] This versatility becomes very important when designing a complex which must possess specific properties, in order to perform a particular task.

The choice of functional group to attach to the bipyridine ligand or complex, is obviously dependant on the purpose of the research being undertaken. The literature contains numerous examples of such work with functionalities ranging from: secondary metallated polypyridyl groups,[33] to calixarenes,[13,30,34] and phenothiazines,[35,36] from crown ethers,[11,37] to [60]fullerene,[38] metallocenes,[39-41] and porphyrins[42-44]. An important feature of each of these polynuclear compounds, aside from the coordinated units themselves, are the bridging ligands between these centres. The nature of the bridge between the bipyridine and its functionality, has a direct influence not only on the degree of

communication between the two units, but also the properties of the resultant complex. Bpy ligands have been functionalised through direct coupling,[44] flexible linking groups,[45] and rigid spacers[46].

1.2.1 Modes of connection

Through the combination of their length, geometry, and chemical nature, the linking groups in polynuclear compounds play a crucial role in determining the rate of energy, and electron transfer processes of the compound. Many different linking groups have been utilised in conjunction with the functionalisation of bipyridines. A selection of those most repeatedly used are summarised in the following table.

Mode of connection	Linking group	comment	references
Direct link	**A.** bpy—≀		17,44
Flexible linkages	**B.** bpy–(CH$_2$)$_n$–≀	n = 1, 2, 4	14,16,18,21, 27,35,36,43
	C. bpy–C(=O)–NH–(CH$_2$)$_n$–≀	n = 2, 4	12,13,23,45, 47,48
Ether linkages	**D.** bpy–O–≀		33
	E. bpy–O–≀		31,49,50
Vinylic link	**F.** bpy–≀		28,34,40,41, 51,52
Ethyne link	**G.** bpy–≡–≀		11,37,46

Table 1
Linkages commonly used for the functionalisation of bpy ligands.

As is apparent, there have been a vast number of functionalised bpy compounds synthesised to date. When the purpose of synthesising such a compound is for its potential ability to perform light induced functions, the choice of linking group is very important. When synthesising a compound with a bpy ligand connected to a second conjugated species, for this or any other application, it may be beneficial to extend this conjugation throughout the linkage. This would result in a fully conjugated binuclear or polynuclear compound which could facilitate electron flow throughout the complex, a useful property for a potential molecular device. A direct link (see Table 1, example A) is not always viable. By bringing

the two groups so close together, a strained system is likely to be induced, as was discovered by Sessler *et al.*[44] (see Figure 1.2-11, p.15). In order to avoid this problem many researchers working on the functionalisation of bipyridines for various different applications have elected vinylic links (see Table 1, example F), as their linking group of choice. A vinylic bridge provides a three bond couple between two centres, extending the conjugation from the bpy ligand to the functional group. For this reason, the vinyl group was chosen as the linker of choice for this research programme.

1.2.2 The vinylic bridge

There are two primary methods of connecting two centres *via* a vinylic bridge. The first method uses lithium diisopropylamide (LDA), and involves the reaction between an alkyl group, and a carbonyl group, Figure 1.2-1.

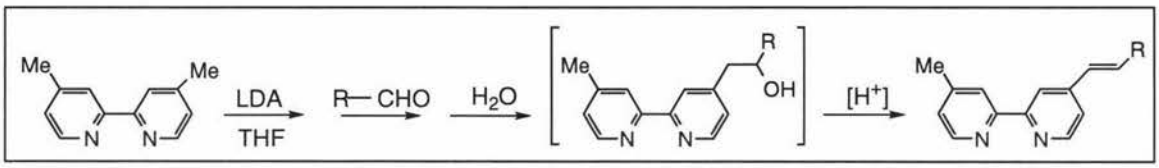

Figure 1.2-1
Functionalisation of a bipyridine ligand *via* a vinylic bridge. LDA method.

This method was successfully used by both Beer,[51] and Bourgault,[40] to functionalise bipyridine ligands with π-donor appendages (see Section 1.2.3, from p.9). However, the LDA method requires the use of a very strong base, which could induce other undesired side-reactions. If the functional group involved is susceptible to such a strong nucleophile, then another methodology should be employed.

An alternative methodology for the formation of a vinylic bridge between a bipyridine and a functional group utilises the classic Wittig reaction. Wittig chemistry involves the formation of a phosphonium ylide from its corresponding phosphonium salt in the presence of a base. The ylide then reacts with a carbonyl compound to form the vinylic bridge, Figure 1.2-2.

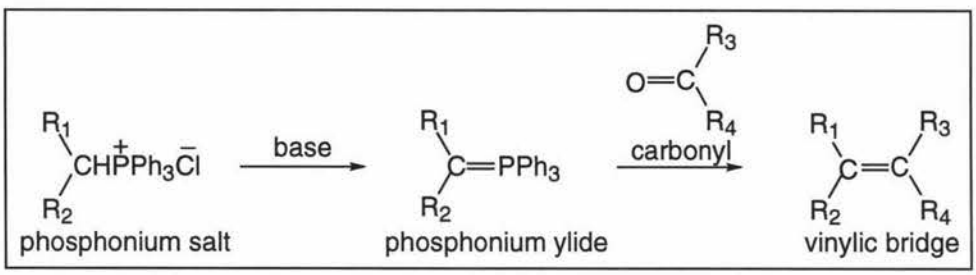

Figure 1.2-2
The Wittig reaction.

Depending on the nature of the R groups, the vinylic compound formed could have a *cis*- or *trans*-configuration. Sterically, the *trans*-isomer is more favourable. In practice, a mixture of products is usually formed with the *trans*-isomer predominating. A final isomerisation step in the reaction sequence will often procure *cis* to *trans* conversion.

The following section contains a summary of the research carried out on the synthesis and study of complexes containing bipyridine units functionalised through vinylic bridges.

1.2.3 Bipyridine ligands functionalised *via* vinylic bridges

The synthesis of complexes containing bipyridine ligands functionalised through vinyl linkages with compounds such as ferrocenes, phenothiazines, crown ethers, and various π-donor groups, is becoming a widely studied area of research. The vinylic linker affords an extended conjugated system between the bipyridine and its appendage, facilitating a possible communication channel between the two centres. This property, along with the relatively straight-forward methodologies involved in incorporating vinyl linking groups into polynuclear compounds, has made such linkers common tools in many research laboratories around the world. This section describes examples of such research.

Because of the significance of bimetallic species in many important biological processes, Burkhard König and his research team in Braunschweig, Germany, are synthesising bimetallic molecular structures. Their model system utilises the bipyridine ligand for its strong bidentate coordination of transition metal ions, functionalised with a redox-active ferrocene moiety. Their model compound, bis(6-vinyl-6'-methyl-2,2'-bipyridyl)ferrocene shown in Figure 1.2-3, acts as a molecular tweezer in the multi-dentate binding of transition metal ions.[41]

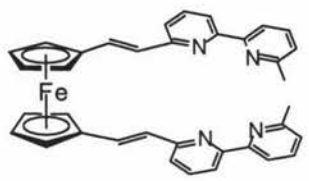

Figure 1.2-3
Ferrocene functionalised bipyridyl "molecular tweezer".

Synthesis of this complex involved a two step condensation reaction of ferrocene-1,1'-dicarbaldehyde with 6,6'-dimethyl-2,2'-bipyridine, a derivation of the LDA method. The isomeric bis(4-vinyl-4'-methyl-2,2'-bipyridine)ferrocenyl compound was also synthesised from a 4,4'-dimethyl-2,2'-bipyridine starting material. To date, studies have shown that

these complexes successfully bind Ag^+ and Cu^+ metal ions in a "molecular tweezer" type fashion. Further studies with various metal ions are underway.

Paul Beer *et al.*[51] are working on the preparation of polymeric films containing chromophore-electroactive quencher systems. They have synthesised two new ferrocene functionalised bpy ligands, $\mathbf{L_1}$ and $\mathbf{L_2}$ (Figure 1.2-4). Both ligands were synthesised from 4,4'-dimethyl-2,2'-bipyridine *via* a three step mrthodology based on the LDA method. Lithiation of bpy followed by the addition of ferrocenecarbaldehyde and then dehydration, yielded bpy ligands, appended with ferrocene functionalities through vinyl linkers.

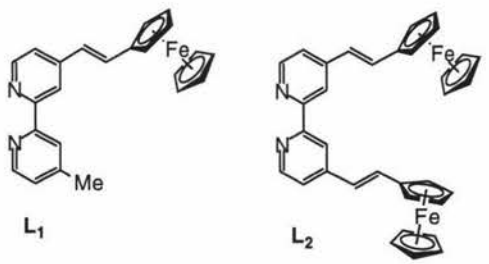

Figure 1.2-4
Ferrocene functionalised bipyridine ligands for complexation and electropolymerisation.

One equivalent of each ligand ($\mathbf{L_1}$ and $\mathbf{L_2}$), were reacted with $[Ru^{II}Cl_2(bpy)_2].2H_2O$ to form ruthenium(II)trisbipyridine complexes containing one and two ferrocenyl functionalities respectively. Through electrochemical analyses, it was found that the complex containing the ligand $\mathbf{L_2}$ successfully formed a polymeric film, whereas the complex with the single $\mathbf{L_1}$ ligand did not electropolymerise. This was rationalised on the basis of radical-radical coupling, which is absent in the latter case due to the complex possessing only a single olefinic ligand. The two tris(ligand)ruthenium(II) complexes; $[Ru(L_1)_3][PF_6]_2$, and $[Ru(L_2)_3][PF_6]_2$, (Figure 1.2-5 below) were also synthesised, by quenching a refluxed mixture of the appropriate ligand with $RuCl_3.3H_2O$.

From previous studies on similar systems,[53] it was expected that these two trisbipyridine complexes would electropolymerise successfully and at a faster rate than the complex containing one $\mathbf{L_2}$ ligand. This assumption was based on findings by Calvert *et al.*[53] that rate of electropolymerisation is proportional to the number of functionalised bipyridine ligands present. However, no electrochemical measurements were able to be taken of either of these octahedral ruthenium(II) species due to product insolubility.

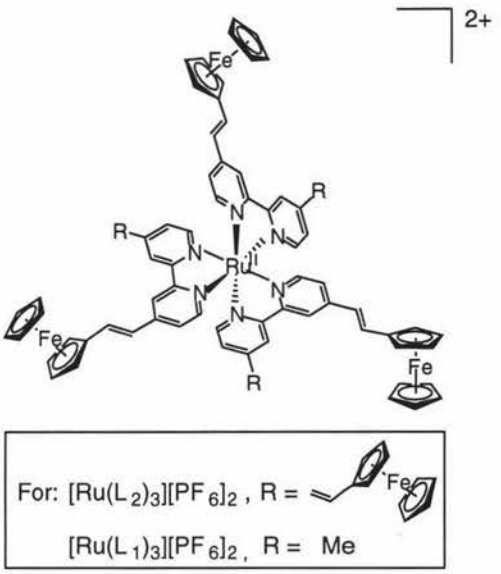

Figure 1.2-5
Tris- and hexa-ferrocenyl functionalised ruthenium(II)trisbipyridyl complexes.

Bourgault *et al.* are designing and synthesising π-donor functionalised bipyridine ligands, with a particular interest in the second-order nonlinear optical (NLO) properties of their metal complexes.[40] This interest has developed since measurements were recorded for the octahedral ruthenium complex containing three bis-4,4'-di-*n*-butylaminostyryl-2,2'-bipyridine ligands (Figure 1.2-6). This complex revealed a giant octupolar nonlinearity, with one of the highest β-values ever reported.[54]

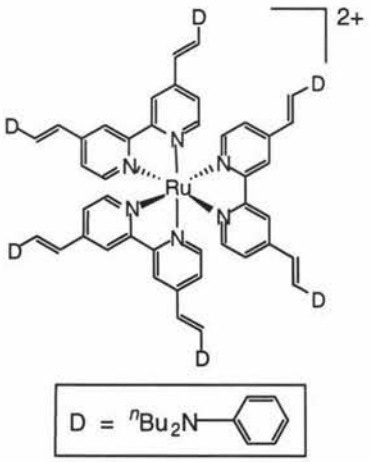

Figure 1.2-6
Ruthenium(II)tris(bis-functionalised)bipyridine complex possessing remarkable NLO properties.

A number of other π-donor functionalised bipyridine ligands have now been synthesised which Bourgault *et al.* believe could possess similar NLO properties when complexed to transition metals. The functionalised ligands have been synthesised *via* four step preparations from 4,4'-dimethyl-2,2'-bipyridine. One of these ligands is identical to Beer *et*

al.'s ferrocene functionalised $\mathbf{L_1}$ ligand (see Figure 1.2-4 above). The results from the NLO studies of these complexed ligands have not yet been reported.

1.2.4 Porphyrin-functionalised bipyridines

During recent years, there has developed a growing interest in the synthesis of mixed photoactive component structures containing bipyridyl complexes. This research is having an enormous impact on the development of molecular scale devices for biomimetic studies. Despite complex syntheses, the combination of transition metal binding bipyridyl complexes and porphyrin rings is becoming increasingly popular. This section summarises the research done on the synthesis and study of compounds containing both bipyridine and porphyrin moieties.

A research group in Princeton, New Jersey, led by Hamilton and Bocarsly, are interested in the synthesis of systems capable of photochemical energy conversion.[29] In recent years, many attempts to formulate such systems have been based around the excited state chemistry of either $Ru(bpy)_3^{2+}$ complexes, or metalloporphyrins. However, this research team could see the potential of combining the properties of both moieties into one photoactive complex. Through a long and complex process, a ruthenium(II)trisbipyridine complex, covalently linked across the face of a porphyrin (Figure 1.2-7) was synthesised. The two flexible, covalent ester linkages connect through the 5- and 5'-positions of one of the bipyridine ligands, to *trans* β-pyrrolic positions of the porphyrin moiety.

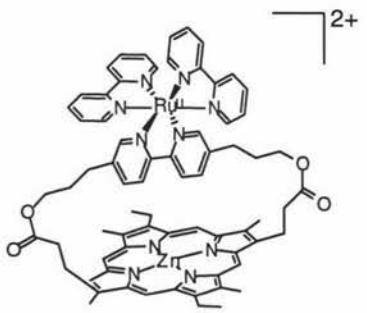

Figure 1.2-7
Porphyrin covalently linked to $Ru(bpy)_3^{2+}$, synthesised by Hamilton *et al.*.

The synthesis involved making 5,5'-bis(3-hydroxypropyl)-2,2'-bipyridine *via* a seven step synthesis from bpy. A diacid chloride substituted porphyrin, was synthesised from a tetrasubstituted pyrrole and a trisubstituted pyrrole in fourteen steps.[55] Condensation of the porphyrin with the diol, followed by reaction with $Ru^{II}(bpy)_2Cl_2$ and then metallation of the porphyrin ring, yields the complex (Figure 1.2-7) in relatively low overall yield. Luminescence and electrochemical studies revealed a strong interaction between the two

photoactive centres, causing stabilisation of the ruthenium(II)trisbipyridyl moiety. This was presumed to be due to the covalent connection between the bipyridine and the β-pyrollic positions of the porphyrin, causing a fixed proximity of approximately 4Å between the two units.[29]

Manganese peroxidase (MnP), an important heme enzyme found in plants and fungi, catalyses the H_2O_2-dependent oxidation of Mn^{2+} to Mn^{3+}. The resulting Mn^{3+} in turn oxidises a wide variety of organic substrates amongst which is lignin, the strengthening cross-linking matrix of wood. A French research group have synthesised a model system based on MnP activity.[42] This is an area of research relatively neglected compared to other hemeproteins due to difficulties in preventing unselective reactions in the model system.[56] Policar *et al.* synthesised a heterobimetallic complex containing a highly fluorinated iron porphyrin, with a manganese site covalently linked at a proximity which mimics that found in MnP (Figure 1.2-8). The manganese-binding bipyridyl complex is covalently attached to the porphyrin ring through the *meta* position of the unsubstituted *meso*-phenyl group of the porphyrin, by way of a five membered, di-amine containing, flexible bridge.

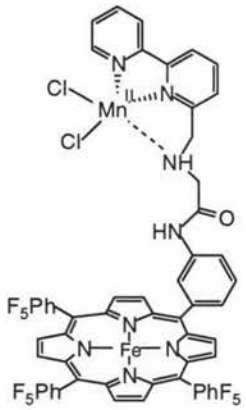

Figure 1.2-8
Binuclear [Mn^{II}(bpy)-Fe^{III}(porphyrin)] complex, biomimetic of MnP.

The complex was synthesised in seven steps from a free base 5,10,15-tris(hexafluoro)phenyl-20-*o*-nitrophenyl porphyrin, and a 6-monosubstituted-2,2'-bipyridine ligand. In the presence of iodosylarene, this model proved to undergo an efficient electron transfer between the Mn^{II} complex and the Fe^{III} porphyrin species to result in Mn^{III} formation. On addition of a substrate this Mn^{III} is converted back to Mn^{II}, mimetic of the functioning of MnP. This model favours the electron transfer between Mn^{II} and the iron-oxo species, eliminating other competitive electron transfer reactions. Policar *et al.*[42] ascribe this property to the particular covalent linkage used. This link holds the two metallocentres at a cognate proximity to that found between the manganese binding site and the heme active site in MnP.

A Brazilian research team are interested in the modification of electrodes with multilayered films. Generally, such electrodes are prepared through either ionic polymer absorption, or by monomer electropolymerisation, and often utilise the properties of ruthenium polypyridine derivatives. Araki *et al.*[32] have synthesised a new polyruthenated nickel porphyrin film which contains four ruthenium(II)bisbipyridine complexes (Figure 1.2-9). The complexes are connected to the porphyrin moiety through direct links between the four Ru metal ions and the 1-position of the four *meso*-pyridyl substituents of the central porphyrin.

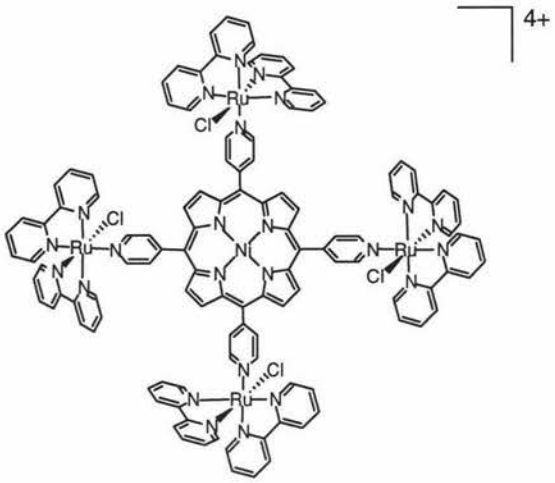

Figure 1.2-9
Tetraruthenated nickel porphyrin complex used for electrode modification.

The complex was synthesised by reacting the *meso*-tetra(4-pyridyl)porphyrinato nickel(II) moiety with excess $Ru(bpy)_2Cl_2$. Unlike the complex modified electrode preparations of the past, this film is easily obtainable by dip-coating. The complex is dissolved in methanol to transfer onto a clean electrode surface. Evaporation of the solvent results in an orange coloured film on platinum electrode surfaces, or a bright violet film when applied to glassy carbon electrodes. The film was found to exhibit well controlled electrochemical and photoelectrochemical responses, and showed maxima resembling absorption patterns from both the peripheral ruthenium(II) complexes, as well as the central nickel porphyrin moiety. Araki *et al.* plan to design further modified electrodes to elaborate on the photochemical properties found for this tetraruthenated nickel porphyrin film.[32]

Harriman and Ziessel[46] are constructing multicomponent, photoactive molecular scale wires containing transition metal bound polypyridine units. Palladium catalysed reactions were employed to bridge the photoactive components with polyyne spacer groups. These rigid triple bond linkers were used in order to maintain strong electronic communication between metal centres. One structure they have synthesised consists of a ruthenium(II)trisbipyridine

unit, equipped with a peripheral light harvesting metalloporphyrin (Figure 1.2-10). The two chromophoric moieties are linked to a central platinum(II) ion through rigid ethyne couples.

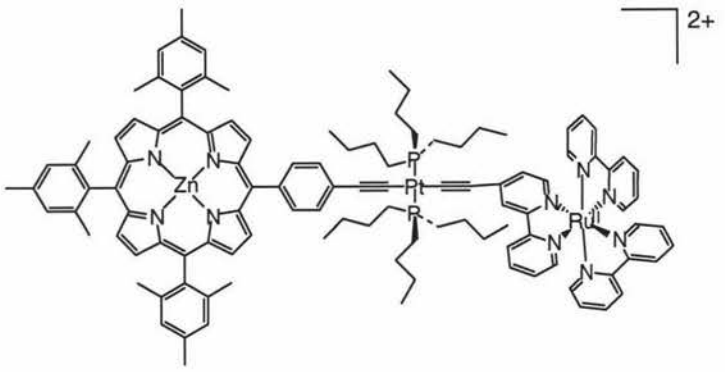

Figure 1.2-10
Harriman and Ziessel's photoactive wire consisting of a metalloporphyrin and a $Ru(bpy)_3^{2+}$ complex.

This complex was found to be kinetically stable in solution and resistant to thermal and photochemical isomerisation. However, in order to produce an efficient photoactive wire, larger scale systems are required. Harriman and Ziessel are currently working on a methodology to enable them to produce long, "molecular clotheslines" with specific cationic complexes at predetermined binding sites along the wire.[46]

Sessler *et al.*[44] have synthesised a complex containing two $Ru^{II}(bpy)_3$ units, directly connected to opposite *meso*-positions of a free base porphyrin ring (Figure 1.2-11).

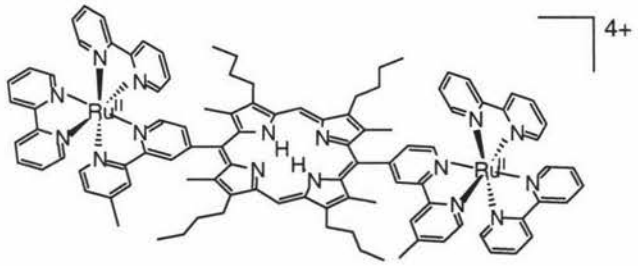

Figure 1.2-11
Reaction scheme showing synthesis of orthogonal bisruthenium(II)trisbipyridine porphyrin bound complex.

This complex was synthesised in modest overall yield by reaction of 4-formyl-4'-methyl-2,2'-bipyridine with dipyrrylmethane under modified Lindsey conditions,[52] followed by complexation with $Ru^{II}(bpy)_2Cl_2.2H_2O$. The aim of the work was to determine whether the porphyrin moiety had any significance on the bridging or mediation of electronic interactions between the two ruthenium metal centres. Static absorption and emission spectra revealed that the two types of chromophore essentially did not interact. It was suspected that this non-interaction was due to the constrained orthogonality at the bipyridyl-porphyrin linkage.[44]

It is clear from the aforementioned examples that the research currently being undertaken using bipyridine ligands functionalised with porphyrin moieties is being targeted for a number of possible future applications. In most cases, complex, multiple step synthetic methodologies have been employed to form these polynuclear complexes. However, the positive results being obtained are establishing the potential of such systems for the development of molecular scale devices for biomimetic functions. There is a noticeable absence in the above examples of the use of vinyl linkers in these complexes. To the best of this author's knowledge, there are no examples yet published containing bipyridine ligands functionalised with porphyrin moieties through vinylic bridging ligands by way of either the LDA method or Wittig chemistry.

1.3 Research proposal

The research carried out for this thesis comprises an investigation into connecting photoactive moieties to bipyridine complexes through vinylic linking groups. As is described in Sections 1.1 and 1.2, there is precedent from the literature that such complexes may possess the potential to perform useful light-induced functions. The purpose of this study is to formulate an efficient method by which such complexes could be synthesised, so as to determine their value in this area of research.

The chromophoric appendage chosen for this study is the porphyrin moiety. Porphyrins are integral components in the light harvesting complexes of green plants and photosynthetic bacteria.[25,57,58] The optical, electronic, and photophysical properties of porphyrins and porphyrin dimers have made them key components for the study of; artificial light harvesting devices,[25,59-62] enzyme mimics,[63] small molecule activation,[64] and the four electron reduction of water[65,66].

To date, combining the two photo-active units has resulted in a variety of complexes with interesting properties for a number of possible applications (see Section 1.2.4). However, the connection of two porphyrin units to a bpy ligand using conjugated vinylic bridges is a novel approach. The complexation of such ligands to transition metal ions, particularly ruthenium, could potentially form complexes with the ability to perform light induced functions.

The chosen methodology of functionalisation for this project utilises Wittig chemistry. This methodology requires a phosphonium salt, and a carbonyl compound. Recently, the synthesis of a porphyrin phosphonium salt was developed in our laboratories and was shown to undergo Wittig reactions with a number of aldehydes.[60,67,68] Reaction of this

phosphonium salt with 4,4'-diformyl-2,2'-bipyridine could produce a bipyridine-porphyrin conjugate as outlined in Figure 1.3-1.

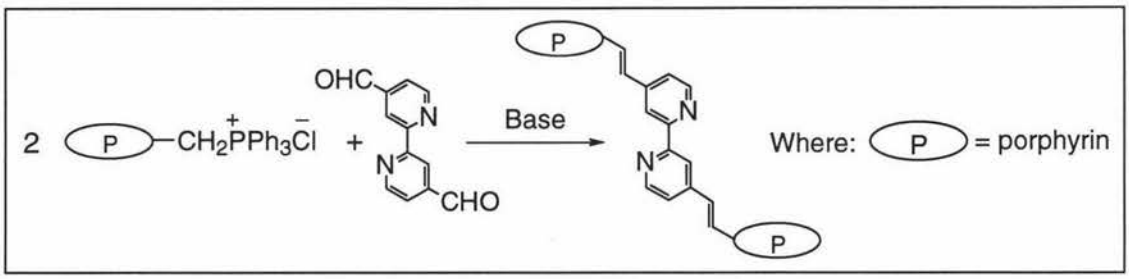

Figure 1.3-1
Synthesis of target bi-functionalised bipyridine ligand *via* Wittig chemistry.

Complexation of this ligand could produce a wide variety of transition metal complexes with exciting photophysical properties.

The first stage of this research was to synthesise the two starting materials required for the Wittig chemistry, the 4,4'-diformyl-2,2'-bipyridine, and the porphyrin phosphonium salt. Once these two precursors were produced, synthesis of the bipyridyl-porphyrin ligand was investigated and its metal-binding ability explored.

1.4 References

(1) Balzani, V.; Juris, A.; Venturi, M.; Campagna, S.; Serroni, S. *Chem. Rev.* **1996**, *96*, 759-833.

(2) Balzani, V. A. *New Scientist* **1994**, *144*, 31-34.

(3) Juris, A.; Balzani, V.; Barigelletti, F.; Campagna, S.; Belser, P.; Von Zelewsky, A. *Coord. Chem. Rev.* **1988**, *84*, 85-277.

(4) Constable, E. C. *Chem. Ind.* **1994**, *1*, 56-59.

(5) Harding, M. H.; Koert, U.; Lehn, J.-M.; Rigault, A. M.; Piguet, C.; Siegel, J. *Helv. Chim. Acta* **1991**, *74*, 594-610.

(6) Hasenknopf, B.; Lehn, J.-M.; Kneisel, B. O.; Baum, G.; Fenske, D. *Angew. Chem. Int. Ed. Eng.* **1996**, *35*, 1838-1839.

(7) Koert, U.; Harding, M. M.; Lehn, J.-M. *Nature* **1990**, *346*, 339-342.

(8) Lehn, J.-M.; Rigault, A. *Angew. Chem. Int. Ed. Eng.* **1988**, *27*, 1095-1097.

(9) Grover, N.; Ciftan, S. A.; Thorp, H. H. *Inorg. Chim. Acta* **1995**, *240*, 335-338.

(10) Palmer, C. R.; Sloan, L. S.; Adrian, J. C.; Cuenoud, B.; Paolella, D. N.; Schepartz, A. *J. Am. Chem. Soc.* **1995**, *117*, 8899-8907.

(11) Beer, P. D.; Kocian, O.; Mortimer, R. J.; Ridgway, C. *J. Chem. Soc., Chem. Commun.* **1991**, 1460-1463.

(12) Beer, P. D.; Szemes, F. *J. Chem. Soc., Chem. Commun.* **1995**, 2245-2247.

(13) Szemes, F.; Hesek, D.; Chen, Z.; Dent, S. W.; Drew, M. G. B.; Goulden, A. J.; Graydon, A. R.; Grieve, A.; Mortimer, R. J.; Wear, T.; Weightman, J. S.; Beer, P. D. *Inorg. Chem.* **1996**, *35*, 5868-5879.

(14) Meyer, T. J. *Acc. Chem. Res.* **1989**, *22*, 163-170.

(15) Péchy, P.; Rotzinger, F. P.; Nazeeruddin, M. K.; Kohle, O.; Zakeeruddin, S. M.; Humphry-Baker, R.; Grätzel, M. *J. Chem. Soc., Chem. Commun.* **1995**, 65-66.

(16) Sun, L.; Hammarstrom, L.; Norrby, T.; Berglund, H.; Davydov, R.; Andersson, M.; Borje, A.; Korall, P.; Philouze, C.; Almgren, M.; Styring, S.; Akermark, B. *J. Chem. Soc., Chem. Commun.* **1997**, 607-608.

(17) Yamamoto, T.; Yoneda, Y.; Kizu, K. *Macromol. Rapid Commun.* **1995**, *16*, 549-556.

(18) Goulle, V.; Harriman, A.; Lehn, J.-M. *J. Chem. Soc., Chem. Commun.* **1993**, 1034-1036.

(19) Benniston, A. C.; Goulle, V.; Harriman, A.; Lehn, J.-M.; Marczinke, B. J. *J. Phys. Chem.* **1994**, *98*, 7798-7804.

(20) Heimer, T. A.; D'Arcangelis, S. T.; Farzad, F.; Stipkala, J. M.; Meyer, G. J. *Inorg. Chem.* **1996**, *35*, 5319-5324.

(21) Ghosh, P. K.; Spiro, T. G. *J. Am. Chem. Soc.* **1980**, *102*, 5543-5549.

(22) Gould, S.; Leasure, R. M.; Meyer, T. J. *Chem. Brit.* **1995**, 891-893.

(23) Dabestani, R.; Bard, A. J.; Campion, A.; Fox, M. A.; Mallouk, T. E.; Webber, S. E.; White, J. M. *J. Phys. Chem.* **1988**, *92*, 1872-1878.

(24) Coghlan, A. *New Scientist* **1995**, *1*, 22.

(25) Lin, V. S. Y.; Dimagno, S. G.; Therien, M. J. *Science* **1994**, *264*, 1105-1111.

(26) Rebek, J.; Trend, J. E.; Wattley, R. V.; Chakravorti, S. *J. Am. Chem. Soc.* **1979**, *101*, 4333-4336.

(27) Lopez, C.; Moutet, J.-C.; Saint-Aman, E. *J. Chem. Soc., Faraday Trans.* **1996**, *92*, 1527-1532.

(28) Frank, M.; Nieger, M.; Vogtle, F.; Belser, P.; Von Zelewsky, A.; De Cola, L.; Balzani, V.; Barigelletti, F.; Flamigni, L. *Inorg. Chim. Acta* **1996**, *242*, 281-291.

(29) Hamilton, A. D.; Rubin, H.-D.; Bocarsly, A. B. *J. Am. Chem. Soc.* **1984**, *106*, 7255-7257.

(30) Casnati, A.; Fischer, C.; Guardigli, M.; Isernia, A.; Manet, I.; Sabbatini, N.; Ungaro, R. *J. Chem. Soc., Perkin Trans. II* **1995**, 395-399.

(31) Deschenaux, R.; Ruch, T.; Deschenaux, P.-F.; Juris, A.; Ziessel, R. *Helv. Chim. Acta* **1995**, *78*, 619-628.

(32) Araki, K.; Angnes, L.; Toma, H. E. *Adv. Mater.* **1995**, *7*, 554-558.

(33) Constable, E. C.; Harverson, P.; Oberholzer, M. *J. Chem. Soc., Chem. Commun.* **1996**, 1821-1822.

(34) Regnouf-de-Vains, J.-B.; Lamartine, R. *Tetrahedron Lett.* **1996**, *37*, 6311-6314.

(35) Larson, S. L.; Elliott, C. M.; Kelley, D. F. *Inorg. Chem.* **1996**, *35*, 2070-2076.

(36) Coe, B. J.; Friesen, D. A.; Thompson, D. W.; Meyer, T. J. *Inorg. Chem.* **1996**, *35*, 4574-4584.

(37) An, H.; Bradshaw, J. S.; Izatt, R. M.; Yan, Z. *Chem. Rev.* **1994**, *94*, 939-991.

(38) Maggini, M.; Dono, A.; Scorrano, G.; Prato, M. *J. Chem. Soc., Chem. Commun.* **1995**, 845-846.

(39) Beer, P. D. *Chem. Soc. Rev.* **1989**, *18*, 409-450.

(40) Bourgault, M.; Renouard, T.; Lognone, B.; Mountassir, C.; Le Bozec, H. *Can. J. Chem.* **1997**, *75*, 318-325.

(41) Konig, B.; Nimtz, M.; Zieg, H. *Tetrahedron* **1995**, *51*, 6267-6272.

(42) Policar, C.; Artaud, I.; Mansuy, D. *Inorg. Chem.* **1996**, *35*, 210-216.

(43) DiMagno, S. G.; Lin, V. S. Y.; Therien, M. J. *J. Org. Chem.* **1993**, *58*, 5983-5993.

(44) Sessler, J. L.; Capuano, V. L.; Burrell, A. K. *Inorg. Chim. Acta* **1993**, *204*, 93-101.

(45) Mecklenburg, S. L.; Peek, B. M.; Erickson, B. W.; Meyer, T. J. *J. Am. Chem. Soc.* **1991**, *113*, 8540-8542.

(46) Harriman, A.; Ziessel, R. *J. Chem. Soc., Chem. Commun.* **1996**, 1707-1716.

(47) Leasure, R. M.; Kajita, T.; Meyer, T. J. *Inorg. Chem.* **1996**, *35*, 5962-5963.

(48) McCafferty, D. G.; Bishop, B. M.; Wall, C. G.; Huges, S. G.; Mecklenberg, S. L.; Meyer, T. J.; Erickson, B. W. *Tetrahedron* **1995**, *54*, 1093-1106.

(49) Dupray, L. M.; Meyer, T. J. *Inorg. Chem.* **1996**, *35*, 6299-6307.

(50) Worl, L. A.; Strouse, G. F.; Younathan, J. N.; Baxter, S. M.; Meyer, T. J. *J. Am. Chem. Soc.* **1990**, *112*, 7571-7578.

(51) Beer, P. D.; Kocian, O.; Mortimer, R. J. *J. Chem. Soc., Dalton Trans.* **1990**, 3283-3288.

(52) Lindsey, J. S.; Schreiman, I. C.; Hsu, H. C.; Kearney, P. C.; Marguerettaz, A. M. *J. Org. Chem.* **1987**, *52*, 827-836.

(53) Calvert, J. M.; Schmehl, R. H.; Sullivan, B. P.; Facci, J. S.; Meyer, T. J.; Murray, R. W. *Inorg. Chem.* **1983**, *22*, 2151-2162.

(54) Dhenaut, C.; Ledoux, I.; Samuel, I. D. W.; Zyss, J.; Bourgault, M.; Le Bozec, H. *Nature* **1995**, *374*, 339-342.

(55) Chang, C. K. *J. Am. Chem. Soc.* **1977**, *99*, 2819-2822.

(56) Artaud, I.; Ben-Aziza, K.; Mansuy, D. *J. Org. Chem.* **1993**, *58*, 3373-3380.

(57) Hu, X.; Ritz, T.; Damjanovic, A.; Schulten, K. *J. Phys. Chem. B* **1997**, *101*, 3854-3871.

(58) Boxer, S. G.; Goldstein, R. A.; Lockhart, D. J.; Middendorf, T. R.; Takiff, L. *J. Phys. Chem.* **1989**, *93*, 8280-8294.

(59) Lin, V. S. Y.; Therien, M. J. *Chem. Eur. J.* **1995**, *1*, 645-651.

(60) Burrell, A. K.; Officer, D. L.; Reid, D. C. W. *Angew. Chem. Int. Ed. Eng.* **1995**, *34*, 900-902.

(61) Officer, D. L.; Burrell, A. K.; Reid, D. C. W. *J. Chem. Soc., Chem. Commun.* **1996**, 1657-1658.

(62) Crossley, M. J.; Try, A. C.; Walton, R. *Tetrahedron Lett.* **1996**, *37*, 6807-6810.

(63) Marvaud, V.; Vidal-Ferran, A.; Webb, S. J.; Sanders, J. K. M. *J. Chem. Soc., Dalton Trans.* **1997**, 985-990.

(64) Collman, J. P.; Hutchison, J. E.; Lopez, M. A.; Tabard, A.; Guilard, R.; Seok, W. K.; Ibers, J. A.; L'Her, M. *J. Am. Chem. Soc.* **1992**, *114*, 9869-9877.

(65) Collman, J. P.; Herrmann, P. C.; Boitrel, B.; Zhang, X.; Eberspacher, T. A.; Fu, L. *J. Am. Chem. Soc.* **1994**, *116*, 9783-9784.

(66) Collman, J. P.; Ennis, M. S.; Offord, D. A.; Chng, L. L.; Griffin, J. H. *Inorg. Chem.* **1996**, *35*, 1751-1752.

(67) Bonfantini, E. E.; Officer, D. L. *Tetrahedron Lett.* **1993**, *34*, 8531-8534.

(68) Burrell, A. K.; Campbell, W.; Officer, D. L. *Tetrahedron Lett.* **1997**, *38*, 1249-1257.

Chapter Two

Synthesis of 4,4'-diformyl-2,2'-bipyridine

There has been substantial interest during the past ten years in investigations into the synthesis of side-chain derivatives of 4,4'-dimethyl-2,2'-bipyridine.[1-5] However, amongst the work published in this area, there is a noticeable under-representation of syntheses of 4,4'-diformyl-2,2'-bipyridine. The majority of research in this area has focused on either the synthesis of mono-substituted, or multi-hetero-substituted bipyridine ligands, with only the occasional mention of a 4,4'-diformyl-2,2'-bipyridine by-product[6]. Of the few publications reporting the synthesis of this product, the methodologies used were either not included in the article, and/or very complex multi-step and low yielding procedures.

2.1 Previous reports of 4,4'-diformyl-2,2'-bipyridine syntheses

Sessler *et al.* [2] reported the connection of two $Ru^{II}(bpy)_3$ units to a porphyrin ring (see Figure 1.2-11, Section 1.2.4, p.15). The synthetic methodology used to make the compound employed modified Lindsey conditions[7] to connect 4-formyl-4'-methyl-2,2'-bipyridine to a dipyrrylmethane, to form the bisruthenium(II)trisbipyridine porphyrin. The mono-formylated bipyridyl precursor was synthesised in 30% yield from 4,4'-dimethyl-2,2'-bipyridine through a SeO_2 oxidation, as depicted in Figure 2.1-1.

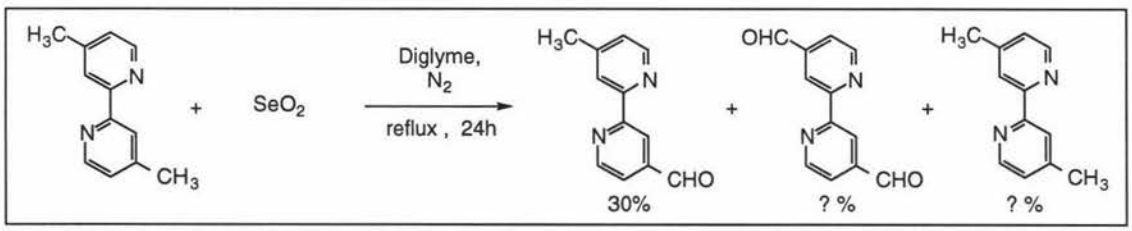

Figure 2.1-1
Synthetic methodology for the formation of 4-formyl-4'-methyl-2,2'-bipyridine *via* a SeO_2 oxidation.

Sessler *et al.* recovered an undisclosed amount of the starting material as well as the over-oxidised by-product, 4,4'-diformyl-2,2'-bipyridine. The yield of the dialdehyde by-product was not stated in the article.

An alternative method of formation of 4-formyl-4'-methyl-2,2'-bipyridine was reported by Meyer *et al.* in 1989.[1] Activated MnO_2 was the oxidising agent used to produce the desired

product in 58% yield. The authors undertook the research simply as an investigation into the synthesis of 2,2'-bipyridine compounds with single functionalised side chains, and made no mention of any by-products recovered from the reactions.

A group of chemists with a noticeable interest in bipyridine chemistry throughout the past decade is Paul Beer and his associates in the U.K. In 1990, an article was published describing the synthesis of polytopic macrocyclic compounds containing multiple bipyridine moieties[4] such as the tetrametallic macrocycle shown in Figure 2.1-2.

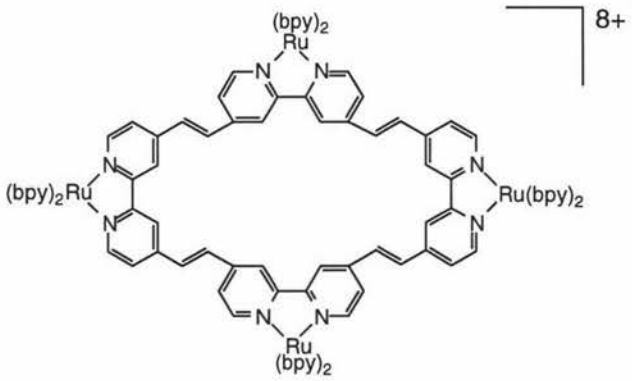

Figure 2.1-2
Polymetallic transition metal macrocyclic complex synthesised by Beer *et al.*.

These macrocycles which contain bipyridine complexes connected through vinylic linkers, were synthesised by linking the 4,4'-diformyl-2,2'-bipyridine units using a variant of the LDA method (see Section 1.2.2, p.8) followed by metal complexation. Despite claiming their 4,4'-diformyl-2,2'-bipyridine precursor as a new compound, the publication contained no formal experimental section, only a brief description of the manner in which the products were formed. The article stated that the dialdehyde was synthesised in four steps (34% overall yield) from 4,4'-dimethyl-2,2'-bipyridine. The only reaction details mentioned were the reagents used in each step and the product yields, as represented in Figure 2.1-3.

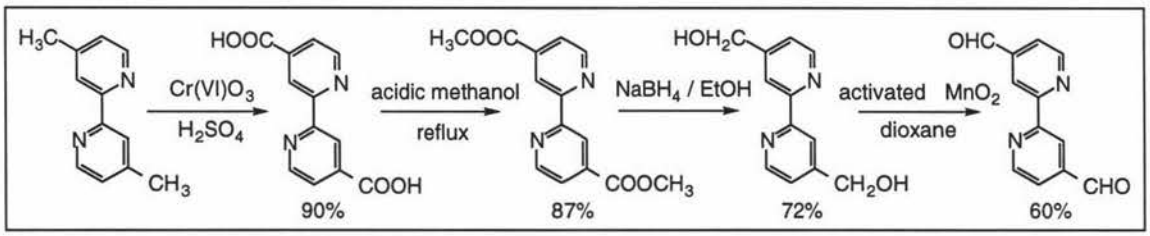

Figure 2.1-3
Reaction scheme showing synthetic route to 4,4'-diformyl-2,2'-bipyridine.

Two years later, a publication focusing on the formation of cryptand molecules containing both functionalised ferrocene and 4,4'-bipyridine moieties was released by the same

authors.[5] Once again experimental details were omitted, however amongst the text it was disclosed that the dialdehyde was prepared in 75% yield from the corresponding dialcohol *via* a Swern oxidation, an alternative and higher yielding procedure to that reported in the 1990 paper. It was later revealed,[8] that in the activated MnO_2 methodology, a side-reaction between the manganese and the nitrogen atoms of the bipyridine ligand was an unavoidable occurrence. Thus, they investigated alternative methods of oxidation for this final step. The Swern oxidation resulted in a 12% increase in yield of the desired product so became the preferred methodology for converting the dialcohol to the dialdehyde.

After the majority of the experimental work carried out for this thesis was completed, an article was published which described an alternative synthetic route to 4,4'-diformyl-2,2'-bipyridine.[9] Le Bozec and his research group could see the potential of this ligand and its derivatives as useful synthons for the elaboration of functionalised bipyridines and oligobipyridines. They were aware that conventional syntheses of such compounds involved several steps, and generally resulted in low yielding formation of the dialdehyde product. This group therefore developed the following methodology by which the commercially available starting material could be converted to the desired product in two steps (outlined in Figure 2.1-4) with an overall yield of 71%.

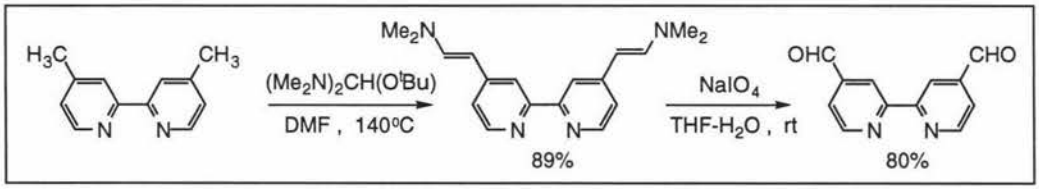

Figure 2.1-4
New two step method for synthesising 4,4'-diformyl-2,2'-bipyridine.

This new method was not utilised in this thesis as the publication was released after the majority of the laboratory research had been completed.

2.1.1 Summary

At the commencement of the research undertaken for this thesis, the literature contained little information on a direct synthesis of the desired precursor, 4,4'-diformyl-2,2'-bipyridine. The occurrence of the dialdehyde by-product in the work carried out by Sessler *et al.* (Section 2.1, p.21), suggests that a one step SeO_2 oxidation of 4,4'-dimethyl-2,2'-bipyridine could be a potential route to the synthesis of this precursor. To the best of the author's knowledge the only published methodology available at the time of commencement of this research project for the synthesis of this ligand, was the four step procedure developed by Beer *et al.*. This method not only significantly lacked detail, but also seemed

relatively low yielding for the amount of work involved. However the four step procedure is a tested and published preparation of the dialdehyde, therefore it was the method followed, to synthesise 4,4'-diformyl-2,2'-bipyridine.

2.2 Four step synthesis of 4,4'-diformyl-2,2'-bipyridine

The first reaction of the four step procedure involves oxidation of the commercially available 4,4'-dimethyl-2,2'-bipyridine to diacid **1** (Figure 2.2-1).

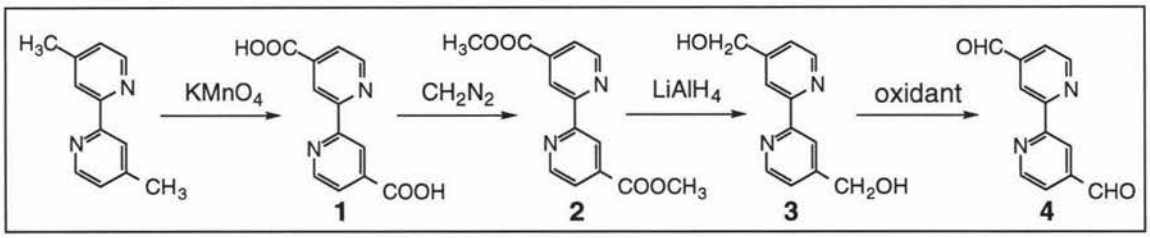

Figure 2.2-1
Four step procedure used to synthesise 4,4'-diformyl-2,2'-bipyridine.

The initial method employed to produce diacid **1** was by way of the readily available oxidising agent potassium permanganate, according to the procedure of Launikonis *et al.*.[10] This successfully yielded dicarboxylic acid **1** as a white solid in 51% yield. Characterisation by Launikonis *et al.* consisted of elemental analysis and ^{1}H NMR spectroscopy in deuterated trifluoroacetic acid. Compound **1** was characterised as the dicarboxylic acid according to mass and infrared spectral data. In the publication by Beer, a 90% yield was quoted for this first step using chromium (VI) oxide in sulphuric acid.[4,11] This same result was later duplicated by a post-doctoral researcher in these laboratories.

Subsequent conversion of **1** to **2** in the literature preparation[4] was achieved in 87% yield by refluxing **1** in acidic methanol. An alternative esterification technique using diazomethane was explored to take the very insoluble diacid compound through to the diester. Diazomethane was synthesised from diazogen (N-methyl-N-nitrosotoluene-p-sulphonamide) and potassium hydroxide based on the procedure outlined in 'Advanced Practical Organic Chemistry'.[12] Four and a half equivalents of diazomethane were required to convert **1** into **2**. The reaction was effectively monitored by tlc with an aqueous Fe^{3+} dip, as bipyridine ligands readily complex with Fe^{3+}. Such complexes are highly coloured red, pink, or purple species, a feature which is captured on the thin layer plate. For the diazomethane reaction, the Fe^{3+}-stained red spot moved from off the baseline (diacid), to an $R_f = 0.15$ corresponding to the monoester, 4-carboxylic acid-4'-methylester-2,2'-bipyridine. As the reaction reached completion this red spot was replaced by a pink-stained spot at $R_f = 0.77$.

Isolation of this compound produced dimethyl-2,2'-bipyridine-4,4'-dicarboxylate, **2**, in 92% yield.

Beer *et al.*[4] used sodium borohydride ($NaBH_4$) in ethanol to reduce diester **2** to dialcohol **3** in 72% yield. Attempts to duplicate this result proved problematic due to insolubility of dialcohol **3** in organic solvents. The most successful attempt did appear to convert the diester to compound **3** according to tlc analysis, as the pink Fe^{3+}-stained spot at $R_f = 0.77$ was replaced by a deep crimson coloured spot on the baseline. Due to the relative polarities of the diester and dialcohol, this result appeared very positive. However, all attempts to isolate the product were unsuccessful due to the solubility problem. Therefore, an investigation into the use of the reducing agent $LiAlH_4$ was carried out. The procedure used[13,14] involved an aqueous work-up and ether extraction of the organic substance, however in all attempts dialcohol **3** remained in the aqueous layer. Extraction of the dialcohol product in any reasonable yield proved to be unsuccessful. It was therefore concluded that a non-aqueous work-up procedure was necessary to isolate the desired compound. A recently released article by Kocienski *et al.*[15] was found to contain a method of converting a single methyl ester group into a hydroxymethyl appendage using $LiAlH_4$ with a non-aqueous work-up procedure. A modification of this method was tested and proved to be successful. The procedure was optimised on a 250 mg scale to give a 90% yielding synthesis of dialcohol **3** from diester **2**.

The final stage of the four step procedure involved the conversion of dialcohol **3** to the desired product 4,4'-diformyl-2,2'-bipyridine, **4**. The preferred methodology for this conversion according to the literature is by means of a swern oxidation. Using this procedure, Beer *et al.*[5] claim to have obtained the dialdehyde in 75% yield from the corresponding dialcohol. Various modified versions of a general Swern oxidation procedure[16,17] were attempted to try to form dialdehyde **4**. Problems arose due to the insolubility of the dialcohol in the solvent systems required for this procedure, and subsequently with the extraction of the product from the quenched reaction mixture. After numerous attempts, the most successful reaction was only able to produce the dialdehyde **4** in 29% yield (Method A, p.33-34). This result fell far short of the 75% yield claimed in the literature. Oxidation reactions using the Swern procedure were therefore discontinued and a final attempt was made using a relatively new oxidising agent, Dess Martin periodinane (D.M.P.).[18,19] The reagent was synthesised according to an optimised version of the procedure developed by Dess and Martin.[20,21] A number of attempts were made to form dialdehyde **4** using this reagent with little reward. The most successful reaction produced only a 12% yield of 4,4'-diformyl-2,2'-bipyridine, **4** (Method B, p.34). Subsequently, attempts to optimise the four step procedure proposed by Beer *et al.*[4] were abandoned as despite the time and effort invested, only a maximum overall yield of 22% was obtained for

synthesis of the dialdehyde over four steps. From the perspective of the objectives for this research, the development of a more direct, higher yielding methodology for synthesising 4,4'-diformyl-2,2'-bipyridine was becoming increasingly urgent. The production of the dialdehyde by-product in the work done by Sessler *et al.*[2], (Section 2.1, p.21) set the precedent for a SeO_2 oxidation as a potential method to synthesise the dialdehyde in a single step reaction. Therefore investigations into the feasibility of this synthetic methodology were begun.

2.3 4,4'-Diformyl-2,2'-bipyridine *via* a SeO_2 oxidation

Variations of the SeO_2 oxidation procedure used by Sessler *et al.* to produce 4-formyl-4'-methyl-2,2'-bipyridine[2] were explored for the synthesis of dialdehyde **4**, as indicated in Figure 2.3-1.

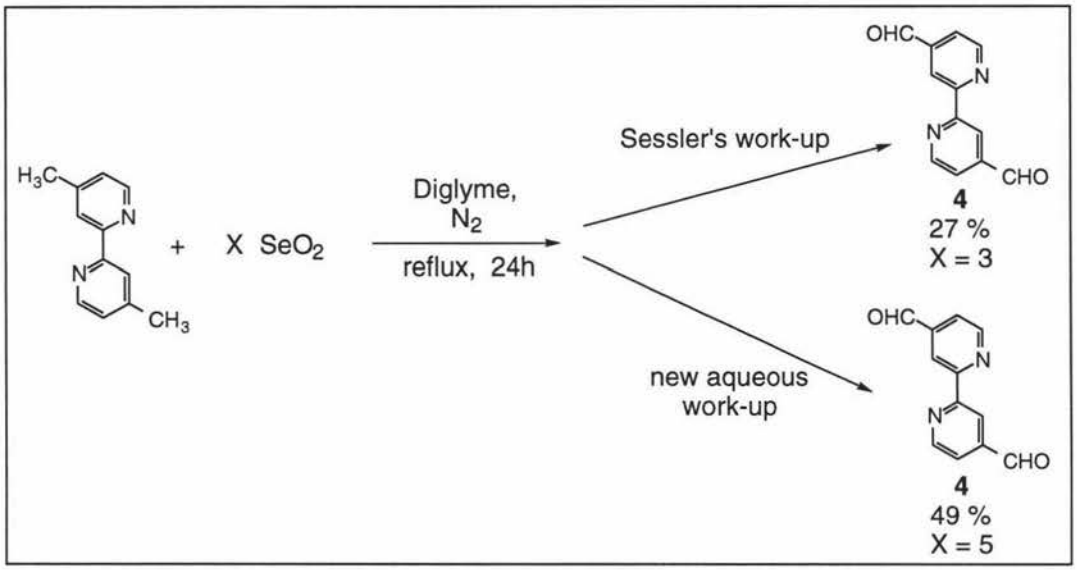

Figure 2.3-1
Synthesis of 4,4'-diformyl-2,2'-bipyridine using SeO_2 as the oxidising agent.

4,4'-Dimethyl-2,2'-bipyridine was refluxed in diglyme with SeO_2 and the reaction was followed by tlc. The use of an aqueous Fe^{3+} dip (as mentioned in Section 2.2), provided an efficient monitoring system to indicate dialdehyde formation during these reactions. However, the tlc results obtained were perplexing and substantially different to the results obtained by Sessler *et al.* in the 1993 article[2]. A summary of the trends seen in both cases is shown below in Figure 2.3-2.

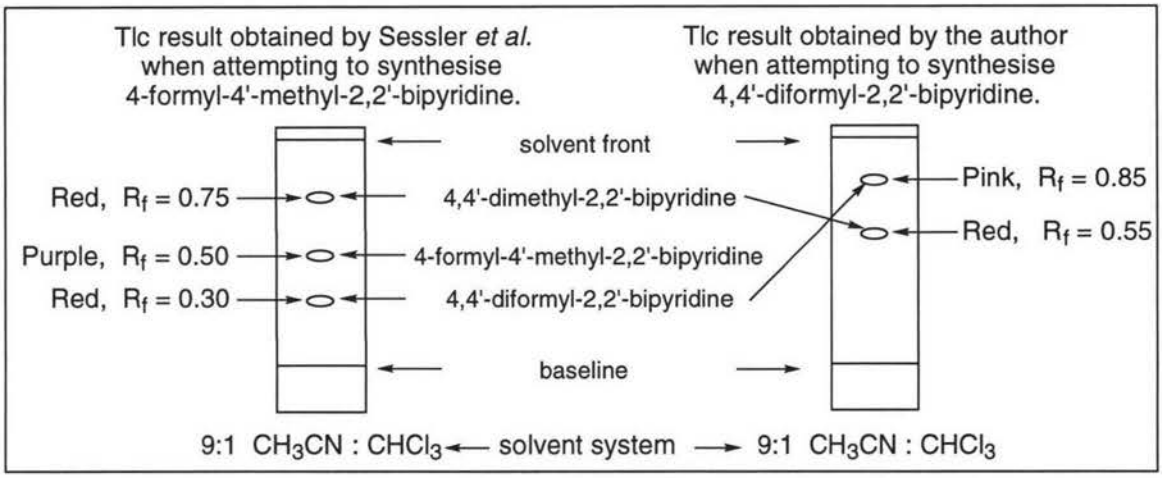

Figure 2.3-2
Comparison between tlc results obtained and those published by Sessler *et al.*.

The pattern observed by Sessler *et al.*[2]. can be readily rationalised as it emulates a direct correlation between the polarity of the compound and its decreasing R_f value on the tlc plate. Figure 2.3-2 above represents this data in a schematic diagram, shown in comparison with the tlc result obtained by the author in all reactions performed. This tlc was run before the completion of a reaction in order to demonstrate the position of both the dialdehyde product and the commercially available starting material. It is noteworthy that no monoformylated product was observed, the reaction appeared to form the dialdehyde directly from the 4,4'-dimethyl-2,2'-bipyridine starting material. Consistently, the dialdehyde product travelled to a higher R_f value than the starting material. This assiduous reversal of trend is very unusual, was unexpected, and is unable to be sensibly rationalised, however, the nature of the tlc plates must be the most likely suspect

Purification by column chromatography (Sessler's work-up) proved problematic as the dialdehyde product was not particularly soluble in suitable organic solvent systems. When performing large scale reactions, a significant quantity of the product was lost through crystallisation on the column, resulting in low yields. Also, residual SeO_2 proved difficult to remove even by column chromatography, leaving all samples of 4,4'-diformyl-2,2'-bipyridine containing SeO_2 impurities. The contamination was not detectable by the spectroscopic techniques employed to characterise the compounds (see Section 2.5, p.31-35), however the distinctive odour of SeO_2 was strongly apparent in all samples. In the 1993 paper Sessler *et al.*[2]. made no mention of any problem relating to unwanted residual SeO_2. This could be due to the smaller proportion of SeO_2 required for their single methyl to formyl group oxidation, thus resulting in less residual reagent to remove from the desired product. In addition, 4-formyl-4'-methyl-2,2'-bipyridine appears to be more soluble in organic solvents than the dialdehyde, making it both easier to chromatograph and perhaps wash free from the water soluble SeO_2. The most successful synthesis of the dialdehyde

obtained by this method required a 3:1 ratio of SeO_2 to 4,4'-dimethyl-2,2'-bipyridine. This resulted in an optimum 27% yield of dialdehyde **4**, a cream coloured solid possessing a distinct smell of SeO_2 (see Section 2.5 compound **4**, Method C, p.34). Clearly this preliminary result leaves great scope for improvement in both yield and purity of product.

Since this work was done it was discovered that a number of research groups have tried to synthesise 4,4'-diformyl-2,2'-bipyridine using SeO_2 and have encountered similar problems.[8,22] As a result none of this work has been published. Despite such difficulties, this procedure has enormous potential as an efficient synthetic route to 4,4'-diformyl-2,2'-bipyridine due to its one-step nature. The preliminary results obtained above, provide the justification to attempt to optimise the reaction conditions in order to eliminate unwanted excess reagent and increase the product yield. Consequently, further investigation of the reaction conditions were made, with specific emphasis on the work-up procedure in an attempt to achieve these goals.

2.3.1 Revised SeO_2 oxidation procedure

In collaboration with Dr. Kirstie Wild (post-doctoral researcher) a new work-up procedure was developed in order to minimise residual SeO_2 in the desired end product. Due to the insolubility of the dialdehyde, and the solubility of the unwanted SeO_2 in water, an aqueous based work-up procedure was developed. This procedure was then optimised to eliminate the residual SeO_2 (see Section 2.5, compound **4**, Method D, p.34-35), and resulted in a reasonable yield of a white solid with no distinctive smell of SeO_2. Dialdehyde **4** was pure according to all characterisation techniques used including FAB HRMS. The development of this new work-up procedure has allowed the use of a larger excess of oxidising agent in order to ensure that the reaction reaches completion. Through a number of trials it was found that the greatest yield of pure dialdehyde **4** was achieved using a 5:1 ratio of the reagents SeO_2 and 4,4'-dimethyl-2,2'-bipyridine respectively (see Table 2).

Eq. of SeO_2	Eq. of bipyridine starting material	% yield of product: 4,4'-diformyl-2,2'-bipyridine
3	1	26.0 %
4	1	27.0 %
5	1	48.7 %
6	1	34.5 %

Table 2

Yields of 4,4'-diformyl-2,2'-bipyridine obtained from reactions using varying quantities of the two reagents.

This new aqueous procedure appears sufficient to deal with the residual oxidising agent left after the completion of the reaction, with no adverse effect on the yield of pure product

recovered. This approach proved to be very rewarding, resulting in a relatively straight-forward 49% yielding one-step synthesis of 4,4'-diformyl-2,2'-bipyridine, **4**. Due to the uncomplicated nature of the chemistry involved, and the inexpense of the reagent required, this optimised single step procedure could be considered almost equivalent in terms of efficiency to the 71% overall yielding two step synthesis developed by Le Bozec *et al.*.[9] For the purpose of this research project, the new 49% yielding SeO_2 procedure was considered a satisfactory preparation of 4,4'-diformyl-2,2'-bipyridine.

2.4 Compound characterisation

All samples were characterised by ^1H NMR spectroscopy with the exception of the highly insoluble dicarboxylic acid **1**. Compounds **2**, **3** and **4** gave typically simple spectra of the form seen below for 4,4'-diformyl-2,2'-bipyridine, **4**.

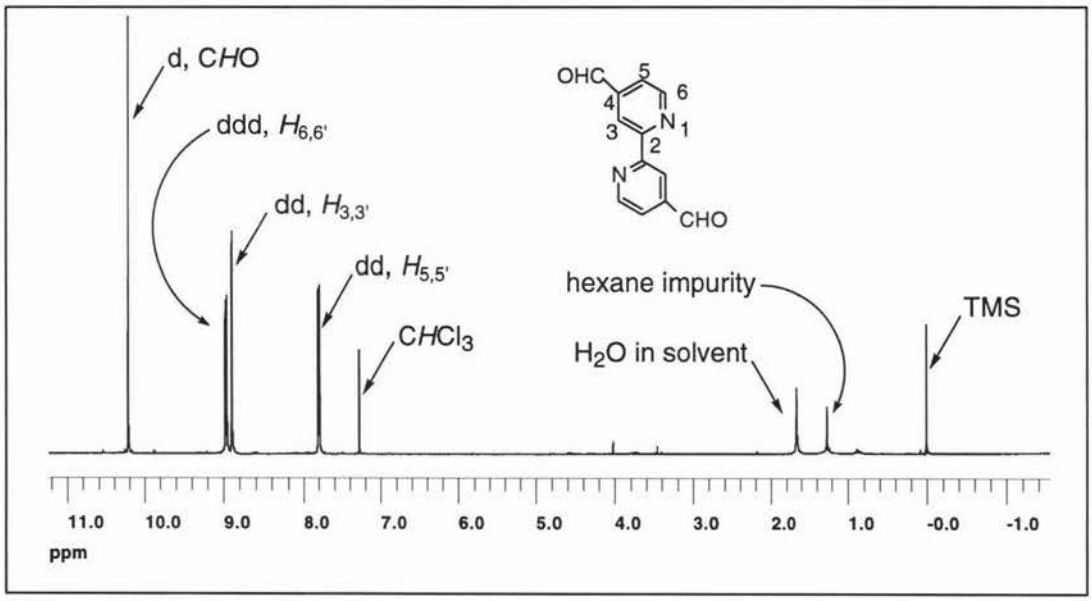

Figure 2.4-1
^1H NMR spectrum of 4,4'-diformyl-2,2'-bipyridine, **4**.

The spectrum of dialdehyde **4** has the distinctive peak at 10.21 ppm corresponding to the two equivalent aldehyde protons. A very weak five bond coupling to the the respective H_6 or $H_{6'}$ proton splits the peak into a doublet with a small coupling constant (J) of 0.4 Hz. The peak for the two equivalent $H_{6,6'}$ protons is shifted downfield from the other two ring protons to 8.96 ppm due to its position adjacent to the nitrogen of the bipyridine ring. It is split into a doublet of doublet of doublets (ddd) through a strong three bond coupling to the $H_{5,5'}$ protons (J = 4.8 Hz), and two five bond couplings to the $H_{3,3'}$ and the aldehyde group protons (J = 0.9 Hz and 0.4 Hz respectively). The doublet of doublets (dd) corresponding

to the two $H_{3,3'}$ protons is downfield shifted to 8.89 ppm due to its proximity to the nitrogen atom of the opposite ring and its three bond separation from the nitrogen atom of its own ring. It is split by a four bond coupling to the $H_{5,5'}$ protons (J = 1.3 Hz) and a smaller five bond coupling to the $H_{6,6'}$ protons (J = 0.9 Hz). The remaining dd at 7.80 ppm is further upfield from the other two as it is not shifted significantly by the nitrogen atoms. This peak corresponds to the two $H_{5,5'}$ protons and is split by both the adjacent $H_{6,6'}$ protons (J = 4.8 Hz) and the $H_{3,3'}$ protons (J = 1.5 Hz).

The ^{1}H NMR spectrum of dialcohol **3** is consistent with the pattern seen for dialdehyde **4**. Two additional peaks including a large singlet at 4.63 ppm corresponding to the four CH_2 protons, and a very broad peak at 5.47 ppm due to the two equivalent -O*H* protons are also present in the spectrum of dialcohol **3**. The spectrum for dimethyl-2,2'-bipyridine-4,4'-dicarboxylate, **2**, differs slightly. A large singlet at 4.01 ppm is present which is due to the six methyl group protons. While the dd corresponding to the two $H_{5,5'}$ protons is at a similar position (7.92 ppm), the peaks due to the $H_{6,6'}$ and $H_{3,3'}$ protons have exchanged positions compared to the spectra of compounds **3** and **4**. The dd due to the $H_{3,3'}$ protons is shifted further downfield than the $H_{6,6'}$ peak due to its proximity to the two oxygen atoms of the ester appendage. Thus ^{1}H NMR spectroscopy provides a reasonably well-defined characterisation for these compounds.

UV/Vis spectra were run on the two more soluble compounds, the diester, **2**, and the dialdehyde, **4** (shown in Figure 2.4-2). The spectra contain one weak broad band, positioned around 310 nm which corresponds to a ligand centred π- π^* transition (LC transition) of the bpy ligand.

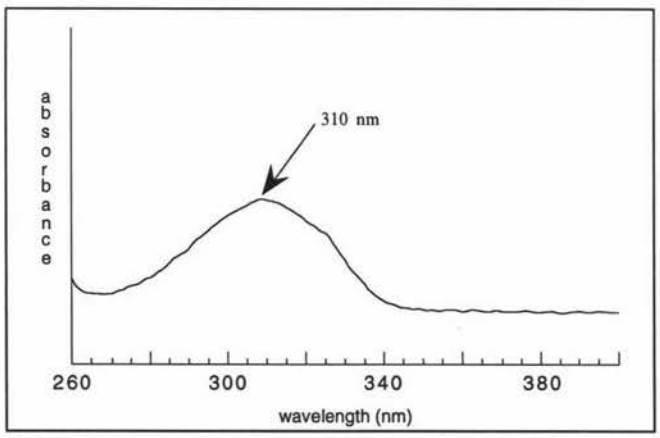

Figure 2.4-2
UV/Vis spectrum of 4,4'-diformyl-2,2'-bipyridine, **4**.

Infrared spectroscopy was used to confirm the presence of the carbonyl, methoxy, or hydroxyl groups. High resolution mass spectra were obtained, and in all cases supported the identity of the compound synthesised.

2.5 Summary

A four step procedure for the synthesis of 4,4'-diformyl-2,2'-bipyridine was first published by Beer *et al.* in 1990,[4] then optimised in 1992[5]. This optimised method claimed to produce the dialdehyde in an overall yield of 42%. Exhaustive efforts to duplicate this result were unsuccessful. An alternative one-step SeO_2 oxidation was developed and optimised to produce the desired dialdehyde precursor **4**, in 49% yield. This is an efficient procedure as it uses inexpensive reagents and straight-forward chemical techniques to give a reasonable yield of the dialdehyde in a single step. Synthesis of dialdehyde **4** *via* method D is the preferred option, and has provided the first reagent necessary for the proposed synthesis of the novel bipyridine-porphyrin conjugates. Therefore, the next task is to prepare the second Wittig reagent required, the porphyrin phosphonium salt.

2.6 Experimental procedures

2.6.1 General methods

When necessary, solvents and reagents were dried according to the methods of Perrin and Amarego.[23] Diazomethane was synthesised according to the method of Mann and Saunders.[12]

Proton nuclear magnetic resonance spectroscopy (^{1}H NMR) was performed using a JOEL JMN-GX270 FT-NMR Spectrometer. Except when stated otherwise, the data is expressed in parts per million (ppm) downfield from tetramethylsilane (TMS), and referenced to $CHCl_3$ ($\delta = 7.270$). In some cases crude spectra were run on a 60 MHz Hitachi R-1200 Permanent Magnet RS-NMR Spectrometer.

Electronic absorption spectra were obtained using a Shimadzu UV-3101PC UV-VIS-NIR scanning spectrophotometer. Band positions are expressed in wavelengths (nm) with the log molar absorptivity ($\log \varepsilon$).

Infrared spectra were run on a Perkin-Elmer PARAGON 1000 FT-IR spectrometer. Samples were run as Nujol mulls and the data reported in wavenumbers (cm^{-1}).

Mass spectra were recorded using a Varian VG70-250S double focusing magnetic sector mass spectrometer. Samples were analysed by fast atom bombardment in the positive mode (FAB^+), for low or high resolution mass spectra (LRMS or HRMS) and were supported in a

p-nitrobenzyl alcohol matrix. Major fragmentations when present are recorded as a percentage relative to the base peak intensity.

Column chromatography was carried out using silica gel (0.032-0.063 mm, Merck Kieselgel 60). The silica column's were packed under pressure (argon cylinder or compressed air) then topped with a layer of acid-washed sand in order to protect the surface of the silica. Flash column chromatography was done using the same media according to the method of Still *et al.*.[24] Thin layer chromatography was performed using precoated plastic-backed silica plates (Merck Kieselgel $60F_{254}$).

2.6.2 Experimental section

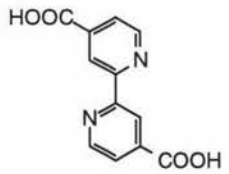

(1) 2,2'-Bipyridine-4,4'-dicarboxylic acid

4,4'-Dimethyl-2,2'-bipyridine (5 g, 0.027 mol) was oxidised using $KMnO_4$ under the conditions described by Launikonis *et al.*[10] Diacid **1** was formed as a fine white powder in 51% yield (literature yield[10] 45%).

R_f = baseline, 1:1 Toluene:EtOAc.

IR (Nujol): 1714 (s, C=O), 3440 (br. s, OH) cm^{-1}.

FAB HRMS [M^+] calcd. for $C_{12}H_8N_2O_4$ 244.0484, obs. 244.0485.

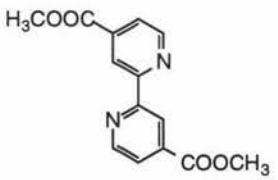

(2) Dimethyl-2,2'-bipyridine-4,4'-dicarboxylate

A 250 mL round bottomed flask was charged with a suspension of diacid **1** (2.27 g, 9.30 mmol) in Et_2O (85 mL). While vigorously stirring, an ethereal solution of CH_2N_2 (60 mL, 0.5 M) was added causing the solution to turn a brownish orange colour and the suspended solid appear cream coloured. After 24 h, analysis by tlc revealed that the reaction had not reached completion so a further quantity of CH_2N_2 (28 mL, 0.5 M) was added. After 2 h the solvent was removed and the resultant residue was dried under vacuum for 4 h to yield diester **2** (2.33 g, 92.1%).

R_f = 0.77, 1:1 Hexane:EtOAc.

^{1}H NMR (270 MHz, $CDCl_3$): δ 4.01 (s, 6H, CH_3), 7.92 (dd, ^3J = 4.8 Hz, ^4J = 1.6 Hz, 2H; $H_{5,5'}$), 8.88 (dd, ^3J = 4.9 Hz, ^5J = 0.8 Hz, 2H; $H_{6,6'}$), 8.97 (dd, ^4J = 1.6 Hz, ^5J = 0.8 Hz, 2H; $H_{3,3'}$).

UV/Vis (CH_2Cl_2): λ_{max} (log ε) = 300 (2.85) nm.

IR (Nujol): 1732 (s, C=O) cm^{-1}.

FAB HRMS [M^+] calcd. for $C_{14}H_{12}N_2O_4$ 272.0797, obs. 272.0804.

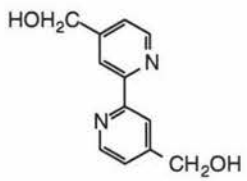

(3) 4,4'-Dihydroxylmethyl-2,2'-bipyridine

In a 25 mL round bottomed flask, a stirring solution of diester **2** (0.25 g, 0.92 mmol) in dry distilled THF (9 mL) was cooled to 0°C using an ice/salt bath. Once cooled $LiAlH_4$ (0.119 g, 3.14 mmol) was added slowly, causing a vigorous effervescence. After stirring for 10 mins the ice bath was removed and the reaction mixture was heated at reflux temperature for 25 mins. The flask was allowed to cool to RT before reducing the temperature back down to 0°C. While the mixture was vigorously stirred, the reaction was quenched with 2:1 THF / H_2O (4.5 mL). After 2 h the solvent was removed *in vacuo* and the resultant residue dried under vacuum overnight. The resultant flaky brown solid was taken up in methanol and stirred for 24 h before filtering through a pad of celite. The light yellow filtrate was reduced to dryness then further dried on the high vacuum pump until no further weight loss occurred to yield dialcohol **3** (0.178 g, 89.6%).

R_f = baseline, 1:1 Hexane:EtOAc.

^{1}H NMR (270 MHz, d_6-DMSO and referenced to DMSO at δ = 2.52 ppm): δ 4.63 (s, 4H; CH_2), 5.47 (br. s, 2H; O*H*), 7.37 (dd, ^3J = 4.8 Hz, ^4J = 1.8 Hz, 2H; $H_{5,5'}$), 8.38 (d, ^4J = 1.8 Hz, 2H; $H_{3,3'}$), 8.59 (d, ^3J = 4.8 Hz, 2H; $H_{6,6'}$).

FAB HRMS [M^+] calcd. for $C_{12}H_{12}N_2O_2$ 216.0899, obs. 216.0896.

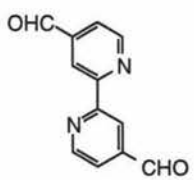

(4) 4,4'-Diformyl-2,2'-bipyridine

Method A: A 10 mL 2-neck round bottomed flask fitted with a drying tube and septum was charged with a solution of oxalyl chloride (116 μL, 1.33 mmol) in CH_2Cl_2 (1.5 mL). The stirring solution was cooled to -55°C with a liquid air/isopropyl alcohol cooling bath

before the addition of DMSO (181 μL, 2.55 mmol) in CH_2Cl_2 (0.30 mL). After two minutes a suspension of dialcohol **3** (0.115 g, 0.532 mmol) in 3:1 DMSO:CH_2Cl_2 (2 mL) was added dropwise. Then after 15 mins triethylamine (742 μL, 5.32 mmol) was added. After a further 5 mins the reaction mixture was allowed to warm to RT. No starting material remained by tlc so the reaction was quenched with H_2O (2.8 mL). Organic and aqueous layers were separated and the aqueous phase extracted with $CHCl_3$ (7 x 5 mL). The combined organic layers were washed with sat. NaCl, dried over $MgSO_4$ and filtered. The filtrate was re-washed with dil. HCl (1%), H_2O, dil. Na_2CO_3, and H_2O (x3), dried over $MgSO_4$ and filtered. The solvent was removed and the resultant residue dried under high vacuum until no further weight loss occurred. This yielded dialdehyde **4** as a cream coloured solid (0.033 g, 29%).

Method B: Dialcohol **3** (0.051 g, 0.24 mmol) was introduced into a 50 mL 2-neck round bottomed flask fitted with an argon source. Dry distilled THF (4 mL) was added forming a suspension. While vigorously stirring, D.M.P. (0.239 g, 0.564 mmol, 2.4 equivalents) was added. After 30 mins the argon source was removed and the reaction was quenched with a solution of sodium thiosulphate (1 g) in 1:4 sat. aq. $NaHCO_3$ / CH_2Cl_2 (25 mL). Using a small amount of H_2O, the mixture was transferred to a sep. funnel and the organic and aqueous phases separated. The aqueous phase was re-extracted with CH_2Cl_2 (4 x 4 mL). The combined organic phases were washed with sat. aq. $NaHCO_3$, H_2O, and sat. NaCl, dried over $MgSO_4$, filtered and reduced to dryness *in vacuo*. The resultant residue was purified by flash column chromatography with 9:1 CH_3CN:$CHCl_3$. The appropriate fractions from tlc analysis were combined, filtered and dried *in vacuo,* then under high vacuum until no further weight loss occurred. This yielded pure 4,4'-diformyl-2,2'-bipyridine **4** (0.006 g, 12%).

Method C: A 50 mL round-bottomed flask was charged with 4,4'-dimethyl-2,2'-bipyridine (1.00 g, 5.43 mmol), SeO_2 (1.81 g, 0.0163 mol) and diglyme (22 mL). The flask was flushed with argon and heated at reflux temperature for 24 h. The hot mixture was filtered through pre-warmed celite, cooled, then filtered again through celite. The filtrate was reduced to dryness *in vacuo* then the resultant residue was extracted with acetone. After filtering this suspension, the acetone was removed. The residue was then extracted with CH_2Cl_2 and filtered through celite. After removing the solvent, the resultant residue was purified by column chromatography using 9:1 CH_3CN:$CHCl_3$ as the elution solvent. Fractions were analysed by tlc, developed first under UV light and then with an aqueous Fe^{3+} dip. The appropriate fractions were combined, solvent removed on a rotary evaporator and dried under high vacuum to yield the product **4** as a cream coloured solid (308 mg, 26.7%).

Method D: A 500 mL round-bottomed flask was charged with 4,4'-dimethyl-2,2'-bipyridine (3.00 g, 0.016 mol), SeO_2 (9.04 g, 0.082 mol) and diglyme (300 mL). The flask was flushed with argon and heated at reflux temperature for 24 h. The hot mixture was

filtered into hot water (2.5 L). The aqueous solution was then filtered through pre-warmed celite, cooled, and extracted with $CHCl_3$ (6 x 200 mL). The organic phases were combined and reduced on a rotary evaporator. The remaining diglyme was removed under vacuum distillation. The resultant off-white solid was stirred for 24 h in water (800 mL). The suspension was filtered and the undissolved solid was extracted with $CHCl_3$. After removal of the $CHCl_3$ *in vacuo*, the residue was again washed by stirring for 24 h with water (800 mL). The solid was collected and dried under high vacuum to yield dialdehyde **4** as a white powder (1.68 g, 48.7%).

R_f = 0.85, 9:1 CH_3CN:$CHCl_3$.

^1H NMR (270 MHz, $CDCl_3$): δ 7.80 (dd, ^3J = 4.8 Hz, ^4J = 1.5 Hz, 2H; $H_{5,5'}$), 8.89 (dd, ^4J = 1.3 Hz, ^5J = 0.9 Hz, 2H; $H_{3,3'}$), 8.96 (ddd, ^3J = 4.8 Hz, ^5J = 0.9 Hz, ^5J = 0.4 Hz, 2H; $H_{6,6'}$), 10.21 (d, ^5J = 0.4 Hz, 2H, C*H*O).

UV/Vis (CH_2Cl_2): λ_{max} (log ε) = 310 (4.04) nm.

IR (Nujol): 1703 (s, CHO) cm^{-1}.

FAB HRMS [M^+] calcd. for $C_{12}H_8N_2O_2$ 212.0586, obs. 212.0585. LRMS *m/z* = 154 (M^+ - $(CHO)_2$, 21%), 106 (M^+ - C_5H_3N-CHO, 5%).

2.7 References

(1) Della Ciana, L.; Hamachi, I.; Meyer, T. J. *J. Org. Chem.* **1989**, *54*, 1731-1735.

(2) Sessler, J. L.; Capuano, V. L.; Burrell, A. K. *Inorg. Chim. Acta* **1993**, *204*, 93-101.

(3) Harding, M. H.; Koert, U.; Lehn, J.-M.; Rigault, A. M.; Piguet, C.; Siegel, J. *Helv. Chim. Acta* **1991**, *74*, 594-610.

(4) Kocian, O.; Mortimer, R. J.; Beer, P. D. *Tetrahedron Lett.* **1990**, *31*, 5069-5072.

(5) Beer, P. D.; Kocian, O.; Mortimer, R. J.; Spencer, P. *J. Chem. Soc., Chem. Commun.* **1992**, 602-604.

(6) McCafferty, D. G.; Bishop, B. M.; Wall, C. G.; Huges, S. G.; Mecklenberg, S. L.; Meyer, T. J.; Erickson, B. W. *Tetrahedron* **1995**, *54*, 1093-1106.

(7) Lindsey, J. S.; Schreiman, I. C.; Hsu, H. C.; Kearney, P. C.; Marguerettaz, A. M. *J. Org. Chem.* **1987**, *52*, 827-836.

(8) Communication with a member of Dr. Paul Beer's research team.

(9) Dupau, P.; Renouard, T.; Le Bozec, H. *Tetrahedron Lett.* **1996**, *37*, 7503-7506.

(10) Launikonis, A.; Lay, P.; Mau, A.; Sargeson, A.; Sasse, W. *Aust. J. Chem.* **1986**, *39*, 1053-1062.

(11) Cooper, G. H.; Rickard, R. L. *Synthesis* **1971**, *1*, 31.

(12) Mann, F. G.; Saunders, B. C. *Practical Organic Chemistry*; 4th ed.; Longman Group Limited: London, **1960**, 430-433.

(13) Kingston, J. F.; Weiler, L. *Can. J. Chem.* **1977**, *55*, 785-791.

(14) Morrison, R. T.; Boyd, R. N. *Organic Chemistry*; 5th ed.; Allyn & Bacon Inc.: Massachusetts, **1987**, 778-779, 832, 844.

(15) Kocienski, P.; Raubo, P.; Davis, J. K.; Boyle, F. T.; Davies, D. E.; Richter, A. *J. Chem. Soc. Perkin Trans. 1* **1996**, 1797-1808.

(16) Mancuso, A.; Huang, S.; Swern, D. *J. Org. Chem.* **1978**, *43*, 2480-2482.

(17) Omura, K.; Swern, D. *Tetrahedron* **1978**, *34*, 1651-1660.

(18) March, J. *Advanced Organic Chemistry: Reactions, Mechanisms and Structure*; 4th ed.; John Wiley & Sons, Inc.: New York, **1992**, 1168.

(19) Dess, D. B.; Martin, J. C. *J. Org. Chem.* **1983**, *48*, 4155-4156.

(20) Dess, D. B.; Martin, J. C. *J. Am. Chem. Soc.* **1991**, *113*, 7277-7287.

(21) Ireland, R. E.; Liu, L. *J. Org. Chem.* **1993**, *58*, 2899.

(22) Communication with a member of Dr. Keith Gordon's research team.

(23) Perrin, D. D.; Armarego, W. L. F. *Purification of Laboratory Chemicals*; Pergamon Press:, **1988**,.

(24) Still, W. C.; Kahn, M.; Mitra, A. *J. Org. Chem.* **1978**, *43*, 2923-2925.

Chapter Three

Synthesis of the porphyrin phosphonium salt

The functionalisation of porphyrin compounds has challenged organic chemists due to difficulties with reactivity, solubility and stability. Subsequently, before endeavouring to perform such a functionalisation using a phosphonium salt appendage, familiarisation with the general properties of porphyrin compounds was necessary. Porphyrins differ from other aromatic compounds in that they possess two sites (with different reactivities), where electrophilic substitution reactions can take place, the four *meso*-positions or the eight β-pyrrolic positions. A recent article describing a study of the mechanism of electron transfer reactions for porphyrin-quinone systems,[1] reported that the electronic ground state of the porphyrin is greatly influenced by the position of a substituent. It was discovered that connection through a β-pyrrolic carbon atom provides for easier photochemical oxidations. Thus for the purpose of this research, connection of the phosphonium salt appendage to a β-pyrrolic carbon of the porphyrin macrocycle is favourable. To achieve this structure, porphyrin macrocycles possessing *meso*-substituents were employed so that subsequent reactions to form the phosphonium salt would be centred at the desired β-pyrrolic position. Macrocycles such as 5,10,15,20-tetraphenylporphyrin (TPP), shown in Figure 3.0-1, were used.

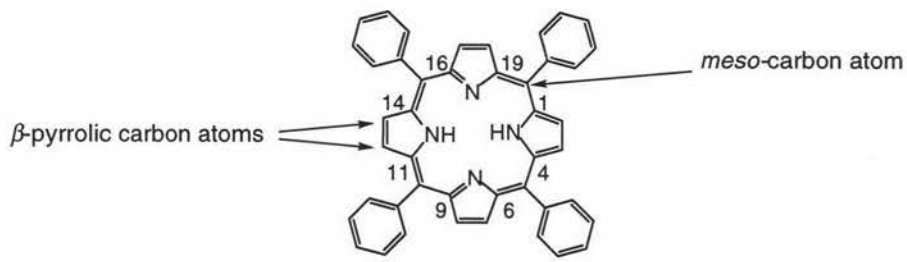

Figure 3.0-1
5,10,15,20-Tetraphenylporphyrin (TPP) showing β-pyrrolic and *meso* carbon atoms. The four *meso*-phenyl substituents are drawn flat for clarity but are in fact orthogonal to the plane of the porphyrin ring.

Pyrrole and benzaldehyde undergo a condensation reaction to form the tetra *meso*-substituted porphyrin TPP.[2,3] Eighteen of the twenty-two π-electrons of the porphyrin ring system (discounting *meso*-substituents) are delocalised about the ring resulting in a stabilised cyclic structure possessing a strong anisotropic ring current.[4,5] The distinctive anisotropic properties of porphyrins produce characteristic patterns with both ^{1}H NMR and UV/Vis spectroscopy allowing, relatively straight-forward identification of compounds. The general pattern observed for the ^{1}H NMR spectra of free-base porphyrin compounds is illustrated below with the ^{1}H NMR spectrum of TPP (Figure 3.0-2). This spectrum contains a

distinctive broad singlet at -2.75 ppm due to the two nitrogen-bound hydrogen atoms in the centre of the ring (N*H* protons). The peak is shifted to this upfield position due to a strong shielding effect from the anisotropic ring current of the porphyrin. The remaining β-pyrrolic and phenyl protons of the porphyrin macrocycle are positioned around the periphery of the ring, thus are deshielded by the anisotropic ring current. Consequently, the peaks due to these sets of protons are shifted downfield from their unsubstituted positions (where they are seen for pyrrole and benzene).

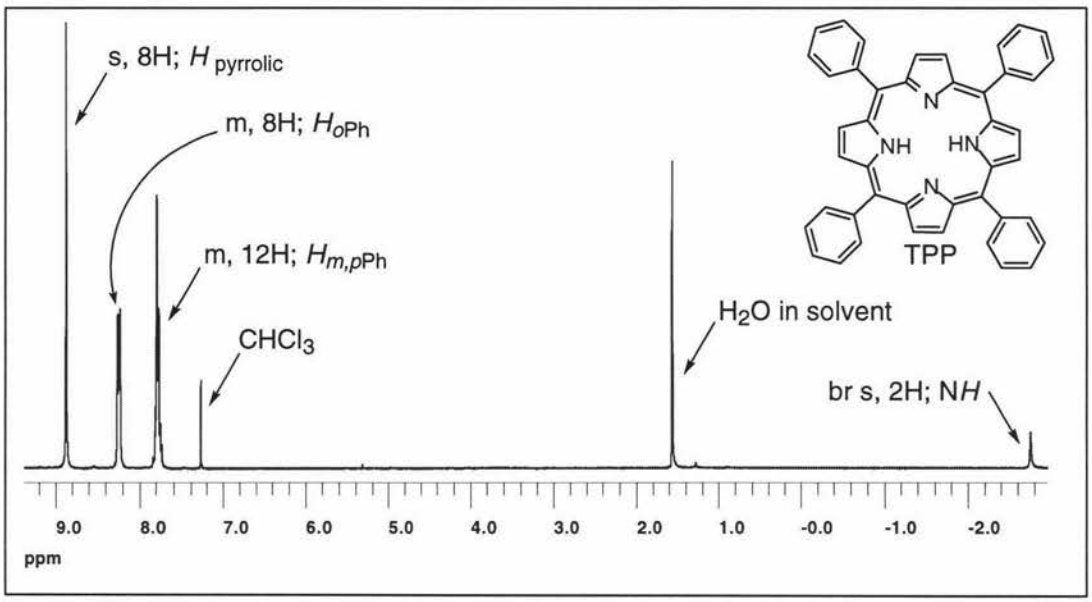

Figure 3.0-2
^{1}H NMR spectrum of TPP, referenced to $CHCl_3$.

Upon metallation, the two N*H* protons are replaced with the metal ion, thus the ^{1}H NMR spectrum will no longer contain the peak upfield of zero ppm.

A typical absorption spectrum of a porphyrin compound consists of two sets of peaks. One in the near-ultraviolet region, and the other in the visible region (see Figure 3.0-3 below). Both free base and metallated porphyrins produce spectra that contain one dominant peak termed the B band (or Soret band), which is found in the near-UV region of the spectrum typically between 390-425 nm. These peaks often show molar extinction coefficients (ε) of 200,000-400,000 $dm^3mol^{-1}cm^{-1}$ (see Experimental procedures, p.43-49).

Where: $$\varepsilon = \frac{\text{concentration of solution (c)} \times \text{path length of instrument (l)}}{\text{absorbance (A)}}$$

It is this strong transition in the near-UV region of the spectrum which is responsible for the characteristic purple colour of porphyrin compounds. In the visible region of the absorption

spectra of free base porphyrins, usually between 480-700 nm, are found four much weaker Q bands (see Figure 3.0-3, solid line). Metallation of the porphyrin ring often results in a more symmetrical macrocycle, and consequently the number of Q bands usually decreases from four to two (see Figure 3.0-3, dashed line).

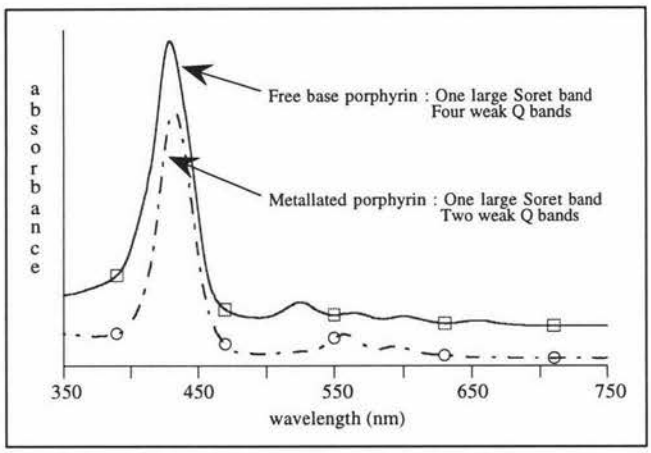

Figure 3.0-3
Typical UV/Vis spectrum of both a free base porphyrin and a metallated porphyrin.

The positions, relative intensities, and number of bands in the absorption spectrum, can be indicative of the substitution pattern of the porphyrin, whether or not it is metallated, and if so, the relative stability of the metal complex.[6,7]

3.1 TPP phosphonium salt

Previous research carried out in these laboratories has developed a methodology towards the synthesis of a phosphonium salt of *meso*-tetraphenylporphyrin.[8] This novel compound has a methyl phosphonium chloride appendage which is connected through a β-pyrrolic position of the ring as is shown below in Figure 3.1-1.

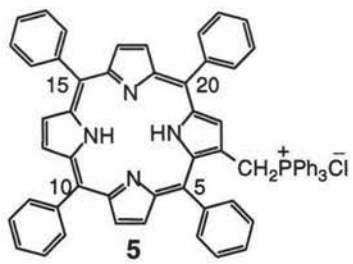

5

Figure 3.1-1
2-(*meso*-Tetraphenylporphyrin)yl)methyltriphenylphosphonium chloride (TPP-CH_2PPh_3Cl).

The synthetic methodology developed by Bonfantini and Officer produces TPP-CH_2PPh_3Cl, **5**, in a six step synthesis from the two commercially available precursors pyrrole and benzaldehyde.[8] In these laboratories, phosphonium salt **5** has successfully been used in Wittig reactions with a range of different carbonyl compounds.[8-10] One such molecule synthesised by Burrell *et al.*[9] is the benzaldehyde-appended TPP shown below in Figure 3.1-2, compound **A**. Insertion of a copper ion into the centre of the porphyrin ring allowed crystals of sufficient size and quality for X-ray diffraction, to be obtained (structures **B** and **C**, Figure 3.1-2). The X-ray crystallographic characterisation revealed the coplanarity of the olefin group and the benzaldehyde. It also showed that the torsion angle between the olefin and the porphyrin ring is small (~17°). Therefore, excluding the orthogonal *meso*-phenyl groups this complex is essentially planar.

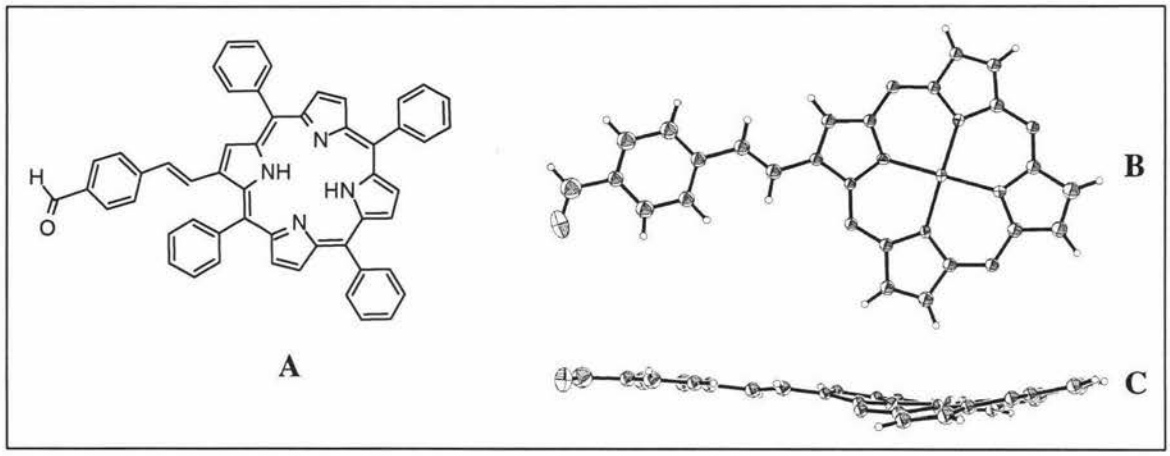

Figure 3.1-2
A)Burrell *et al.*'s 2-vinyl-substituted tetraphenylporphyrin compound.
B) Crystal structure of A, top view - *meso*-phenyl substituents omitted for clarity.
C) Crystal structure of A, side view.

This planarity combined with interesting spectroscopic results indicate the possibility of conjugation between the porphyrin and the aldehyde moieties. This could have an enormous impact on the rate of electron transfer in larger compounds of this kind. Burrell *et al.* carried out a second Wittig reaction on compound **A** with phosphonium salt **5**, in order to connect a second porphyrin ring to the benzaldehyde.[9] This reaction was also successful however it produced a dimeric porphyrin compound with very low solubility due to the occurrence of π-π interactions between molecules.

This lack in solubility of the dimeric compound synthesised by Burrell *et al.*, was a cause for concern. The compounds to be synthesised for this thesis are similar to the aforementioned porphyrin dimer, except would contain a central bipyridyl moiety between the two porphyrin rings in place of the phenyl group. It was strongly suspected that the solubility problems seen by Burrell *et al.* would be accentuated in the bipyridine work due to the introduction of

the larger, highly conjugated bipyridyl-bridging ligand. Consequently, the synthesis of a more soluble porphyrin phosphonium salt was investigated.

3.2 TXP phosphonium salt

Small variations in the structure of substituted porphyrins have large effects on the solubility of the resultant compound. For both the research carried out for this thesis as well as other projects underway in these laboratories, a methodology for the synthesis of a more soluble porphyrin phosphonium salt based on *meso*-tetraxylylporphyrin, **8** was developed (see Figure 3.2-1, p.42). The new phosphonium salt, **13**, is identical to TPP-CH_2PPh_3Cl discussed in section 3.1 above, except that the four *meso*-phenyl substituents are replaced by four *meso*-3,5-dimethylphenyl (xylyl) appendages. The two methyl groups projecting from the orthogonal phenyl rings extend the structure further from the plane of the porphyrin ring than the unsubstituted phenyl rings of TPP. Subsequently, π-π interactions between phosphonium salt molecules are inhibited resulting in a more soluble porphyrin. The methodology for the synthesis of this more soluble compound was derived from the preparation for TPP-CH_2PPh_3Cl developed by Bonfantini and Officer.[8] The new phosphonium salt synthesis was optimised in collaboration with David Reid resulting in an eight step synthesis from the starting materials, mesitylene and pyrrole (see Figure 3.2-1, p.42).

3,5-Dimethylbenzyl bromide, **6**, was prepared *via* an NBS bromination of mesitylene according to a modified procedure of that published by Newman and Lee.[11] Excess mesitylene (with respect to NBS) was used in the bromination step (**i**) in order to eliminate the production of unwanted dibromide by-products. The unreacted mesitylene is able to be recovered and recycled. A 60 MHz ^{1}H NMR spectrum of the crude bromide was obtained which revealed the presence of residual solvent and *N*-hydroxysuccinimide contaminants. Neither impurity affects the following step thus the crude bromide, **6**, was oxidised in step **ii** using a Sommelet oxidation.[11] A small portion of the crude product was purified by column chromatography, and a 60 MHz ^{1}H NMR spectrum was recorded of this yellow oil. The spectrum revealed the presence of both aldehyde **7** and residual unreacted mesitylene in a ratio of 2.9:1, hence calculation of the yield of 3,5-dimethylbenzaldehyde **7** (70 g, 63% over two steps) was possible. The residual mesitylene is easily removed during the filtration of the next step and has no negative effect on reaction **iii**.

Condensation of aldehyde **7** with pyrrole based on reported procedures[3,6] produced TXP, **8**, as a relatively insoluble purple solid in 19% yield. The ^{1}H NMR spectrum of **8** was very similar to that of TPP (see Figure 3.0-2, p.38). The broad singlet due to the highly shielded

central hydrogen atoms was shifted slightly further upfield and the β-pyrrolic and phenyl proton peaks were slightly broader than those for TPP. A new peak at 2.63 ppm corresponds to the methyl protons of the four xylyl groups. UV/Vis spectroscopy revealed a spectrum typical of a free base porphyrin with a strong Soret band at 416 nm with ε= 427,000 $dm^3mol^{-1}cm^{-1}$ (log ε = 5.63), and four Q bands in the visible region.

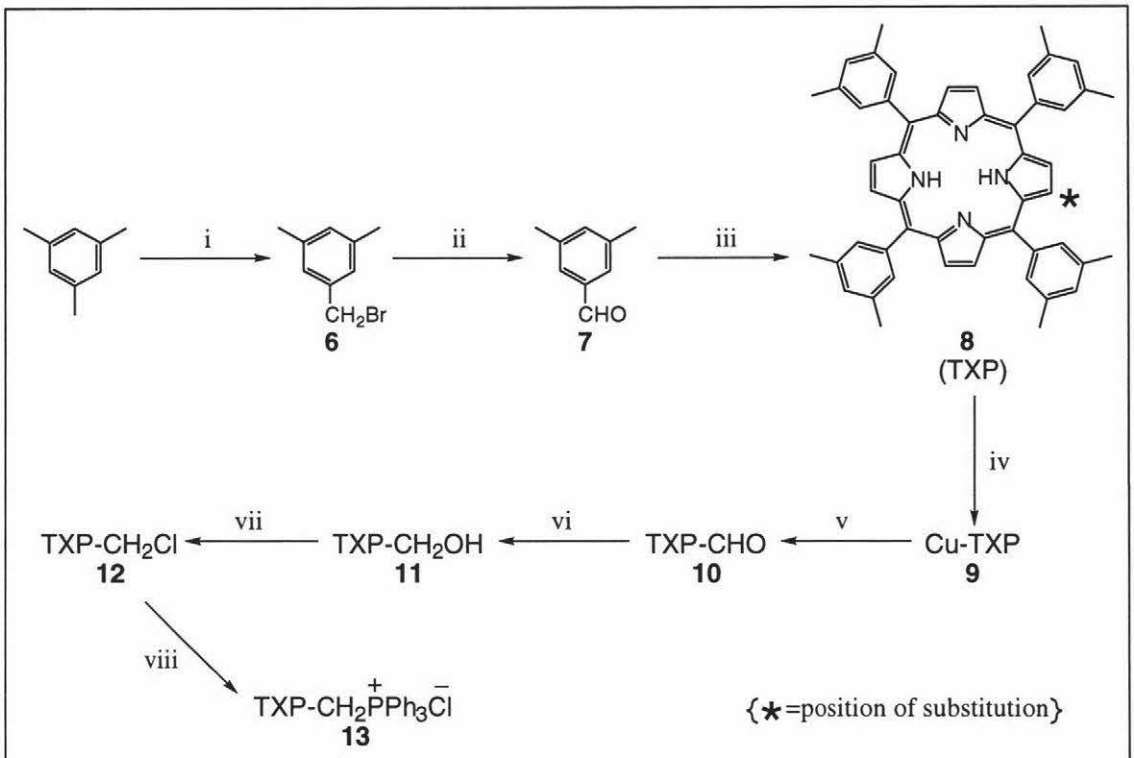

Conditions and reagents: **i**) NBS, CH_2Cl_2, *hv*, reflux, 3 h; **ii**) HMTA, EtOH/H_2O, reflux, 4 h; c.HCl, reflux, 30 mins; **iii**) 4eq. **7**, 4eq. pyrrole, propanoic acid, reflux, 40 mins; **iv**) $Cu(OAc)_2.H_2O$ / MeOH / H_2O, $CHCl_3$, reflux, 10 mins; **v**) DMF, $POCl_3$, $ClCH_2CH_2Cl$, reflux, 7 h; c.H_2SO_4, RT, 10 mins; **vi**) $NaBH_4$, THF, RT, 30 mins; **vii**) pyridine, $SOCl_2$, 0°C, 15 mins, RT, 30 mins; **viii**) PPh_3, $CHCl_3$, reflux, 2 d.

Figure 3.2-1
Schematic diagram of the synthetic route to the new porphyrin phosphonium salt, TXP-CH_2PPh_3Cl, **13**.

Metallation of porphyrin **8** with copper(II) by way of the acetate method,[6] followed by recrystallisation produced Cu-TXP **9** as a relatively insoluble maroon solid in 94% yield. ^1H NMR analysis was of little use as all peaks were severely broadened due to the presence of the copper ion. UV/Vis spectroscopy also supported the metal coordination as the four Q bands observed for free base porphyrin, **8**, were reduced to two Q-bands. Aldehyde **10** was synthesised by refluxing Cu-TXP in dichloroethane with a Vilsmeier complex (made from DMF and $POCl_3$)[12]. The copper(II) ion was then removed by treatment of the reaction mixture with conc. H_2SO_4. Following a large scale aqueous work-up, and flash column chromatography, the aldehyde was isolated in 87% yield. A distinctive peak at 9.39 ppm in the ^1H NMR spectrum of **10** corresponds to the aldehyde appendage, and a broad singlet at

-2.56 ppm due to the two N*H* protons indicates the return to a free base porphyrin. The absorption spectrum of **10** contains four Q bands, which also confirms the removal of the Cu(II) ion. Further purification of this crude product is achieved by careful chromatography followed by slow recrystallisation from $CHCl_3$ with MeOH, however this is time consuming and causes the loss of a significant quantity of product. The crude material **10** is therefore carried through to the next step. Alcohol **11** is synthesised by a sodium borohydride reduction of the aldehyde. An aqueous work-up isolated TXP-CH_2OH, **11**, in 85% yield. Characterisation by UV/Vis spectroscopy is typical of a free base porphyrin and the ^1H NMR spectrum exhibits a triplet at 2.04 ppm and a doublet at 4.97 ppm corresponding to the hydroxymethyl protons respectively. Chlorination of **11** was achieved by reaction of the alcohol with pyridine and thionyl chloride. Isolation of chloride **12** gave an insoluble purple solid which proved to be unstable on silica therefore was not further purified. Phosphonium salt **13** was prepared by refluxing the crude chloride with excess triphenylphosphine in chloroform for two days. Isolation by column chromatography through silica gel (using a slow gradient elution with 1:100 to 15:100 MeOH:CH_2Cl_2), gave TXP-CH_2PPh_3Cl, **13**, in 62% yield over four steps (from the Cu-TXP) as a bright purple powder. Phosphonium salt **13** was characterised according to ^1H NMR, UV/Vis, and mass spectral results (see Section 3.3, compound **13**, p.49). As expected phosphonium salt **13** showed an increased solubility in organic solvents compared to the analogous TPP phosphonium salt.

The next stage of this research involved the reaction of the phosphonium salts with dialdehyde **4** under Wittig conditions. The objective of this work was to synthesise novel bipyridine-porphyrin conjugates as described in section 1.3 (p.16-17), and then to investigate their metal-binding propensity.

3.3 Experimental procedures

For general procedures see Chapter Two, Section 2.6.1, p 31-32.
When necessary, reactions involving light sensitive porphyrin compounds were carried out under aluminium foil and stored in the dark in order to protect them from both reacting with light and decomposition.

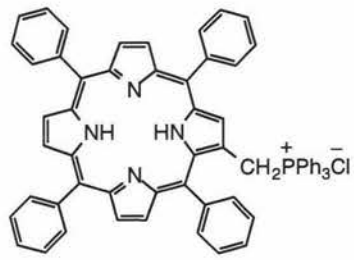

(5) TPP-CH_2PPh_3Cl

Synthesised according to the procedure developed by Bonfantini and Officer.[8]

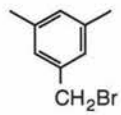

(6) 3,5-Dimethylbenzyl bromide

A 2 L round bottomed flask was fitted with a condenser and a drying tube and then charged with a suspension of mesitylene (500 mL, 3.59 mol) and NBS (148 g, 0.832 mol) in dry distilled CH_2Cl_2 (500 mL). While vigorously stirring, the reaction mixture was irradiated and heated at reflux temperature for 3 h using a UV lamp. Tlc analysis showed the production of the bromide as a more polar, slower running spot than the mesitylene starting material. The reaction mixture was allowed to cool to room temperature and then to 0°C in an ice/water bath. Filtration removed the crystallised *N*-hydroxysuccinimide contaminant. Removal of the solvent *in vacuo* revealed compound **6** as a crude yellow oil which was carried through to the oxidation step.

$R_f = 0.60$, Hexane ($R_{f\,[mesitylene]} = 0.89$, Hexane).

^1H NMR (60 MHz, $CDCl_3$): δ 2.30 (s, 6H; CH_3), 4.43 (s, 2H; CH_2), 7.01 (s, 2H; $H_{o\text{Ph}}$), 7.15 (s, 1H; $H_{p\text{Ph}}$).

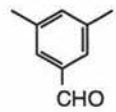

(7) 3,5-Dimethylbenzaldehyde

Crude 3,5-dimethylbenzyl bromide **6**, (assumed a maximum yield of 0.83 mol) was placed in a 2 L round bottomed flask with hexamethylenetetramine (HMTA) (280 g, 2.00 mol), ethanol (250 mL), and water (250 mL). The reaction was heated at reflux temperature for 4 h. Concentrated hydrochloric acid (130 mL) was added slowly and the reaction was refluxed for a further 30 mins. After allowing to cool to RT the reaction mixture was extracted with diethyl ether (4 x 200 mL). The organic phases were combined and washed with H_2O (2 x 400 mL) and sat. aq. $NaHCO_3$ (400 mL). The solvent was removed *in vacuo* and the resulting yellow liquid was stirred with sat. aq. $Na_2S_2O_5$ (200 mL) to give a

gelatinous white solid. Slow filtration followed by ether and *n*-hexane rinses removed unreacted starting material from the isolated white solid. The filtrate was reduced to dryness and the resultant mesitylene recycled. The solid bisulphite complex was transferred to a large beaker and decomposed with sat. aq. $NaHCO_3$ (500 mL) and ether (500 mL). The organic layer was separated, washed with H_2O (2 x 200 mL) then sat. aq. $NaHCO_3$ (200 mL), dried over $MgSO_4$ and filtered. The solvent was removed *in vacuo* to give a yellow oil (92 g). A 60MHz NMR spectrum was obtained of a sample of the oil purified by column chromatography, which revealed the presence of the benzaldehyde product **7** and residual unreacted mesitylene in a ratio of 2.9:1 respectively. This allowed the calculation of the yield of 3,5-dimethylbenzaldehyde **7** (70 g, 63% over two steps).

$R_f = 0.63$, 1:9 Ethyl acetate:Hexane.

^1H NMR (60 MHz, $CDCl_3$): δ 2.40 (s, 6H; C*H*$_3$), 7.32 (s, 1H; *H*$_4$), 7.53 (s, 2H; *H*$_{2,6}$), 10.01 (s, 1H; C*H*O).

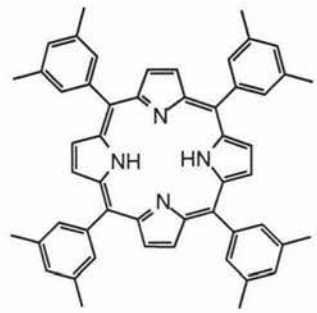

(8) meso-Tetraxylylporphyrin, (TXP)

A 5 L round bottomed flask was charged with propionic acid (2.3 L) which was then heated to reflux temperature. While the acid was refluxing, pyrrole (42.5 mL, 0.613 mol) followed by dimethylbenzaldehyde **7** (82.4 g, 0.614 g) were added quickly through the condenser. After 40 mins, the reaction mixture was allowed to cool to RT, and the resultant bright purple crystalline solid was collected by filtration. The solid was rinsed with methanol until the filtrate became clear, then rinsed with water and again with methanol. Drying under high vacuum for 30 mins yielded pure TXP, **8**, (21.1 g, 19%).

$R_f = 0.81$, 1:1 CH_2Cl_2:Hexane (greenish/brown spot).

^1H NMR (270 MHz, $CDCl_3$): δ -2.76 (br s, 2H; N*H*), 2.63 (s, 24H; C*H*$_3$), 7.44 (s, 4H, *H*$_{p\text{Xy}}$), 7.87 (s, 8H; *H*$_{o\text{Xy}}$), 8.91 (s, 8H; *H*$_{\text{pyrrolic}}$).

UV/Vis (CH_2Cl_2): λ_{max} (log ε) = 416 (5.63), 449 (4.22), 484 (3.70), 516 (4.38), 551 (4.07) nm.

FAB HRMS [MH^+] calcd. for $C_{52}H_{47}N_4$ 727.3801, obs. 727.3833.

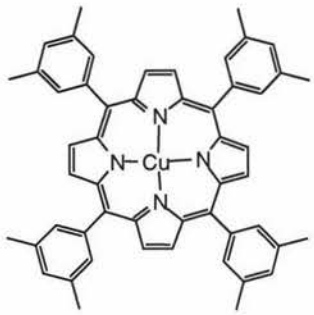

(9) meso-Tetraxylylporphyrinato copper(II), (Cu-TXP)

TXP, **8**, (10.0 g, 13.8 mmol) was dissolved in $CHCl_3$ (1 L) in a 3 L round bottomed flask. To the stirring solution was added a slurry of $Cu(OAc)_2.H_2O$ (12.2 g, 61.1 mmol) in $MeOH/H_2O$ (30 mL:4 mL). The reaction mixture was heated at reflux temperature for 10 mins. The hot solution was poured through a pre-warmed silica column and eluted with $CHCl_3$ until the eluent faded to a pale red colour. The $CHCl_3$ was reduced *in vacuo* to a volume of approximately 300 mL. Methanol (300 mL) was added and the solution was placed in a dark cupboard to slowly recrystallise. The recrystallised solid was collected by filtration, rinsed with methanol and dried under high vacuum to yield Cu-TXP, **9**, (10.2 g, 94%) as a maroon crystalline solid.

$R_f = 0.94$, 1:1 CH_2Cl_2:Hexane (rust coloured spot).

^1H NMR (270 MHz, $CDCl_3$): δ ~2.5 (24H; CH_3), ~7.3 (12H; $H_{o,p\mathrm{Xy}}$), peaks due to pyrrolic protons not evident in spectrum. All peaks severely broadened by the Cu ion.

UV/Vis (CH_2Cl_2): λ_{max} (log ε) = 416 (5.73), 539 (4.40), 573 (3.60) nm.

FAB HRMS [M^+] calcd. for $C_{52}H_{44}N_4{}^{63}Cu$ 787.2862, obs. 787.2835.

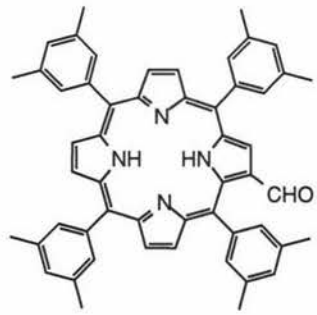

(10) 2-Formyl-meso-tetraxylylporphyrin, (TXP-CHO)

A 250 mL round bottomed flask was charged with a solution of Cu-TXP **9** (2.40 g, 3.04 mmol) dissolved in dry distilled $ClCH_2CH_2Cl$ (196 mL). The solution was stirred under Ar and cooled in an ice/water bath for 15 mins. At the same time, a 500 mL round bottomed flask was charged with dry DMF (23 mL, 0.297 mol), flushed with Ar and cooled in an ice/water bath. $POCl_3$ (19 mL, 0.204 mol) was added to the DMF to form a thick golden Vilsmeier complex. The Cu-TXP solution was added to the Vilsmeier complex and the Ar source was replaced with a condenser and drying tube. The flask was allowed to

warm to RT then was heated at reflux temperature for 7 h. The reaction mixture was left to cool overnight. With vigorous stirring, concentrated H_2SO_4 (39 mL) was added slowly through the condenser. The acidified solution was stirred for a further 10 mins. The reaction mixture (now green) was poured into a 5 L separating funnel containing ice cold aq. NaOH (72 g in 2.5 L H_2O). $CHCl_3$ (1.4 L) was added and the mixture was shaken until no sign of the green colour remained in the brown two-phase mixture. The organic layer was separated, washed twice with sat. aq. $NaHCO_3$ (2 x 1 L), dried over $MgSO_4$ and filtered. The solvent was reduced to ~100 mL *in vacuo* which was then crudely purified by flash chromatography with CH_2Cl_2 in order to remove any highly polar impurities. The solvent was removed to give crude TXP-CHO, **10**, (2.0 g, 87%) as a brown solid. Smaller quantities of the crude solid can be further purified by careful chromatography followed by recrystallisation from $CHCl_3$/MeOH to give pure TXP-CHO, **10**, in 61% yield.

R_f = 0.60, 3:2 CH_2Cl_2:Hexane (green spot).

^{1}H NMR (270 MHz, $CDCl_3$): δ -2.56 (br s, 2H; N*H*), 2.59-2.60 (m, 24H; C*H*$_3$), 7.40 (s, 3H;H_pXy), 7.44 (s, 1H, H_pXy), 7.78 (s, 2H, H_oXy), 7.82 (br s, 4H; H_oXy), 7.78 (s, 2H; H_oXy), 8.80-8.97 (m, 6H, $H_{pyrrolic}$), 9.24 (s, 1H; $H_{\beta\text{-pyrrolic}}$), 9.39 (s, 1H; C*H*O).

UV/Vis (CH_2Cl_2): λ_{max} (log ε) = 433 (5.52), 526 (4.26), 567 (3.87), 606 (3.75), 664 (3.91) nm.

FAB HRMS [M^+] calcd. for $C_{53}H_{47}N_4O$ 755.3750, obs. 755.3746.

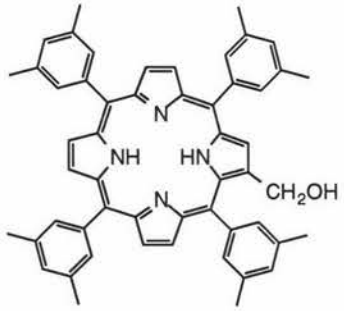

(11) 2-Hydroxymethyl-meso-tetraxylylporphyrin, (TXP-CH_2OH)

A 1 L round bottomed flask was charged with a solution of TXP-CHO (936 mg, 1,24 mmol) dissolved in THF (300 mL) and H_2O (3 mL). $NaBH_4$ (1.17 g, 30.9 mmol) was added portionwise and the reaction mixture was vigorously stirred for 30 mins before diluting with CH_2Cl_2 (400 mL) and quenching with H_2O (200 mL). The two phase mixture was transferred to a 1 L separating funnel and the organic and aqueous layers separated. The organic phase was washed with H_2O (2 x 300 mL) and sat. aq. $NaHCO_3$ (300 mL), then dried over $MgSO_4$, and filtered. The solvent was removed and the resultant solid dried under high vacuum to give TXP-CH_2OH, **11**, (800 mg, 85%) as a purple solid.

R_f = 0.53, 3:2 CH_2Cl_2:Hexane (brown line).

^{1}H NMR (270 MHz, $CDCl_3$): δ -2.81 (br s, 2H; N*H*), 2.04 (t, ^3J = 4.9 Hz, 1H; O*H*), 2.57-2.59 (m, 24H; C*H*$_3$), 4.97 (d, ^3J = 4.9 Hz, 2H; C*H*$_2$), 7.39 (s, 3H; $H_{p\text{Xy}}$), 7.43 (s, 1H; $H_{p\text{Xy}}$), 7.71-7.82 (m, 8H; $H_{o\text{Xy}}$), 8.66-8.87 (m, 6H; H_{pyrrolic}), 8.95 (s, 1H; $H_{\beta\text{-pyrrolic}}$).

UV/Vis (CH_2Cl_2): λ_{max} (log ε) = 419 (5.68), 515 (4.33), 550 (3.87), 590 (3.78), 646 (3.66) nm.

FAB HRMS [MH$^+$] calcd. for $C_{53}H_{49}N_4O$ 757.3906, obs. 757.3913.

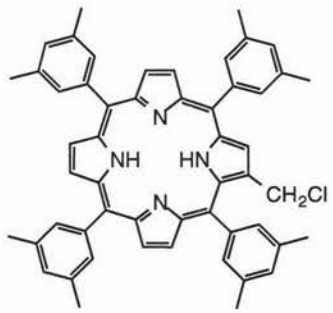

(12) 2-Chloromethyl-meso-tetraxylylporphyrin, (TXP-CH$_2$Cl)

A 500 mL round bottomed flask was charged with a solution of TXP-CH_2OH, **11**, (1.98 g, 2.62 mmol) dissolved in dry distilled CH_2Cl_2 (283 mL), and then cooled in an ice/water bath. By syringe, dry pyridine (2.0 mL, 0.0247 mol) was added, followed by $SOCl_2$ (0.80 mL, 0.011 mol) causing the wine coloured reaction mixture to turn greenish-brown. After 15 mins the reaction was allowed to warm to RT and then stirred for a further 30 mins. No starting material remained by tlc so CH_2Cl_2 (500 mL) was added and the reaction mixture was washed with H_2O (2 x 500 mL) and sat. aq. $NaHCO_3$ (500 mL). The organic phase was dried over $MgSO_4$, filtered, and the solvent removed *in vacuo* to give an insoluble purple solid (1.90 g). This crude TXP-CH_2Cl, **12** was carried through to the next step.

R_f = not recorded as product is unstable on silica, tlc was used only to determine reaction completion by absence of starting material.

^{1}H NMR (270 MHz, $CDCl_3$): δ -2.80 (br s, 2H; N*H*), 2.59-2.61 (m, 24H; C*H*$_3$), 4.84 (s, 2H; C*H*$_2$Cl), 7.42 (s, 3H; $H_{p\text{Xy}}$), 7.45 (s, 1H; $H_{p\text{Xy}}$), 7.74 (s, 2H, $H_{o\text{Xy}}$), 7.77 (s, 6H; $H_{o\text{Xy}}$), 8.73-8.86 (m, 5H; H_{pyrrolic}), 8.99 (s, 1H; $H_{\beta\text{–pyrrolic}}$).

UV/Vis (CH_2Cl_2): λ_{max} (log ε) = 421 (5.76), 488 (3.71), 517 (4.42), 552 (4.00), 593 (3.88) nm.

FAB HRMS [MH$^+$] calcd. for $C_{53}H_{48}N_4Cl$ 775.3568, obs. 755.3599.

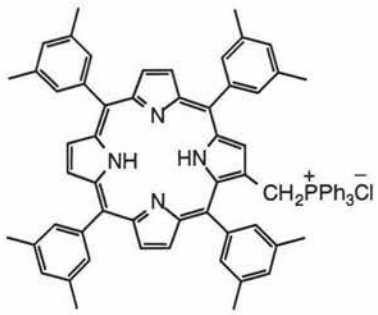

(13) (2-(meso-Tetraxylylporphyrin)yl)methyltriphenylphosphonium chloride (TXP-CH_2PPh_3Cl)

A 500 mL round bottomed flask was charged with a solution of crude TXP-CH_2Cl (2 g, 2.5 mmol) and triphenylphosphine (15.9 g, 60.6 mmol) dissolved in $CHCl_3$ (160 mL). The reaction mixture was heated at reflux temperature for 2 d. The solution was then poured onto a pad of silica and eluted with CH_2Cl_2 to remove nonpolar impurities and residual starting materials. A gradient elution was then carried out with with MeOH:CH_2Cl_2 (1:100 up to 15:100 respectively) to remove the product. Removal of solvent *in vacuo* gave the crude product as shiny purple flakes. Recrystallisation from a $CHCl_3$/acetone/diethyl ether mixture produced TXP-CH_2PPh_3Cl, **13** (2.01 g, 62% yield over four steps from Cu-TXP) as a purple powder.

R_f = 0.40, 10% MeOH in CH_2Cl_2 (brown spot).

^1H NMR (270 MHz, $CDCl_3$): δ -2.79 (br s, 2H; N*H*), 2.48 (s, 6H; CH_3), 2.57 (s, 6H; CH_3), 2.61 (s, 12H; CH_3), 5.10 (d, ^3J = 14.6 Hz, 2H; CH_2), 7.05 (dd, $^3J_{(H\text{-}P)}$ = 12.7 Hz, ^3J = 7.6 Hz, 6H; $H_{o\text{Ph[PPh3]}}$), 7.11 (s, 2H; $H_{p\text{Xy}}$), 7.28 (app t of d, ^3J = 7.3 Hz, $^4J_{(H\text{-}P)}$ = 3.5 Hz, 6H; $H_{m\text{Ph[PPh3]}}$), 7.36 (s, 1H; $H_{p\text{Xy}}$), 7.43 (s, 2H; $H_{o\text{Xy}}$), 7.49 (s, 2H; $H_{o\text{Xy}}$), 7.57 (s, 1H; $H_{p\text{Xy}}$), 7.60-7.65 (m, 3H; $H_{p\text{Ph[PPh3]}}$), 7.82 (s, 4H, $H_{o\text{Xy}}$), 8.19 (d, ^3J = 3.5 Hz, 1H; $H_{\beta\text{-pyrrolic}}$), 8.55 and 8.83 (ABq, ^3J = 4.9 Hz, 2H; H_{pyrrolic}), 8.82 and 8.91 (ABq, ^3J = 4.9 Hz, 2H, H_{pyrrolic}), 8.84 and 8.85 (ABq, ^3J = 4.9 Hz, 2H; H_{pyrrolic}).

UV/Vis (CH_2Cl_2): λ_{max} (log ε) = 426 (5.68), 449 (4.22), 489 (3.65), 521 (4.34), 557 (3.85) nm.

FAB HRMS [M^+] calcd. for $C_{71}H_{62}N_4P$ 1001.4712, obs. 1001.4761.

3.4 References

(1) Sen, A.; Krishnan, V. *Tetrahedron Lett.* **1996**, *37*, 8437-8438.

(2) Adler, A. D.; Longo, F. R.; Finarelli, J. D.; Goldmacher, J.; Assour, J.; Korsakoff, L. *J. Org. Chem.* **1967**, *32*, 476.

(3) Wayland, B. B.; Ba, S.; Sherry, A. E. *J. Am. Chem. Soc.* **1991**, *113*, 5305-5311.

(4) Milgrom, L. R. *The Colours of Life. An Introduction to the Chemsitry of Porphyrins and Related Compounds*; Oxford University Press Inc: Oxford, **1997**, 65-70.

(5) Crossley, M. J.; Harding, M. M.; Sternhell, S. *J. Am. Chem. Soc.* **1992**, *114*, 3266-3272.

(6) Falk, J. E. *Porphyrins and Metalloporphyrins*; Elsevier: Amsterdam, **1975**, 19-27.

(7) Milgrom, L. R. *The Colours of Life. An Introduction to the Chemistry of Porphyrins and Related Compounds*; Oxford University Press Inc.: Oxford, **1997**, 84-89, 194-195.

(8) Bonfantini, E. E.; Officer, D. L. *Tetrahedron Lett.* **1993**, *34*, 8531-8534.

(9) Burrell, A. K.; Officer, D. L.; Reid, D. C. W. *Angew. Chem. Int. Ed. Eng.* **1995**, *34*, 900-902.

(10) Reid, D. C. W. PhD thesis in preparation.

(11) Newman, M. S.; Lee, L. F. *J. Org. Chem.* **1972**, *37*, 4468-4469.

(12) March, J. *Advanced Organic Chemistry: Reactions, Mechanisms, and Structure*; 4th ed.; John Wiley & Sons, Inc.:, **1992**, 542-543.

Chapter Four

Synthesis of bipyridyl-functionalised porphyrins

This chapter describes the synthesis of novel bipyridyl ligands functionalised through vinyl linking groups to porphyrin moieties. The methodology developed herein utilises Wittig chemistry to react 4,4'-diformyl-2,2'-bipyridine (see Chapter Two) with porphyrin phosphonium salts (see Chapter Three), in order to synthesise the desired bipyridine-porphyrin conjugates.

To the best of the author's knowledge the compounds described in this chapter are the first of their kind to be synthesised. There is precedent from the literature (see Chapter One), that the direct combination of the two aforementioned moieties in this direct manner followed by metal complexation, could produce multi-chromophore containing complexes with useful photovoltaic properties. It is anticipated that the incorporation of such complexes into photovoltaic units could produce solar cells with a broader absorption range than has previously been seen with synthetic mono-chromophore containing cells such as that produced by Grätzel *et al.*[1] (see Section 1.1.3, p.4). This study however, is primarily an investigation into the synthesis of these ligands and their metal complexes. Future studies (see Chapter Six) will investigate the potential of such complexes as photovoltaic units for solar cells.

4.1 Synthesis of bipyridyl-bridged TPP compounds

In order to synthesise these bipyridine-porphyrin conjugates, two different porphyrin phosphonium salts were made (see Chapter Three). Tetraphenylporphyrin phosphonium salt, **5**, had previously been studied in these laboratories.[2-4] Thus although TPP-CH_2PPh_3Cl is not as soluble as the newer TXP salt, more was known about its properties and reactivity at the time that this study was commenced. Consequently the TPP salt, **5**, was first employed to explore the synthesis of the novel bipyridyl-functionalised porphyrin compounds.

4.1.1 Synthesis and characterisation of a mono-TPP-bound bipyridyl ligand

The Wittig reaction carried out to synthesise the monomeric porphyrinyl bipyridine compound, **14**, is shown below in Figure 4.1-1. Porphyrinyl bipyridine **14** was

synthesised by reacting equal mole equivalents of the TPP phosphonium salt, **5**, with 4,4'-diformyl-2,2'-bipyridine **4**, under standard Wittig conditions using DBU as the base. Column chromatography using 4% MeOH in CH_2Cl_2 as the eluent gave a *cis/trans* mixture of product **14** with the *trans*-isomer predominating (only the *trans* isomer is pictured in Figure 4.1-1).

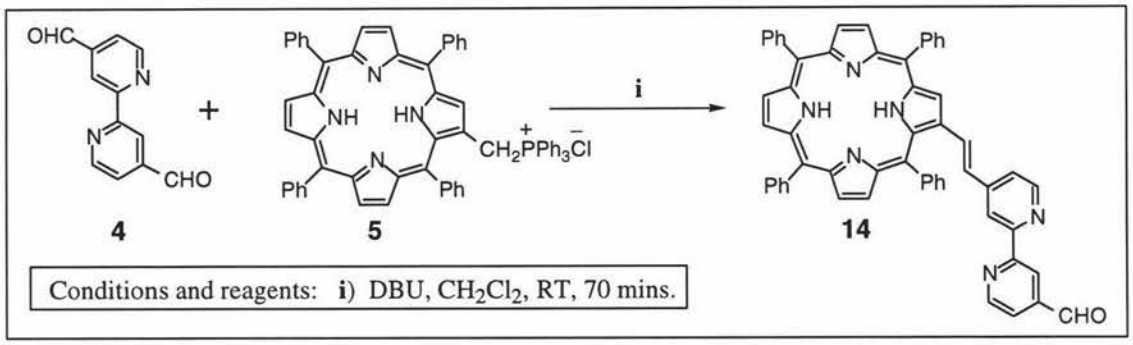

Figure 4.1-1
Wittig reaction between TPP-CH_2PPh_3Cl, **5**, and 4,4'-diformyl-2,2'-bipyridine, **4**.

Isomerisation of the mixture using iodine was attempted in order to convert the *cis*-product to *trans*, however all efforts to isomerise the mixture proved to be unsuccessful. Only very little *cis*-isomer was produced in the reaction, thus further attempts to separate the two isomers were made. The mixture was re-columned slowly using gravity chromatography with a less polar solvent system (1:1 CH_2Cl_2:EtOAc), and separation of the two isomers was achieved. A third, non-polar, red band was the first band recovered off the column, which when analysed by ^1H NMR spectroscopy proved to be a small quantity of methyltetraphenylporphyrin (Me-TPP). According to Johnson[5], the presence of water in a Wittig reaction will react with the phosphonium ylide to produce the methyl product, as is represented in Figure 4.1-2.

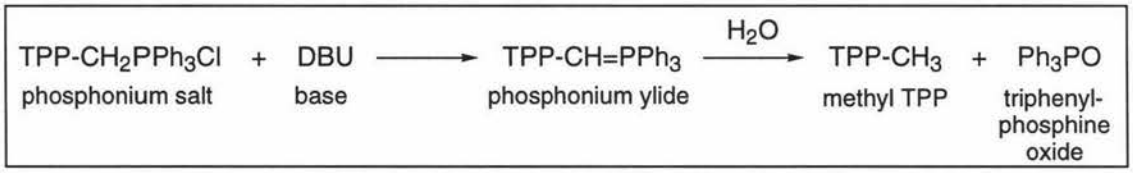

Figure 4.1-2
Formation of Me-TPP during a Wittig reaction.

Removal of water from the reaction was achieved by using dry, distilled solvents and oven dried glassware which eliminated the production of Me-TPP. Compound **14** was therefore able to be synthesised in 84% yield as a purple powder. This compound was reasonably soluble in organic solvents and was characterised using ^1H NMR, UV/Vis and IR spectroscopy and FAB HRMS.

The ^{1}H NMR spectrum of **14** followed the general pattern observed for TPP (see Figure 3.0-2, p 38), with a number of extra peaks corresponding to the bipyridine moiety and the vinylic linking group. Two doublets centred at 7.25 ppm and 7.33 ppm correspond to the two protons of the *trans*-vinylic linking group. Each peak is split into a doublet by a strong three bond coupling to its neighbouring vinylic proton. The coupling constants for these two doublets measured 16.2 Hz, which are typical of a strong *trans*-vinylic couple. A multiplet at 8.77-8.85 ppm corresponds to the six pyrrolic protons remote from the vinylic substitution. The β-pyrollic proton which is closest to the vinyl linker, gives a single peak slightly further downfield at 9.06 ppm. There are seven peaks corresponding to the bipyridyl moiety; a resonance at 10.17 ppm is due to the aldehyde group, and six peaks between 7.10 ppm and 9.10 ppm (four doublets and two singlets) correspond to the remaining six non-equivalent bipyridine protons (see Section 4.4, compound **14**, p.61). UV/Vis spectroscopy produced a spectrum typical of a free base porphyrin with a large Soret band at 426 nm and four weaker Q bands at higher wavelengths. The Soret band recorded a molar extinction coefficient (ε) of over 214,000. A small broad band is also seen at 307 nm which is due to the ligand centred π-π* transition (LC transition) of the bipyridine ligand. The infrared spectrum confirmed the presence of the aldehyde group with a band of medium intensity at 1590 cm^{-1}, and FAB HRMS supported the characterisation (as compound **14** shown above) with an accurate mass reading.

4.1.2 Synthesis of the dimeric TPP-bound bipyridine ligand

The dimeric porphyrin compound **15** was synthesised by reacting compound **14** in a second Wittig reaction with a little over one equivalent of phosphonium salt **5** (depicted below in Figure 4.1-3).

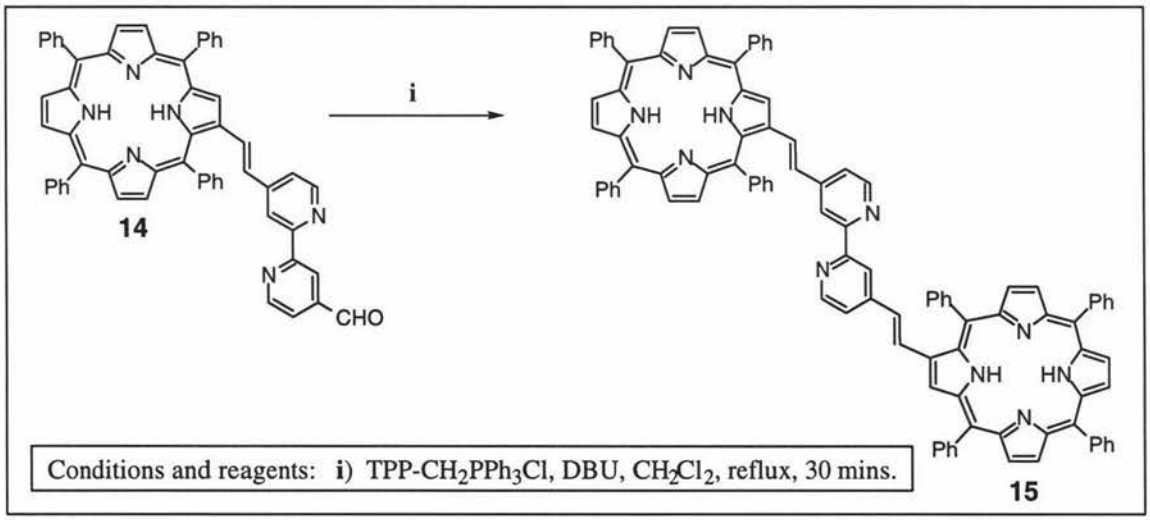

Figure 4.1-3
Synthesis of the dimeric TPP-bound bipyridine ligand, **15**.

The bipyridyl-bridged porphyrin dimer **15**, precipitated out of the reaction mixture and was isolated in 72% yield. As was expected (see Section 3.1, p.40-41), compound **15** proved to be insoluble in all organic solvents and thus was unable to be used in further chemistry. Due the poor solubility, compound **15** could only be characterised by mass spectrometry.

Before proceeding with the option of using the more soluble tetraxylylporphyrin phosphonium salt, **13**, a number of test metallation reactions using the monomeric bipyridine-porphyrin conjugate **14** were explored.

4.1.3 Metallation of the porphyrin ring

Many of the porphyrin containing compounds found in nature consist of arrays of metallated porphyrin moieties. The magnesium porphyrin, chlorophyll, and the iron porphyrin found in haemoglobin are two common examples. As porphyrin rings readily coordinate to many of the transition metal ions, most of the large synthetic porphyrin arrays synthesised to date contain primarily metallated porphyrins.[6-8] As metallation of the porphyrin ring is not the primary focus for this study into bipyridine-porphyrin conjugates, and in order to demonstrate the ease of metal coordination for such systems, only one such metallation was carried out.

Zinc was inserted into the porphyrin ring of compound **14** by way of the acetate method[9] (see Figure 4.1-4). Metallated porphyrin monomer **16** was purified by column chromatography and isolated as a purple powder in 85% yield.

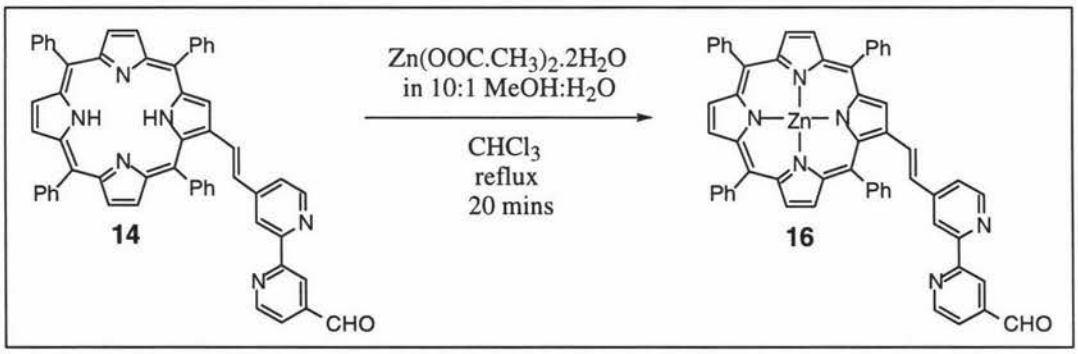

Figure 4.1-4
Metallation of porphyrinyl bipyridine **14** with a zinc metal ion *via* the acetate method.

Analysis of the ^{1}H NMR spectrum of **14** supportes the metallation of the porphyrin ring by the absence of the peak upfield of zero ppm (which corresponds to the two N*H* protons of a free base porphyrin). The remainder of the spectrum was very similar to that of porphyrinyl bipyridine **14** except that the doublets due to the two vinylic protons are positioned much

closer together and so appear as an apparent triplet with a coupling constant of 15.8 Hz. The UV/Vis spectrum of compound **16** (shown in Figure 4.1-5) contains four distinct bands.

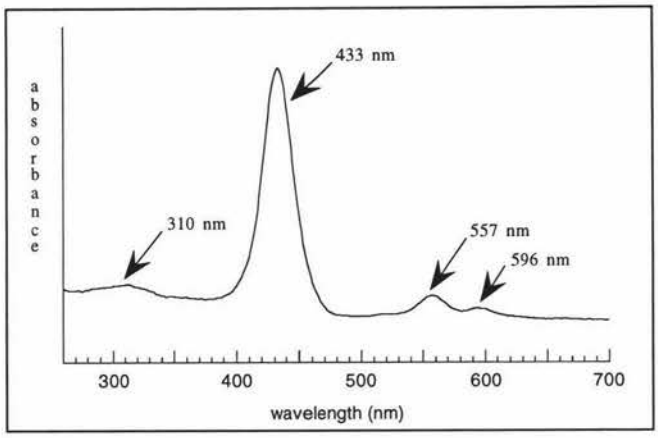

Figure 4.1-5
UV/Vis spectrum of 4-[(*trans*-2''-vinyl-TPPato)zinc(II)]-4'-formyl-2,2'-bipyridine, **16**.

The LC transition of the bipyridine ligand is seen as a broad weak band at 310 nm, the large Soret band due to the porphyrin moiety is at 433 nm, and two weak Q bands are positioned at 557 nm and 596 nm. It is due to the increased symmetry of the porphyrin ring caused by complexation with the zinc metal ion, that the number of Q bands in the UV/Vis spectrum is reduced to two (as opposed to four for a free base porphyrin). A peak at 1590 cm^{-1} in the infrared spectrum confirmed the presence of the aldehyde group, and FAB HRMS supported the proposed identity of the compound with an accurate mass reading.

4.1.4 Metallation of the bipyridine ligand

Due to the availability of the complex, $Re(CO)_5Cl$, rhenium was chosen to attempt the first metallation of the porphyrin appended bipyridine ligand **14** . Compound **14** was refluxed in benzene in an inert atmosphere with the metal complex, $Re(CO)_5Cl$ (represented below in Figure 4.1-6, step **i**). Purification by flash chromatography gave rhenium bipyridyl complex, **17**, as a relatively soluble purple powder in 40% yield. Characterisation of this rhenium complex was relatively straight forward as the ^1H NMR spectrum was almost identical to that seen for compound **14**, since metallation at the bipyridyl nitrogen atoms has no significant effect on the protons of the compound. The UV/Vis spectrum contained a broad weak band due to the bipyridyl LC transition at 304 nm, as well as one large Soret band and four Q bands as expected for the free base porphyrin. The IR spectrum supported both the presence of the aldehyde appendage with a peak of medium intensity at 1604 cm^{-1}, and the three rhenium-bound carbonyl groups with peaks at 1889 cm^{-1}, 1913 cm^{-1}, and 2018 cm^{-1}. Mass spectrometry supported the proposed characterisation of **17** as the rhenium complex of compound **14** with an accurate mass reading of 1129.23 amu.

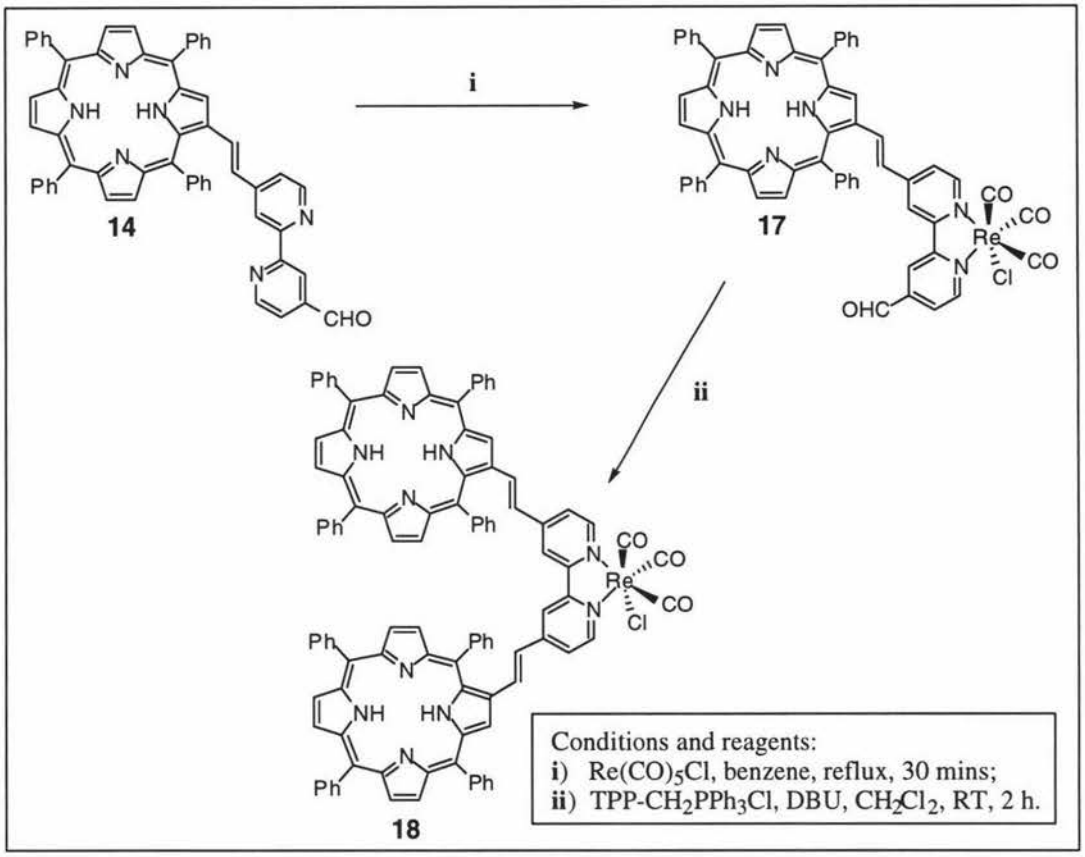

Figure 4.1-6
Metallation of compound **14** and the subsequent Wittig reaction to form the dimeric compound, **18**.

Metallation of porphyrinyl bipyridine **14** was successfully achieved at both the porphyrin ring and the bipyridyl binding site (using zinc and rhenium respectively). This is an extremely positive result as a future aim will be to incorporate these ligands into large multi-centred complexes for use in photovoltaics.

Before moving on to using the TXP salt, one final test reaction was attempted which was to synthesise the bisporphyrinyl metal-bpy complex **18** (shown in Figure 4.1-6). Complex **17** was reacted under standard Wittig conditions with one equivalent of the TPP salt, **5**, and DBU as the base. The dimeric free base porphyrin complex **18** was purified by flash chromatography using CH_2Cl_2 as the elution solvent, and isolated in 78% yield. Due to the symmetry of this dimeric compound, the ^1H NMR spectrum of **18** was relatively simple. The peaks due to the protons of the porphyrin ring are shifted slightly from their positions in unsubstituted TPP (see TPP spectrum, Chapter Three, Figure 3.0-2, p.38) due to effects from the metallated bipyridine appendage and the vinylic linking groups. A broad singlet at -2.50 ppm corresponds to the four N*H* porphyrin ring protons. The peaks for the *meta*- and *para*-phenyl protons overlay the doublets for the four vinylic's, in a large multiplet from 7.74-8.01 ppm. Three peaks, two doublets and one singlet, positioned at 7.92, 8.95, and

8.36 ppm respectively correspond to the three sets of equivalent bipyridyl protons. This pattern is identical to that seen for the corresponding protons in the spectrum of 4,4'-diformyl-2,2'-bipyridine (see Figure 2.4-1, p.29). There are two multiplets for the *ortho*-phenyl and pyrrolic protons at 8.20-8.34 ppm and 8.82-8.90 ppm respectively. A singlet downfield at 9.23 ppm corresponds to the two β-pyrolic hydrogen atoms. This bipyridyl-bridged dimeric porphyrin complex is more soluble than its unmetallated counterpart, **15**, however a more soluble system is still preferred.

This section of work clearly demonstrates the feasibility and the flexibility of this study. Even though the compounds synthesised have tended towards low solubility, all reactions successfully formed the desired products. The step-wise nature of the synthesis used, incorporates flexibility into the methodology. Potentially, large bipyridyl-bridged porphyrin arrays could be built up in a step-wise manner, thus enabling the placement of specific metal ions or ligands to certain positions in the complex. This could allow the synthetic chemist the ability to tune the structure and therefore desired properties of a target complex for a particular purpose or application.

The ever present problem with the solubility of these compounds must be overcome, thus the Wittig chemistry of 4,4'-diformyl-2,2'-bipyridine, **4**, with the more soluble phosphonium salt, TXP-CH_2PPh_3Cl, **13**, was then explored.

4.2 Synthesis of bipyridyl-bridged TXP compounds

This section consists of a discussion of the results obtained for the synthesis and characterisation of bipyridyl-functionalised tetraxylylporphyrin ligands. The objective of this section was to develop an efficient synthetic methodology of a soluble bistetraxylylporphyrinyl bipyridine ligand analogous to compound **15**. To achieve this goal, Wittig chemistry was employed to react bipyridine dialdehyde **4**, with the more soluble tetraxylylporphyrin phosphonium salt, **13**. The synthetic routes investigated towards the synthesis of the new target compound are represented below in Figure 4.2-1.

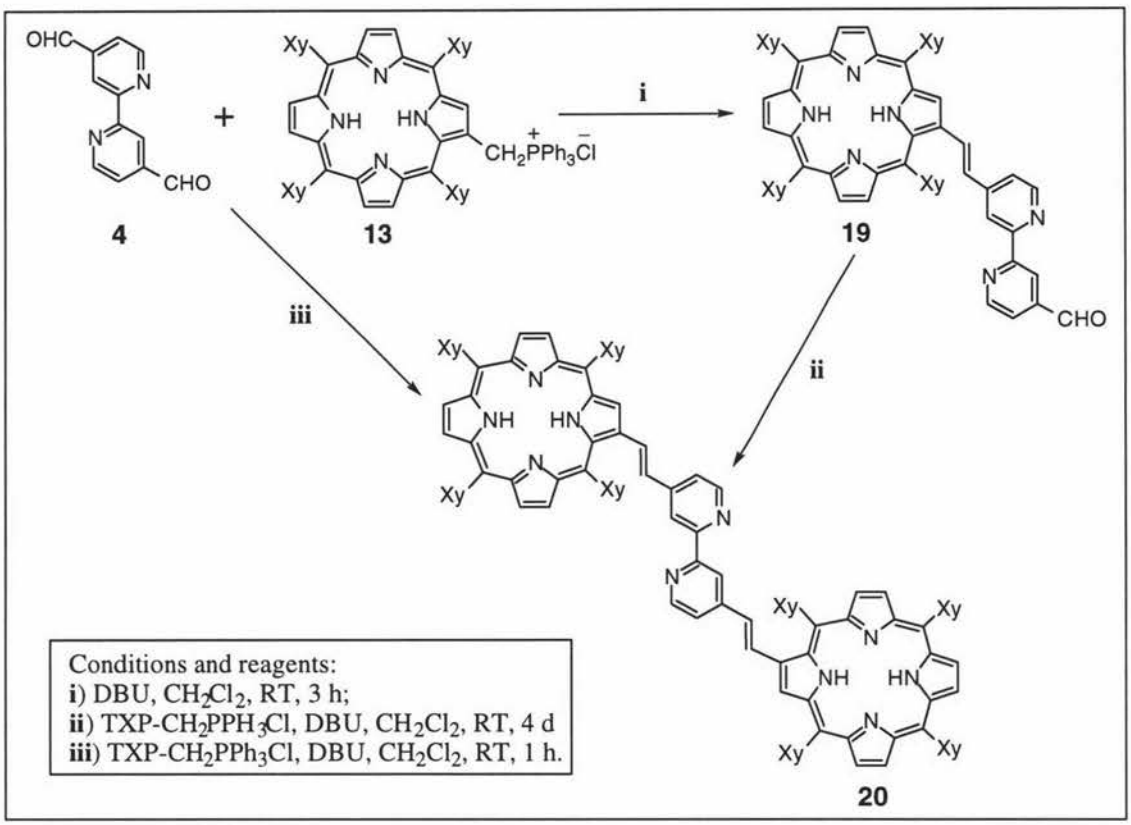

Figure 4.2-1
Wittig reactions on 4,4'-diformyl-2,2'-bipyridine, **4**, using TXP-CH_2PPh_3Cl, **13**.

4.2.1 Synthesis and characterisation of a mono-TXP-bound bipyridyl ligand

4,4'-Diformyl-2,2'-bipyridine, **4**, was reacted with one equivalent of TXP-CH_2PPh_3Cl, **13**, in the presence of DBU under standard Wittig conditions (see Figure 4.2-1, reaction **i**). Purification of the resulting product mixture by column chromatography was carried out with relative ease due to the high solubility of the products. A fast running non-polar band was collected which was characterised as Me-TXP (see Section 4.1.1, p.51). Only a very small quantity of this by-product was produced and thus was of little concern. The second, most prominent band off the column, the desired Wittig product, was isolated as a purple powder in 91% yield. Porphyrinyl bipyridine **19** was readily soluble in organic solvents, CH_2Cl_2, and $CHCl_3$ and was characterised according to the usual spectroscopic techniques.

The ^1H NMR spectrum of **19** contains six singlets due to the six non-equivalent bipyridine hydrogen atoms, with positions ranging from 7.24 ppm up to 9.04 ppm. The pattern of peaks is the same as that observed for the analogous tetraphenylporphyrin compound, **14** (discussed in Section 4.1.1, p.52). A distinctive peak at 10.2 ppm corresponds to the aldehyde proton, and there are two doublets centred at 7.44 ppm and 7.83 ppm due to the two vinylic protons. Three singlets at 2.55, 2.61, and 2.66 ppm correspond to the methyl

groups of the tetraxylylporphyrin ring (split into three groups due to relative proximity to the position of substitution). The remaining peaks due to the *meta-* and *para-* xylyl protons and pyrrolic protons are of similar form and are in similar positions to those of the unsubstituted phosphonium salt (see Section 3.3, compound **13**, p.49). The UV/Vis spectrum of **14** was almost identical to the analogous TPP compound, as was the infrared data. An accurate mass determination was obtained using FAB High Resolution Mass Spectrometry.

4.2.2 Synthesis of the dimeric TXP-bound bipyridine ligand

The next step involved the Wittig reaction of porphyrinyl bipyridine **19** with a second mole equivalent of the porphyrin phosphonium salt, **13**, reaction **ii**, Figure 4.2-1 above. During the course of this reaction a small amount of solid purple material began to precipitate out of solution. Due to the increased solubility of the tetraxylylporphyrin, this solid was easily redissolved by the addition of a small volume of solvent. Column chromatography using a solvent polarity gradient elution, separated the desired product from Me-TXP (a more significant quantity was produced than with previous Wittig reactions). Product **20** (Figure 4.2-1) was then washed with Et_2O in order to remove residual triphenylphosphine and triphenylphosphine oxide. Subsequent drying produced the bipyridyl-bridged dimeric porphyrin compound **20** in 51% yield. The TXP dimer was soluble in CH_2Cl_2 and $CHCl_3$ and was characterised according to the standard spectroscopic techniques used throughout this study. However, this preparation does leave room for improvement as the increased amount of methylporphyrin by-product produced consequently the lowers the yield of product. Therefore, an alternative route to compound **20** (step **iii**, Figure 4.2-1 above) was investigated.

4.2.3 Alternative synthesis of the dimeric TXP-bound bipyridine ligand

Reaction **ii** (Figure 4.2-1 above) discussed in Section 4.2.2, simply repeats the same Wittig reaction executed in step **i**. Therefore, a logical alternative to attempt would be the combination of the two reactions into a single step. A one step methodology would be advantageous as far as the time and effort invested in the synthesis, and the loss of product during work-up procedures could effectively be halved. The problem of the Me-TXP production was addressed in two ways. Firstly, the previous reactions had been carried out with dry distilled solvents in air, therefore the single step reaction was attempted in an inert atmosphere by purging the solution with argon and then bubbling the gas throughout the apparatus for the duration of the reaction. It was also discovered through a number of trials that the concentration of the reaction had a distinct effect on the quantity of Me-TXP produced. Previous Wittig reactions had been performed using minimum volumes of

solvent. It was found that this method produced greater amounts of Me-TXP than if more dilute solutions were used. A 0.05 M concentration (combined moles of reagents per litre of solvent) was found to be most successful for this reaction, eliminating the unwanted by-product and maximising the product yield. Thus, a one step Wittig reaction of 4,4'-diformyl-2,2'-bipyridine, **4**, with 2.2 equivalents of TXP-CH_2PPh_3Cl, **13**, and DBU as the base, was utilised to produce the bipyridine-bisporphyrin conjugate **20**. The pure product was isolated by careful column chromatography using a solvent polarity gradient, followed by slow recrystallisation from $MeOH/CH_2Cl_2$. Optimisation of the procedure (see Section 4.4, compound **20**, Method B, p.66) resulted in pure compound **20** in 68% yield.

Compound **20** was characterised by ^1H NMR spectroscopy (see Figure 4.2-2), which was supported by both UV/Vis spectroscopy and mass spectrometry results. The ^1H NMR spectrum contains the distinctive broad singlet at -2.52 ppm corresponding to the four N*H* protons of the porphyrin rings. The three large singlets at 2.63, 2.65, and 2.68 ppm are due to the forty-eight methyl protons of the xylyl groups. A doublet positioned at 7.30 ppm (^3J = 5.2 Hz) corresponds to the two equivalent 5-position protons of the bipyridyl moiety ($H_{5,5'\text{-bpy}}$) coupled to their respective 6-position proton. Two doublets centred at 7.34 ppm and 7.44 ppm, split with a coupling constant of 16.2 Hz are due to the four vinylic protons (the symmetry of the dimeric compound results in two sets of two equivalent protons). The *para*-xylyl protons are divided into two singlets, each corresponding to four protons (as was seen with the monomeric porphyrin compound, **19**), and a multiplet from 7.87-7.94 ppm corresponds to the sixteen *ortho*-xylyl protons.

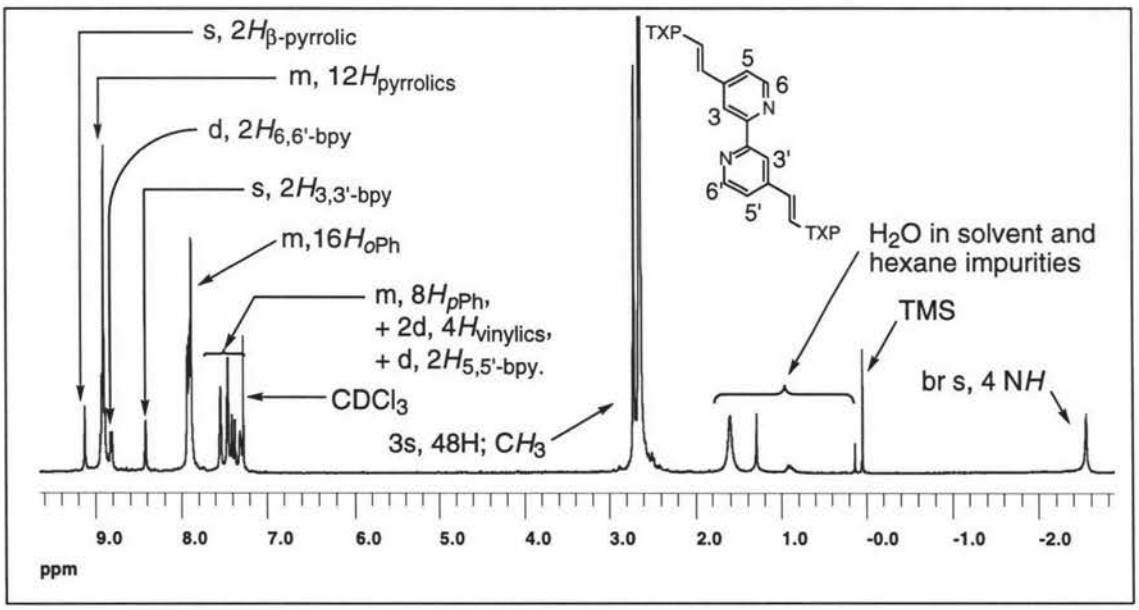

Figure 4.2-2
^1H NMR spectrum of 4,4'-(*trans*-2"-vinyl-TXPyl)-2,2'-bipyridine, **20**.

The two equivalent 3-position bipyridine protons ($H_{3,3'\text{-bpy}}$) give a singlet at 8.41 ppm as they have no adjacent proton with which to couple. The 6-position protons (each coupled to their respective 5-position proton with a coupling constant of 5.2 Hz) produce one doublet centred at 8.81 ppm. A multiplet from 8.87-8.95 ppm corresponds to twelve of the pyrrolic protons, and the two remaining β-pyrrolic protons produce a singlet downfield at 9.12 ppm.

4.3 Summary

The synthesis of a novel bipyridine-bisporphyrin conjugate, using 4,4'-diformyl-2,2'-bipyridine, **4**, and TPP-CH_2PPh_3Cl, **13**, was severely limited due to the insolubility of the resultant dimeric compound **15,** and to a lesser extent rhenium complex **18**. However, test metallation reactions of both the porphyrin ring and the bipyridyl ligand were successfully executed using the monomeric TPP-bound bipyridine ligand. The synthesis of these metal bound complexes, indicates that such metallation reactions using a more soluble system should also be successful, thus confirming the feasibility of the remainder of this proposed study. The solubility problems encountered with this first method were successfully overcome by replacement of the tetraphenylporphyrin phosphonium salt with a more soluble tetraxylylporphyrin analogue, **13**. The use of the new salt was tested and optimised resulting in the synthesis of the soluble bipyridyl-functionalised dimeric porphyrin target compound, **20**, in a one step 68% yielding reaction. This was an exciting development for this research as it provided a simple and efficient synthesis of this key compound. The next and final stage of this research was to explore the metal-binding capabilities of compound **20**, as a preliminary investigation into it's potential as a building block for the synthesis of large multi-chromophore containing complexes.

4.4 Experimental procedures

For general procedures used see Chapter Two, Section 2.6.1, p.31-32.
When necessary, reactions involving light sensitive porphyrin compounds were carried out under aluminium foil and stored in the dark in order to protect them from both reacting with light and decomposition.

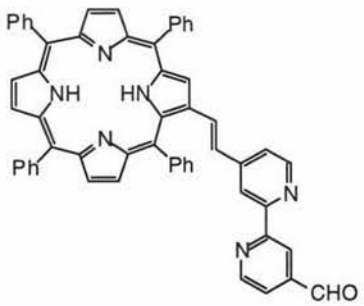

NB: Phenyl rings represented as Ph's.

(14) 4-(trans-2''-Vinyl-TPPyl)-4'-formyl-2,2'-bipyridine

A 25 mL round bottomed flask was charged with a solution of TPP phosphonium salt, **5**, (0.250 g, 0.270 mmol) and 4,4'-diformyl-2,2'-bipyridine, **4**, (0.057 g, 0.270 mmol) in basified CH_2Cl_2 (13 mL). While stirring vigorously at RT, DBU (0.202 mL) was added and the reaction was monitored by tlc. After 70 mins, no starting material remained so the solution was reduced to dryness. The residue was carefully purified by gravity fed chromatography through silica gel using 1:1 CH_2Cl_2:EtOAc as the elution solvent. The third band off the column was collected and the solvent removed under reduced pressure. Drying under high vacuum yielded product **14** as a purple powder (0.187 g, 84%).

R_f = 0.375, 1:1 CH_2Cl_2:EtOAc.

^{1}H NMR (270 MHz, $CDCl_3$): δ -2.58 (br s, 2H; N*H*), 7.160 (d, ^3J = 5.2 Hz, 1H; $H_{5\text{-bpy}}$), 7.25 (d, ^3J = 16.2 Hz, 1H; $H_{trans\text{-vinylic}}$), 7.33 (d, ^3J = 16.2 Hz, 1H; $H_{trans\text{-vinylic}}$), 7.76-7.88 (m, 12H; $H_{m,p\text{Ph}}$), 7.74 (d, ^3J = 4.9 Hz, 1H; $H_{5'\text{-bpy}}$), 8.27 (s, 1H; $H_{3\text{-bpy}}$), 8.20-8.30 (m, 8H; $H_{o\text{Ph}}$), 8.65 (d, ^3J = 5.2 Hz, 1H; $H_{6\text{-bpy}}$), 8.77-8.85 (m, 6H; $H_{\text{pyrrolics}}$), 8.80 (s, 1H; $H_{3'\text{-bpy}}$), 9.01 (d, ^3J = 4.9 Hz, 1H; $H_{6'\text{-bpy}}$), 9.06 (s, 1H; $H_{\beta\text{-pyrrolic}}$), 10.17 (s, 1H; C*H*O).

UV/Vis (CH_2Cl_2): λ_{max} (log ε) = 307 (4.39), 426 (5.33), 523 (4.27), 564 (3.97), 5.99 (3.84), 653 (3.55) nm.

IR (Nujol): 1590 (m, CHO) cm^{-1}.

FAB HRMS [MH$^+$] calcd for $C_{57}H_{39}N_6O$ 823.3185, obs. 823.3182.

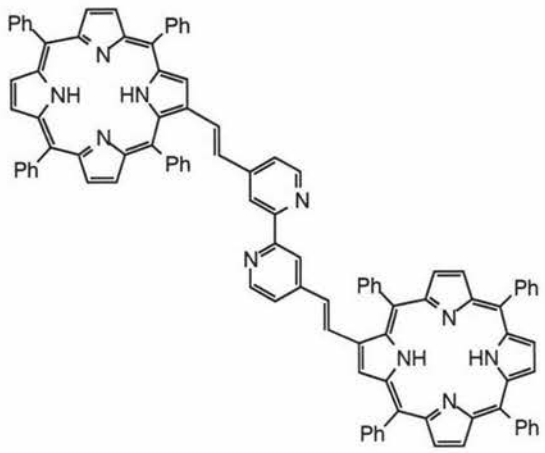

(15) 4,4'-(trans-2''-Vinyl-TPPyl)-2,2'-bipyridine

Porphyrinyl bipyridine **14** (20 mg, 0.024 mmol) and TPP phosphonium salt **5** (27 mg, 0.029 mmol) were stirred in CH_2Cl_2 (4 mL) in a 10 mL round bottomed flask. DBU (18 mL) was added, and after 20 mins a light purple solid precipitated from the reaction mixture. This precipitate was filtered off and dried under vacuum to give product **15** as an insoluble light purple solid (0.025 g, 72%).

FAB HRMS [MH^+] calcd for $C_{102}H_{69}N_{10}$ 1433.5806, obs. 1433.5707.

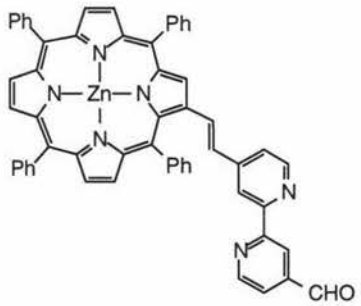

(16) 4-[(trans-2''-Vinyl-TPPato)zinc(II)]-4'-formyl-2,2'-bipyridine

A 25 mL round bottomed flask was charged with a solution of porphyrinyl bipyridine **14** (12 mg, 0.015 mmol) dissolved in $CHCl_3$ (5 mL). With vigorous stirring, a slurry of $Zn(OOCCH_3)_2.2H_2O$ (0.016 g, 0.073 mmol) in 10:1 MeOH:H_2O (2.5 mL) was added. The mixture was heated at reflux temperature for 20 mins. Analysis by tlc showed that the reaction had reached completion so the mixture was allowed to cool. The reaction mixture was then purified by flash chromatography using $CHCl_3$ as the eluent. The desired fraction was reduced to dryness and the product precipitated from CH_2Cl_2 with MeOH. Filtering and drying under vacuum gave metallated porphyrinyl bipyridine **16** as a purple powder (0.011 g, 85%).

R_f = 0.125, 1:1 CH_2Cl_2:EtOAc.

^1H NMR (270 MHz, $CDCl_3$): δ 7.08 (d, ^3J = 5.2 Hz, 1H; $H_{5\text{-bpy}}$), 7.25 (appt t, ^3J = 15.8 Hz, 2H; $H_{trans\text{-vinylic}}$), 7.64 (d, ^3J = 4.9 Hz, 1H; $H_{5'\text{-bpy}}$), 7.75-7.84 (m, 12H;

$H_{m,p\text{Ph}}$), 8.18-8.24 (m, 8H; $H_{o\text{Ph}}$), 8.27 (s, 1H; $H_{3\text{-bpy}}$), 8.40 (d, ^3J = 4.9 Hz, 1H; $H_{6\text{-bpy}}$), 8.53 (s, 1H; $H_{3'\text{-bpy}}$), 8.83 (d, ^3J = 4.6 Hz, 1H; $H_{6'\text{-bpy}}$), 8.87-8.93 (m, 6H; $H_{\text{pyrrolics}}$), 9.13 (s, 1H; $H_{\beta\text{-pyrrolic}}$), 10.02 (s, 1H; C*H*O).

UV/Vis (CH_2Cl_2): λ_{max} (log ε) = 310 (4.39), 433 (5.20), 557 (4.21), 596 (3.92) nm.

IR (Nujol): 1590 (m, CHO) cm^{-1}.

FAB HRMS [MH^+] calcd for $C_{57}H_{37}N_6OZn$ 885.2320, obs. 885.2327.

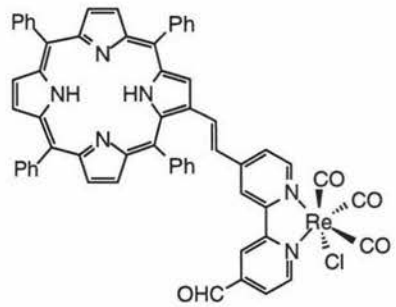

(17) 1,1'-Re(CO)$_3$Cl[4-(trans-2''-Vinyl-TPPyl)-4'-formyl-2,2'-bipyridine]

A 10 mL round bottomed flask was charged with porphyrinyl bipyridine **14** (20 mg, 0.024 mmol), $Re(CO)_5Cl$ (9.7 mg, 0.027 mmol) and C_6H_6 (2 mL). The reaction mixture was heated to reflux temperature under argon. After 30 mins, analysis by tlc showed that the reaction had reached completion. Once cooled, the mixture was purified by flash chromatography using a solvent gradient from CH_2Cl_2 to 1:1 CH_2Cl_2:EtOAc. The second band was collected and the solvent removed. The resultant solid was dried under vacuum to yield product **17** as a purple powder (0.011 g, 40%).

R_f = 0.150, CH_2Cl_2.

^{1}H NMR (270 MHz, $CDCl_3$): δ -2.54 (br s, 2H; N*H*), 7.29 (d, ^3J = 5.8 Hz, 1H; $H_{5\text{-bpy}}$), 7.30 (d, ^3J = 15.1 Hz, 1H; $H_{\text{trans-vinylic}}$), 7.39 (d, ^3J = 15.1 Hz, 1H; $H_{\text{trans-vinylic}}$), 7.75 (d, ^3J = 5.8 Hz, 1H; $H_{5'\text{-bpy}}$), 7.79-8.01 (m, 12H; $H_{m,p\text{Ph}}$), 8.19-8.22 (m, 4H; $H_{o\text{Ph}}$), 8.24 (s, 1H; $H_{3\text{-bpy}}$), 8.27-8.31 (m, 4H; $H_{o\text{Ph}}$), 8.71 (s, 1H; $H_{3'\text{-bpy}}$), 8.77-8.89 (m, 6H; H_{pyrrolic}), 8.91 (d, ^3J = 5.8 Hz, 1H; $H_{6\text{-bpy}}$), 9.10 (s, 1H; $H_{\beta\text{-pyrrolic}}$), 9.37 (d, ^3J = 5.5 Hz, 1H; $H_{6'\text{-bpy}}$), 10.24 (s, 1H; C*H*O)

UV/Vis (CH_2Cl_2): λ_{max} (log ε) = 304 (4.36), 424 (5.01), 524 (4.20), 575 (3.92), 604 (3.82), 662 (3.52) nm.

IR (Nujol): 2018 (m, CO), 1913 (m, CO), 1889 (m, CO), 1604 (m, CHO) cm^{-1}.

FAB HRMS [MH^+] calcd for $C_{60}H_{39}N_6O_4ReCl$ 1129.2266, obs. 1129.2279.

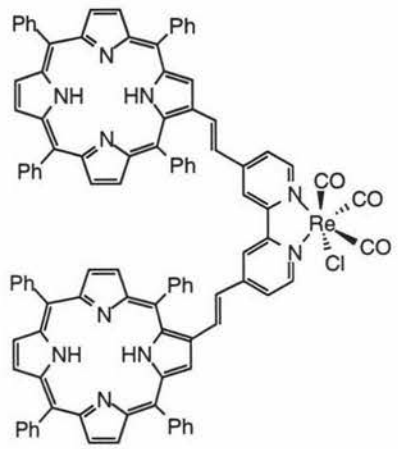

(18) 1,1'-Re(CO)$_3$Cl[4,4'-(trans-2''-Vinyl-TPPyl)-2,2'-bipyridine]

Compound **17** (5 mg, 0.004 mmol) and TPP phosphonium salt **5** (4.1 mg, 0.004 mmol) were dissolved in CH_2Cl_2 (0.5 mL) in a 5 mL round bottomed flask. While stirring at RT, DBU (3.3 μL) was added and the reaction was monitored by tlc. After 2 h the reaction had reached completion by tlc. The product was purified by flash chromatography through silica gel using CH_2Cl_2 as the elution solvent. The second band was collected and the solvent removed. Drying under high vacuum afforded product **18** as a purple solid (6 mg, 78%).

R_f = 0.825, CH_2Cl_2.

^{1}H NMR (270 MHz, $CDCl_3$): δ -2.50 (br s, 4H; N*H*), 7.74-8.01 (m, 28H; 4$H_{trans\text{-vinylic}}$ + 24$H_{m,p\text{Ph}}$), 7.92 (d, ^3J = 5.2 Hz, 2H; $H_{5,5'\text{-bpy}}$), 8.20-8.34 (m, 16H; $H_{o\text{Ph}}$), 8.36 (s, 2H; $H_{3,3'\text{-bpy}}$), 8.82-8.90 (m, 12H; $H_{\text{pyrrolics}}$), 8.95 (d, ^3J = 5.8 Hz, 2H; $H_{6,6'\text{-bpy}}$), 9.23 (s, 2H; $H_{\beta\text{-pyrrolic}}$).

FAB HRMS [MH$^+$] calcd. for $C_{105}H_{69}N_{10}O_3ReCl$ 1739.4890, obs. 1739.4800.

FAB LRMS [MH$^+$ -Cl} obs. 1704.5203.

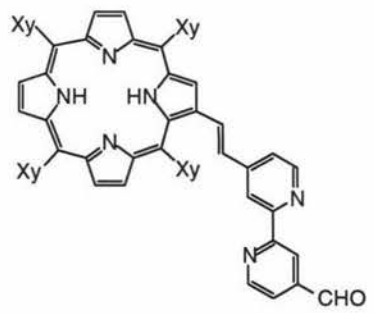

NB: Xylyl groups represented as Xy's

(19) 4-(trans-2''-Vinyl-TXPyl)-4'-formyl-2,2'-bipyridine

A 10 mL round bottomed flask was charged with a solution of TXP phosphonium salt **13** (50 mg, 0.0482 mmol) and dialdehyde **4** (10 mg, 0.0482 mmol) dissolved in basified CH_2Cl_2 (2 mL). While vigorously stirring, DBU (0.036 mL) was added and the reaction was monitored by tlc. After 3 h no starting material remained by tlc. The mixture was then

purified by column chromatography using 4% MeOH in CH_2Cl_2 as the eluent. The second fraction was collected, filtered, and the solvent removed. The resultant purple solid was dried under high vacuum to yield compound **19** (0.041 g, 91%).

R_f = 0.60, 10% MeOH in CH_2Cl_2.

^{1}H NMR (270 MHz, $CDCl_3$): δ -2.61 (br s, 2H; N*H*), 2.55 (s, 6H; CH_3), 2.61 (s, 12H; CH_3), 2.66 (s, 6H; CH_3), 7.24 (d, ^3J = 4.9 Hz, 1H;$H_{5\text{-bpy}}$), 7.29 (s, 2H; $H_{p\text{Ph}}$), 7.44 (s, 2H; $H_{p\text{Ph}}$), 7.44 (d, ^3J = 15.9 Hz, 1H; $H_{trans\text{-vinylic}}$), 7.79 (d, ^3J = 4.9 Hz, 1H; $H_{5'\text{-bpy}}$), 7.82 (s, 8H; $H_{o\text{Ph}}$), 7.83 (d, ^3J = 15.3 Hz, 1H; $H_{trans\text{-vinylic}}$), 8.36 (s, 1H; $H_{3\text{-bpy}}$), 8.67 (d, ^3J = 4.9 Hz, 1H; $H_{6\text{-bpy}}$), 8.83-8.87 (m, 6H; $H_{\text{pyrrolics}}$), 8.90 (s, 1H; $H_{3'\text{-bpy}}$), 9.03 (s, 1H; $H_{\beta\text{-pyrrolic}}$), 9.04 (d, ^3J = 4.9 Hz, 1H; $H_{6'\text{-bpy}}$), 10.2 (s, 1H; C*H*O).

UV/Vis (CH_2Cl_2): λ_{max} (log ε) = 300 (4.31), 429 (5.20), 524 (4.14), 564 (3.85), 600 (3.72), 655 (3.46) nm.

IR (Nujol): 1588 (m, CHO) cm^{-1}.

FAB HRMS [M^+] calcd. for $C_{65}H_{54}N_6O$ 935.4466, obs. 935.4437

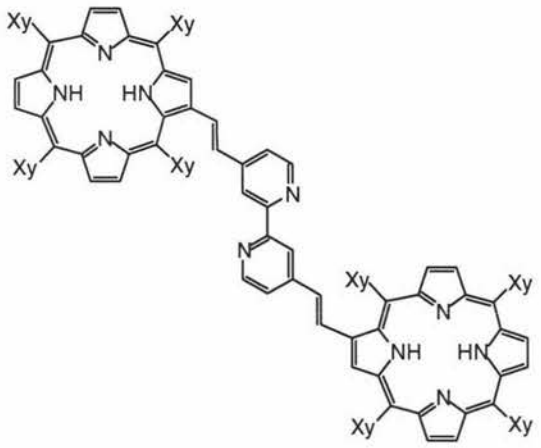

(20) 4,4'-(trans-2''-Vinyl-TXPyl)-2,2'-bipyridine

Method A: A 10 mL round bottomed flask was charged with porphyrinyl bipyridine **14** (20 mg, 0.021 mmol) and phosphonium salt **13** (22 mg, 0.021 mmol) dissolved in basified CH_2Cl_2 (2 mL). DBU (0.016 mL) was added and the reaction was stirred for 4 d. After this time some solid material had precipitated out of solution. $CHCl_3$ (5 mL) and EtOAc (1 mL) were added to redissolve this solid and the mixture was stirred for 1 h. Tlc analysis showed that the reaction had reached completion. The solvent was removed and the resultant residue dissolved in 1:1 CH_2Cl_2:Hexane (1 mL). Purification by column chromatography (eluted with 1:1 CH_2Cl_2:Hexane, then 4% MeOH in CH_2Cl_2) gave two distinct bands. The second band was collected, filtered, and the solvent removed. The residue was washed with Et_2O to remove residual triphenylphosphine and triphenylphosphine oxide, filtered, and dried under high vacuum to yield dimer **20** (0.018 g, 51%, = 46% yield over two steps).

Method B: A 250 mL round bottomed flask was charged with dialdehyde **4** (0.015 g, 0.072 mmol) and phosphonium salt **13** (0.162 g, 0.157 mmol) dissolved in dry distilled CH_2Cl_2 (45 mL). The reaction mixture was purged with argon for 5 mins. DBU (0.108 mL) was then added and the mixture was stirred in an inert atmosphere for 1 h. Analysis by tlc showed that the reaction had reached completion. The solvent was removed *in vacuo* and the resultant residue was purified by column chromatography. The residue was dissolved in 1:1 CH_2Cl_2:Hexane (5 mL) and loaded onto the silica column. The column was eluted using a solvent gradient (from 1:1 CH_2Cl_2:Hexane, to CH_2Cl_2, to 4% MeOH in CH_2Cl_2, then 10% MeOH in CH_2Cl_2) to give three distinct bands. The third band was collected, filtered and reduced to dryness *in vacuo*. The residue was then recrystallised slowly overnight in a dark cupboard from MeOH/CH_2Cl_2. The resultant purple precipitate was collected by filtration, washed with a small volume of methanol and dried under high vacuum to yield the bipyridine-bisporphyrin conjugate **20** (81 mg, 68%).

R_f = 0.48, 4% MeOH in CH_2Cl_2.

^{1}H NMR (270 MHz, $CDCl_3$): δ -2.52 (br s, 4H; N*H*), 2.63 (s, 12H; CH_3), 2.65 (s, 24H; CH_3), 2.68 (s, 12H; CH_3), 7.30 (d, ^3J = 5.2 Hz, 2H; $H_{5,5'\text{-bpy}}$), 7.34 (d, ^3J = 15.7 Hz, 2H; $H_{trans\text{-vinylic}}$), 7.44 (d, ^3J = 15.7 Hz, 2H; $H_{trans\text{-vinylic}}$), 7.45 (s, 4H; $H_{p\text{Ph}}$), 7.53 (s, 4H; $H_{p\text{Ph}}$), 7.87-7.94 (m, 16H; $H_{o\text{Ph}}$), 8.41 (s, 2H; $H_{3,3'\text{-bpy}}$), 8.81 (d, ^4J = 5.2 Hz, 2H; $H_{6,6'\text{-bpy}}$), 8.87-8.95 (m, 12H; $H_{\text{pyrrolics}}$), 9.12 (s, 2H; $H_{\beta\text{-pyrrolic}}$).

UV/Vis (CH_2Cl_2): λ_{max} (log ε) = 299 (4.62), 430 (5.60), 524 (4.54), 565 (4.26), 601 (4.07), 657 (3.71) nm.

FAB HRMS [M^+] calcd. for $C_{118}H_{100}N_{10}$ 1656.8088, obs. 1656.8132.

4.5 References

(1) Péchy, P.; Rotzinger, F. P.; Nazeeruddin, M. K.; Kohle, O.; Zakeeruddin, S. M.; Humphry-Baker, R.; Grätzel, M. *J. Chem. Soc., Chem. Commun.* **1995**, 65-66.

(2) Bonfantini, E. E.; Officer, D. L. *Tetrahedron Lett.* **1993**, *34*, 8531-8534.

(3) Burrell, A. K.; Officer, D. L.; Reid, D. C. W. *Angew. Chem. Int. Ed. Eng.* **1995**, *34*, 900-902.

(4) Reid, D. C. W. PhD thesis in preparation.

(5) Johnson, A. W. *Ylides and imines of phosphorus*; John Wiley & Sons, Inc: North Dakota, **1993**, 130-135.

(6) Officer, D. L.; Burrell, A. K.; Reid, D. C. W. *J. Chem. Soc., Chem. Commun.* **1996**, 1657-1658.

(7) Drain, C. M.; Lehn, J.-M. *J. Chem. Soc., Chem. Commun.* **1994**, 2313-2315.

(8) Anderson, H. L. *Inorg. Chem.* **1994**, *33*, 972-981.

(9) Falk, J. E. *Porphyrins and Metalloporphyrins*; Elsevier: Amsterdam, **1975**, 179-181.

Chapter Five

Metal complexes of bipyridine-porphyrin conjugates

In Chapter Four an efficient synthesis of the target bipyridine-bisporphyrin conjugate **20** was developed. The remainder of the research carried out for this project involved an investigation into the metal binding capabilities of this ligand.

Determination of the metal complexation capabilities of these ligands is important as upon coordination to some transition metal ions, the bipyridyl moiety could acquire chromophoric properties. Therefore, successful metal coordination of the ligands synthesised in Chapter Four could produce multi-chromophore containing complexes, complexes which could have potential for application in the area of photovoltaics.

This chapter describes an introductory investigation into the coordination of different metal ions to the soluble bipyridyl-bridged TXP ligands. The test reactions carried out on ligand **14** in Chapter Four involved metal coordination to the pre-formed bipyridine-bisporphyrin conjugate. The metal complexation reactions described herein investigate the flexibility of this methodology by attempting metal coordination at various stages of ligand formation.

5.1 Molybdenum-bound bipyridine complex

Connection of the porphyrin moiety *via* Wittig chemistry to a pre-metallated bpy ligand has not yet been attempted. Thus, a bipyridyl-molybdenum complex was employed to explore this alternative route for the synthesis of a bipyridyl-bridged porphyrin complex.

Condensation of bipyridine dialdehyde **4** with $Mo(CO)_4(piperidine)_2$ produced complex **21**.[1] The metallated bipyridine dialdehyde was then reacted with a small excess of TXP-CH_2PPh_3Cl, **13**, under Wittig conditions in an inert atmosphere. Previous studies of Wittig reactions performed in these laboratories have found that a number of different bases will successfully form the desired product. In the previous Wittig reactions described, the base employed was always DBU. For this molybdenum reaction an alternative base was used, triethylamine. However, it was found that compared to the reactions using DBU, a much larger excess of the triethylamine was required to take the reaction to completion Purification of the molybdenum complex was achieved by column chromatography with a

polarity gradient elution, followed by recrystallisation from dichloromethane and methanol. Isolation of the recrystallised material afforded product **22** in 75% yield.

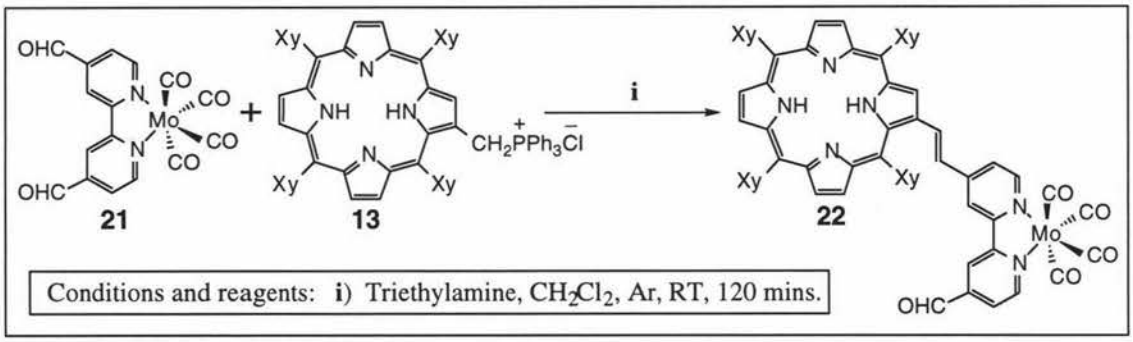

Figure 5.1-1
Wittig reaction to attach TXP to the bipyridine dialdehyde containing molybdenum complex **21**.

The ^1H NMR spectrum of complex **22** shows a similar pattern to that seen for the unmetallated ligand **19** (see p.57-58 for discussion of ^1H NMR spectrum of **19**). For the molybdenum complex **22**, the two doublets corresponding to the two vinylic protons are positioned so close together that they appear as a triplet, rather than two sets of doublets (as was seen in the spectrum of the porphyrinato zinc(II) compound **16**, see Section 4.4, p.62-63).

Electronic absorption analysis of complex **22** revealed a higher molar extinction coefficient for the Soret band (174,000 $dm^3mol^{-1}cm^{-1}$) compared to that seen for the non-metallated analogue **19** (158,000 $dm^3mol^{-1}cm^{-1}$). Thus metal coordination of the bpy ligand has an effect on the absorption of the porphyrin moiety. The infrared spectrum of **22** revealed a band of medium intensity positioned at 1599 cm^{-1}, a typical signal in the spectrum of a complex containing an aldehyde appendage. Four bands positioned close to 2000 cm^{-1} correspond to the four carbonyl groups connected to the molybdenum. These spectral results support the proposed characterisation of the product, as complex **22**. A molecular ion in the FAB HRMS was unable to be obtained for this complex as the fast atom bombardment technique proved to be too vigorous, causing complete fragmentation of the material. However, a major fragment corresponding to the mass of complex **22** with two carbonyl groups removed was observed. The loss of two metal-bound carbonyl's is commonly observed when attempting to acquire mass spectral characterisation of complexes containing transition metal carbonyl groups.[2]

The aim of the work done for this chapter was to attempt the coordination of various metal ions to the bipyridine-tetraxylylporphyrin conjugates. The use of molybdenum was primarily a test reaction as no previous metal coordination had been attempted using the tetraxylylporphyrin appended bipyridine ligand. In Chapter Four it was discovered that a

Wittig reaction on a complex of similar form to complex **22**, could be achieved with relative ease. This was observed when the rhenium-bound bipyridyl TPP monomer **17** was reacted with a second equivalent of TPP-CH_2PPh_3Cl, **5**, to form the bisporphyrinyl complex **18**. However, no further reactions using this molybdenum complex were attempted due to time constraints.

5.2 Rhenium-bound bipyridine complexes

Rhenium complexes, including those containing bipyridyl ligands have been widely used in inorganic chemistry research and spectroscopic studies.[3-5] Helberg *et al.*[6] observed that polypyridyl metal complexes had been studied in detail, especially the d^6 systems such as the Ru^{II} and Os^{II} complexes, for their potential application in the areas of redox catalysis and photoactivated electron transfer. However, it was apparent that there were very few studies of the isoelectronic Re^{I} polypyridyl complexes, which were considered to be a logical extension of the d^6 systems. The particular area of interest of Helberg *et al.* for such Re^{I} complexes was for their potential as π-bases for the activation of unsaturated organic molecules. The coordination of rhenium to our bipyridyl-tetraxylylporphyrin conjugates could produce complexes with interesting chemical and photochemical properties.

The bistetraphenylporphyrinyl rhenium-bound bipyridyl complex **18** (see Chapter Four p.55-56) was synthesised in three steps. An initial Wittig reaction between dialdehyde **4** and phosphonium salt **5** produced TPP-bpy-aldehyde **14**. Complexation to rhenium metal was then achieved by refluxing compound **14** and $Re(CO)_5Cl$ in benzene. This was followed by a second Wittig reaction to form the desired bisporphyrinyl complex **18**. The following section discusses the synthesis and characterisation of **23** (see Figure 5.2-1 below), the tetraxylylporphyrin analogue of complex **18**. However, rather than following the synthetic methodology used to form complex **18**, a more direct route was employed to prepare the tetraxylylporphyrin derivative **23**.

5.2.1 Synthesis and characterisation of $Re^{I}[bpy(TXP)_2](CO)_3Cl$

The bipyridine-bisporphyrinyl conjugate **20**, was refluxed under an inert atmosphere with rhenium pentacarbonyl chloride in dry, distilled benzene, for 90 mins. The reaction mixture had reached completion by tlc so was purified by column chromatography followed by recrystallisation from CH_2Cl_2 with MeOH. This process yielded complex **23** in 74% yield from dimer **20** (or 50% yield over two steps from the TXP phosphonium salt and dialdehyde starting materials). This methodology is more direct and more efficient than the route used to synthesise the bistetraphenylporphyrin rhenium complex **18**. The previous

method required three steps as opposed to a single step, with an overall yield of only 26% from the dialdehyde and phosphonium salt starting materials.

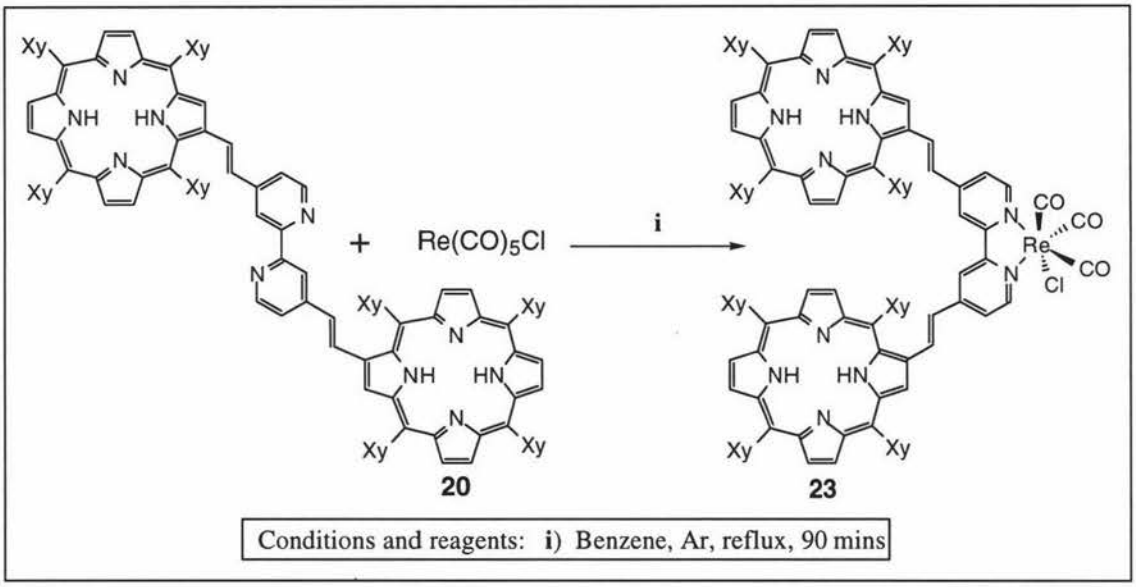

Figure 5.2-1
Synthesis of bisporphyrinyl rhenium(I)bipyridine complex, **23**.

Complex **23** was characterised using mass spectrometry, ^{1}H NMR, UV/Vis, and IR spectroscopy. The ^{1}H NMR spectrum of **23** was very similar to that seen for the uncomplexed bipyridine-bistetraxylylporphyrin conjugate **20** (see Figure 4.2-2, p.60). Upon complexation a degree of the definition seen with ligand **20** was lost, the peaks were pushed a little closer together and broadened. As a result, the two vinylic doublets were masked by the broadened multiplet of the *para*-xylyl protons. The remaining peaks were similar to those seen for the uncomplexed ligand (see Section 5.4, complex **23**, p.80). Electronic absorption data for **23**, was also similar to that seen for the uncomplexed analogue. A weak band at 312 nm corresponds to the LC transition of the bipyridine ligand. The large Soret band is present at 426 nm which has a large molar extinction coefficient of 275,500 $dm^3mol^{-1}cm^{-1}$. Infrared spectroscopy showed three bands of medium intensity around 2000 cm^{-1} which correspond to the three carbonyl groups. Mass spectrometry gave an accurate mass reading to support the proposed characterisation.

The success of the coordination of rhenium and molybdenum show that the connection of transition metal ions to these bipyridine-porphyrin conjugates is possible. This was largely expected as polypyridyl compounds are well known for their ability to coordinate to transition metals. It appears that the presence of the porphyrin appendages, connected through vinylic bonds to the bipyridine ligand, have no adverse effect on the ability of the bpy to coordinate to metals. The molybdenum and rhenium complexes were synthesised by different methods, the Mo complex was formed *via* a Wittig reaction of the phosphonium salt

with the pre-metallated bipyridine dialdehyde ligand. The rhenium complex on the other hand was formed *via* a direct metallation of the bipyridine-bistetraxylylporphyrin conjugate, thus further demonstrating the flexibility of this chemistry.

It is widely accepted through detailed studies that polypyridyl complexes of Ru^{II} and Os^{II} have great potential for application in synthetic solar cells due to their chromophoric properties. Thus the final section of work undertaken for this study was to attempt to synthesise ruthenium complexes of the bipyridine-porphyrin conjugates described in the preceding chapters. It was due to the relative inexpense of ruthenium complexes as opposed to osmium, that Ru^{II} was the transition metal of choice.

5.3 Ruthenium complexes of bpy(TXP)$_2$

There have been extensive studies carried out on transition metal polypyridyl complexes, in particular those of ruthenium(II), due to their interesting photochemical and photophysical properties.[7,8] Of these complexes, $Ru^{II}(bpy)_3$ appears to have been very popular due to its potential use in photocatalytic or electron transfer reactions.[9-13] Consequently, there is a great deal of literature describing the various synthetic methodologies used for the formation of ruthenium bound bipyridyl complexes. There are two possible routes for the complexation of the bipyridine-bisporphyrin conjugates to ruthenium metal. Firstly, the method used to synthesise the rhenium complex **23**, which involved metal complexation of the bisporphyrinyl bipyridine ligand. The other possible route was used to form the molybdenum complex **22**, and involved connection of the porphyrin ring *via* a Wittig reaction to the pre-metallated bipyridine ligand.

Initially, direct connection of a metal complex to the bipyridine-bisporphyrin conjugate **20** was attempted.

5.3.1 The 'ruthenium blue' method for Ru^{II}[bpy(TXP)$_2$] complex formation

One common method used throughout the literature to synthesise ruthenium-bound bipyridine complexes employs a 'ruthenium blue' solution.[14,15] The blue solution is formed by refluxing hydrated ruthenium trichloride ($RuCl_3.3H_2O$) in a mixture of alcohol (generally methanol or ethanol) and water. The hot 'ruthenium blue' solution is added to a solution of the bipyridine ligand in the same solvent. This mixture is then heated at reflux temperature to form the desired complex. This method was attempted a number of times with the bipyridine-bistetraxylylporphyrin conjugate **20**. However in all cases, the reaction proved to be unsuccessful resulting in unreacted starting materials and/or the precipitation of

ruthenium metal. Subsequently, an alternative route to the target compound were explored. This involved the synthesis of a ruthenium-bound 4,4'-diformyl-2,2'-bipyridine complex, followed by Wittig chemistry to connect the porphyrin appendages.

5.3.2 Synthesis of TXP-bpy complexes of Ru(II) using Wittig chemistry

Firstly the $Ru^{II}[bpy(CHO)_2]$ precursor had to be formed. A publication by Anderson *et al.*[16] discusses the synthesis of a polymeric ruthenium complex $[Ru(CO)_2Cl_2]_n$. Reaction of this polymer with bpy ligands such as bpy and Me_2bpy afforded the resultant mono- and bisbpy appended ruthenium complexes. This method was therefore employed to coordinate the 4,4'-diformyl-2,2'-bipyridine, **4**, to ruthenium metal so that a subsequent Wittig reaction with TXP-CH_2PPh_3Cl, **13**, could produce the desired complex (see Figure 5.3-1).

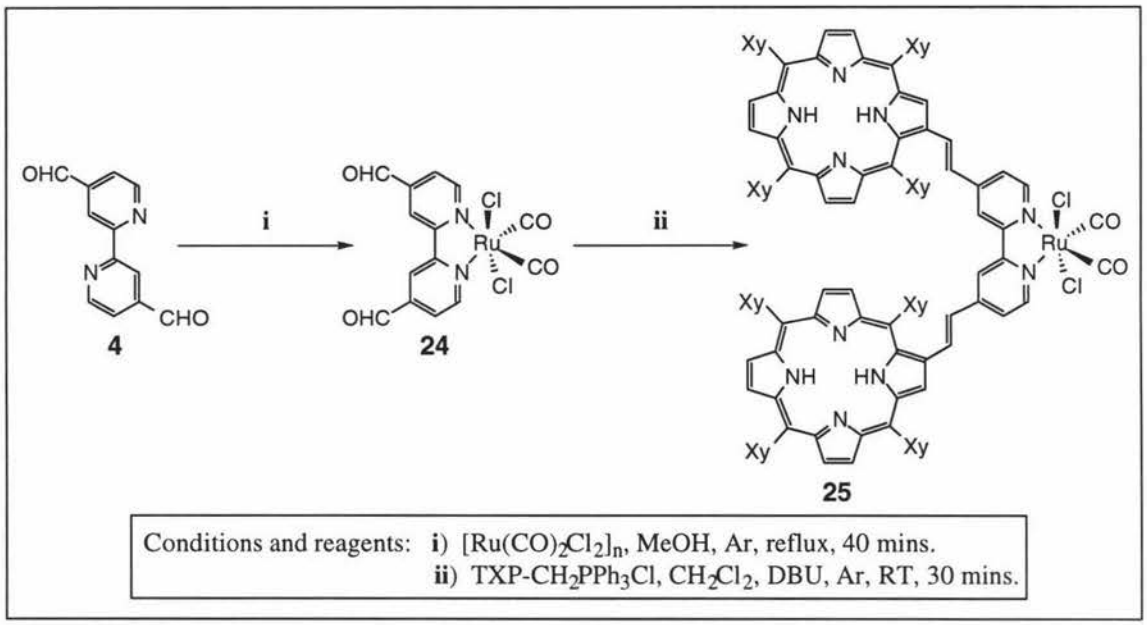

Figure 5.3-1
Successful synthesis of the bisporphyrinyl ruthenium(II)bipyridine complex, **25**.

The ruthenium polymer was synthesised from $RuCl_3.3H_2O$ according to the method of Anderson *et al.*.[16] Equal mole equivalents of the polymeric complex and dialdehyde **4** were suspended in methanol and refluxed in an inert atmosphere (step **i**, Figure 5.3-1). Upon cooling, a lemon yellow solid precipitated out of solution. Isolation of this solid afforded complex **24** in 63% yield. As expected, the ^1H NMR spectrum of complex **24** was of similar pattern to that of dialdehyde **4**, as coordination with the ruthenium metal ion has little effect on the chamical shifts of bpy protons of the ligand. UV/Vis spectroscopy showed a broad band at 315 nm corresponding to the LC transition of the bpy ligand. IR analysis revealed two bands of medium intensity at 1562 cm^{-1} and 1620 cm^{-1} corresponding to the two aldehyde appendages present in complex **24**. The spectrum also contained two very

strong bands at 1997 cm^{-1} and 2073 cm^{-1} which are typical of metal coordinated carbonyl groups, thus the IR data supported the characterisation of the product, as complex **24**. Mass spectrometry also supported the proposed characterisation with an accurate mass reading.

A Wittig reaction of complex **24** was then carried out using two equivalents of the TXP phosphonium salt, **13**, and excess DBU. Analysis by tlc revealed the formation of a non-polar porphyrin containing product, and showed no residual polar TXP phosphonium salt starting material. The reaction mixture was purified by column chromatography followed by recrystallisation from CH_2Cl_2 with MeOH. Isolation of the purple crystalline solid afforded complex **25** in 55% yield (step **ii**, Figure 5.3-1 above).

The ^1H NMR spectrum of complex **25** was almost identical to that seen for the analogous rhenium complex **23**, as the different transition metal ion has little effect on any of the shifts of the hydrogen atoms of the complex. The peaks in the spectrum of complex **25** are broadened in a similar manner to those observed for complex **23**. As a consequence, the doublet corresponding to the two equivalent 5-position bpy protons, and the two doublets due to the four vinylic protons are masked by a multiplet corresponding to six of the *para*-xylyl protons (see Section 5.4, complex **25**, p.81-82). The electronic absorption spectrum of **25** was also similar to that seen for the rhenium analogue. A broad band at 307 nm is due to the LC transition of the bpy ligand, and a large Soret band at 426 nm and four weaker Q bands at higher wavelengths correspond to the equivalent porphyrin rings. The Soret band for this ruthenium complex does possess a larger molar extinction coefficient than the rhenium analogue **23**, recording 334,000 $dm^3mol^{-1}cm^{-1}$ (as opposed to 275,000 $dm^3mol^{-1}cm^{-1}$ for the Re complex). Again, this shows that the addition of a metal ion to the porphyrin containing ligand has an effect on the absorption of the porphyrin moieties, and it appears that the ruthenium(II) metal ion has more of an effect than the rhenium(I) metal ion. Further support for the proposed characterisation of complex **25** was made through infrared analysis which revealed two bands of medium intensity at 1994 cm^{-1} and 2055 cm^{-1}, corresponding to carbonyl stretches of the two CO groups. FAB HRMS gave a parent ion mass value of 1886.653 amu for complex **25** which accurately agrees with the calculated value of 1886.642 amu.

The success of the synthesis of target complex **25** was an exciting breakthrough for this research as it could prove to be a useful building block for large arrays of multichromophore containing complexes. The final target for this research was to attempt to synthesise the tetraporphyrinyl analogue of dimer **25**, $RuCl_2$bis[4,4'-(*trans*-2"-vinyl-TXPyl)-2,2'-bipyridine].

5.3.3 Attempted synthesis of a Ru^{II} bis[bpy(TXP)$_2$] complex

Complex **25** was synthesised from a Wittig reaction between TXP-CH_2PPh_3Cl, **13**, and complex **24** (see Figure 5.3-1 above). The *cis*-$RuCl_2$bis[4,4'-diformyl-2,2'-bipyridine] complex which was required for the Wittig reaction to form the tetraporphyrinyl complex had been synthesised by Dr. A. Burrell. The procedure by which the ruthenium(II)bisbipyridine complex was made involved refluxing $RuCl_2(DMSO)_4$ in benzene with excess dialdehyde **4**, for six hours. Upon cooling, product **26** precipitated out of solution as a very insoluble maroon coloured solid.

Complex **26** was found to be soluble in hot acetonitrile. Thus Wittig reactions were attempted by dissolving the ruthenium(II)bisbipyridyl complex in a minimum volume of CH_3CN, adding dichloromethane, the phosphonium salt, and then base (Figure 5.3-2). Various Wittig reactions with different reaction conditions were attempted without success.

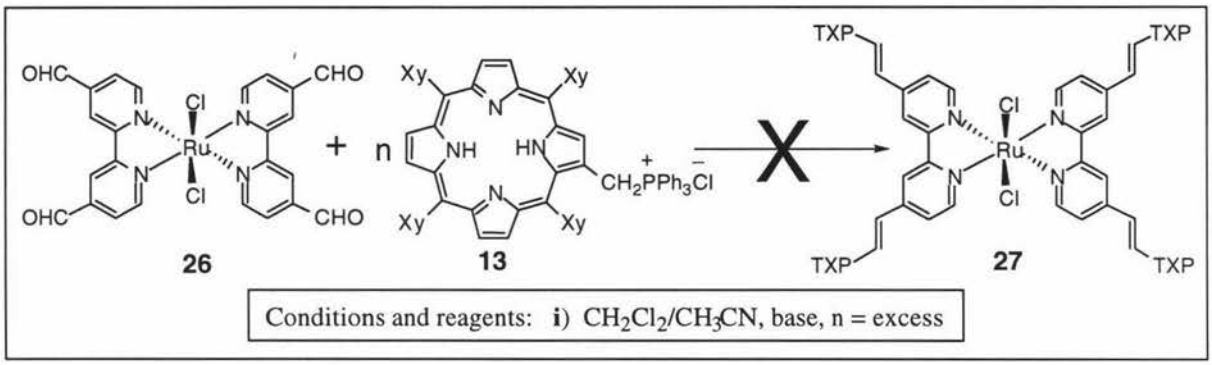

Figure 5.3-2
Attempted synthesis of tetrameric porphyrinyl complex **27**, *via* Wittig chemistry.

An alternative synthetic methodology was therefore explored. Rather than using Wittig chemistry to add the porphyrin appendages to the ruthenium(II)bisbipyridyl complex, a simultaneous coordination of the Ru(II) metal complex to two bipyridine-bistetraxylylporphyrin conjugates was investigated. A similar route was previously unsuccessfully attempted, to synthesise the analogous dimeric porphyrin complex **25** using a 'ruthenium blue' method (see Section 5.3.1, p.72-73). This time, a different ruthenium complex was used.

5.3.4 Reaction of dimer 20 with $Ru^{II}Cl_2(DMSO)_4$

Ruthenium complex **26** was synthesised by Dr. A. Burrell by refluxing $Ru^{II}Cl_2(DMSO)_4$ with 4,4'-diformyl-2,2'-bipyridine, **4**. This reaction produced an insoluble material which precipitated out of solution (see Section 5.3.3). Therefore, a similar reaction using bisporphyrinyl bipyridine **20** in place of the dialdehyde, could produce the desired

tetraporphyrinyl complex in a single step. The solubility problems encountered with complex **26** may be minimised by the presence of the bulky non-planar TXP appendages.

$Ru^{II}Cl_2(DMSO)_4$, with a three fold excess of bisporphyrinyl bipyridine **20** was heated at reflux temperature in benzene, under an inert atmosphere for 20 h (Figure 5.3-3). Tlc analysis showed the appearance of a new non-polar, porphyrin containing band which did not intensify throughout the latter 5 h of the reflux.

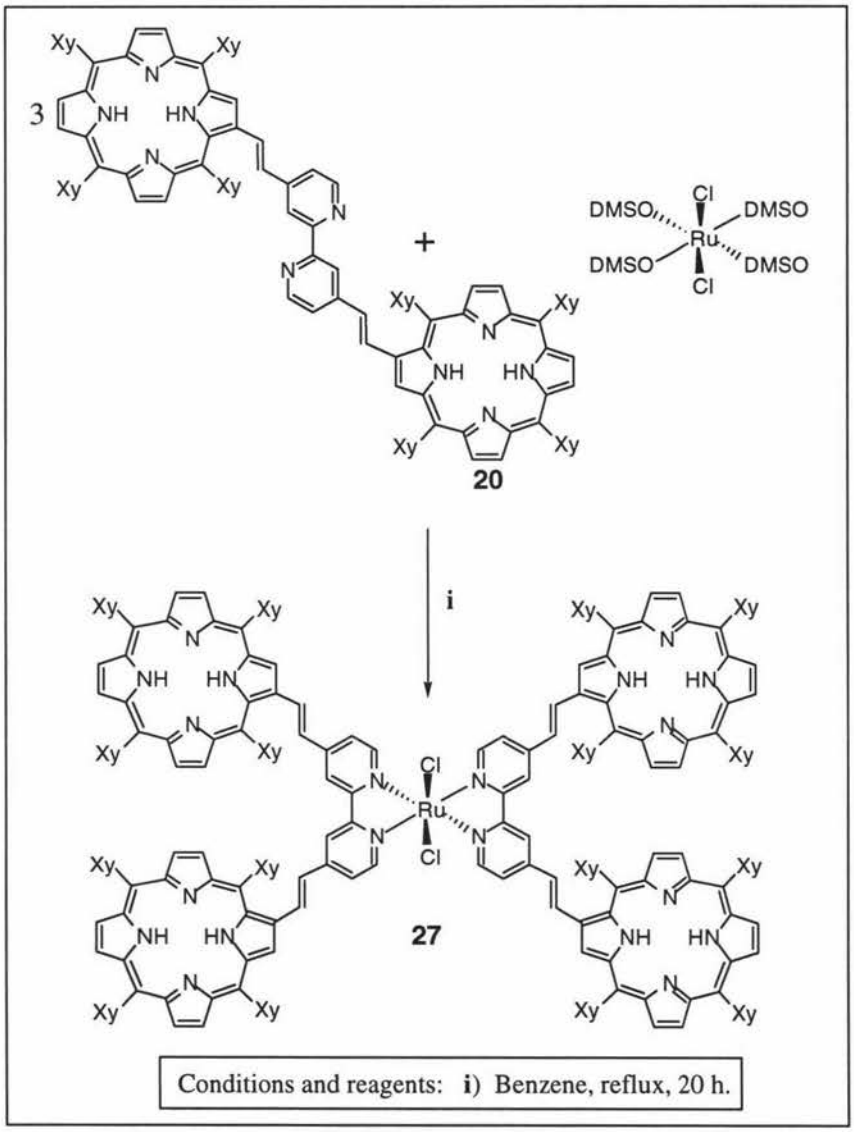

Figure 5.3-3
Synthesis of the tetraporphyrinyl ruthenium(II)bisbipyridine complex **27**.

Purification by column chromatography under a slow stream of argon revealed three bands. The first fraction consisted of pure bipyridine-bisporphyrin conjugate **20** (64% recovery). A second band was characterised as a mixture of ligand **20**, with a small amount of a monomeric bipyridyl ruthenium(II) complex analogous to complex **24** (with DMSO

coordinated in place of the two carbonyl groups), and a tiny quantity of product **27**. The third band off the column was isolated and characterised as complex **27** in 28% yield.

There are two possible configurations of the ligands around the ruthenium ion of complex **27**, and each configuration would give a different ^{1}H NMR spectrum. If the chloride ligands are *trans* to each other, the two bpy ligands will be identical, thus affording a simple spectrum. In contrast, if the chloride atoms of tetraporphyrinyl complex **27** are coordinated to the central ruthenium metal in a *cis*-configuration, the two rings of each bipyridine are no longer equivalent. One ring is *trans* to a chloride atom, and the other is *trans* to a bipyridine ring (represented in Figure 5.3-4). Consequently, the ^{1}H NMR spectrum of complex **27** would show an interesting pattern of peaks, as was seen (see Figure 5.3-5 below).

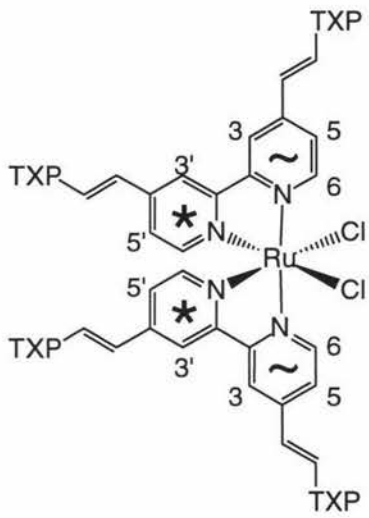

~	=	*trans* to a bipyridyl ring, *cis* to both Cl atoms.
*	=	*trans* to one Cl atom, and *cis* to one Cl atom.

Figure 5.3-4
Diagram of complex **27**.

The ^{1}H NMR spectrum of complex **27** contains six peaks corresponding to the bipyridyl protons, one singlet for the two equivalent $H_{3\text{-bpy}}$ protons (~), one singlet for the two equivalent $H_{3'\text{-bpy}}$ protons (*), one doublet for the two equivalent $H_{5\text{-bpy}}$ protons (~), and so on as is discussed below. There are three important peaks present in the ^{1}H NMR spectrum of complex **27**, which are not shown in Figure 5.3-5 below. A broad singlet is positioned at -2.54 ppm which corresponds to the eight N*H* protons in the centre of the four TXP rings. Two large peaks at 2.60 ppm and 2.63 ppm are due to twenty-four, and seventy-two protons respectively, from the methyl constituents of the xylyl groups. The peak labelled **L** in Figure 5.3-5 below corresponds to $CHCl_3$ from the deuterated solvent used to dissolve the sample. Doublets **K** and **I** positioned at 7.32 ppm and 7.58 ppm,

correspond to the four bipyridyl H_5 and $H_{5'}$ protons. The two peaks are seen as doublets with coupling constants of ^3J = 6.2 Hz, as they are coupled through three bonds to their neighbouring H_6 or $H_{6'}$ proton. The multiplet **J** is positioned between 7.40 ppm and 7.50 ppm, and hides the doublets due to the eight vinylic protons, as well as the sixteen *para*-xylylporphyrin protons.

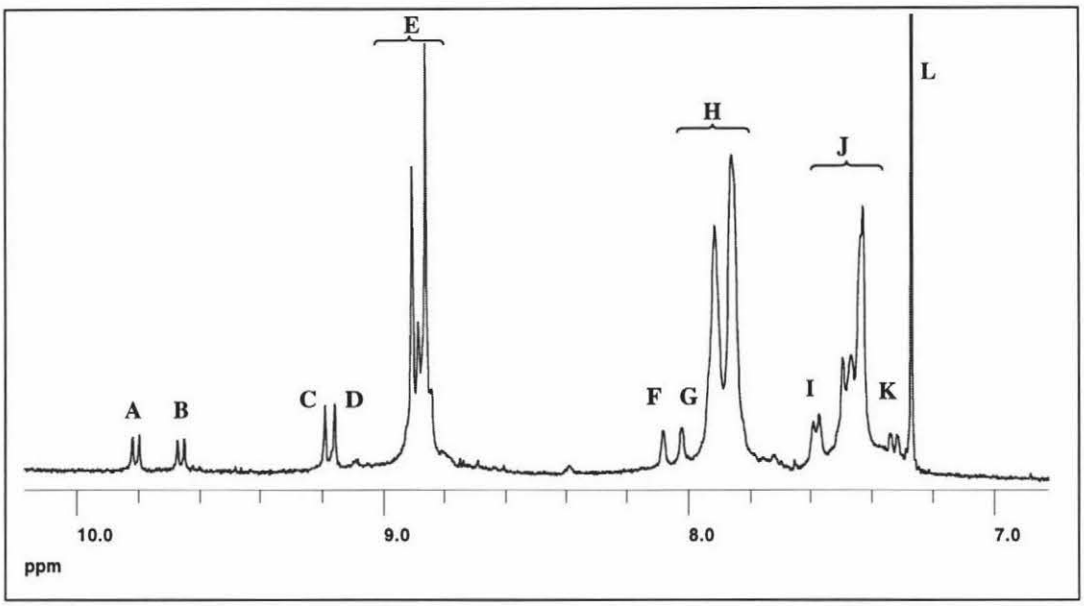

Figure 5.3-5
^{1}H NMR spectrum of complex **27**.

The broadened multiplet, **H**, positioned between 7.80 ppm and 7.93 ppm corresponds to the thirty-two *ortho*-xylylporphyrin protons. The two singlets, **G** and **F**, are due to the H_3 and $H_{3'}$ bipyridyl protons. As with the 5-position bpy protons, there are two peaks as the four 3- and 3'-position protons are split into two groups. The two $H_{3\text{-bpy}}$ protons belong to bpy rings which are *cis* to both chloride atoms thus are equivalent, and correspondingly, the two $H_{3'\text{-bpy}}$ protons (on bpy rings *trans* to a chloride atom) are also equivalent. Twenty-four pyrrolic protons produce a multiplet from 8.83-8.91 ppm labelled **E**. The remaining four β-pyrrolic protons are split into two groups, as two of the β-pyrrolic protons are connected to a bpy ring that is *cis* to both the Cl atoms, and the other two β-pyrrolic protons are connected to a bpy ring that is *trans* to one of the Cl atoms and *cis* to the other. This results in two singlets labelled peaks **D** and **C** at 9.16 ppm and 9.19 ppm respectively. The remaining two doublets positioned at 9.66 ppm, peak **B**, and at 9.81 ppm, peak **A**, correspond to the two 6-position and the two 6'-position bipyridyl protons. The two peaks are split into doublets as the protons are coupled with their adjacent 5- or 5'-position proton with coupling constants of 6.2 Hz.

The electronic absorption spectrum is typical of previous results obtained for the bipyridine-porphyrin conjugate metal complexes. The Soret band for this tetrameric porphyrin complex records a molar extinction coefficient of 382,000 $dm^3mol^{-1}cm^{-1}$. This value is greater than that recorded for the analogous dimeric porphyrin analogue **25** (see Section 5.3.2, p.73), as twice as many porphyrin moieties are present in complex **27**.

The calculated mass value of complex **27** is 3488.286 amu. Samples of the complex were sent to two different mass spectrometry operators in New Zealand who could not find an accurate parent ion in the vicinity of 3500 amu. However, this compound was of significantly greater weight than most samples supplied for mass spectrometric analysis at these institutions, thus a sample was sent to Wollongong University in Australia. This University owns a matrix-assisted laser desorption ionisation (MALDI) mass spectrometer which has a greater capacity for determining accurate mass readings for large compounds. The result of 3488.81 obtained from Wollongong for complex **27** supports the above proposed characterisation.

To the best of the author's knowledge, this is the first Ru(II)bis[bpy(porphyrin)$_2$]$_2$ complex containing vinylic linking groups that has ever been synthesised. Such a complex may have huge potential for application in photovoltaic studies, especially since it has effectively two free sites on the ruthenium metal ion, where the two chloride atoms are presently situated. These sites could be utilised to further functionalise the complex or to attach a tether for connection to a conducting medium for electrochemical studies (see Conclusions and future work, Chapter Six).

5.4 Experimental procedures

For general procedures see Chapter Two, Section 2.6.1, p.31-32.
When necessary, reactions involving light sensitive porphyrin compounds were carried out under aluminium foil and stored in the dark in order to protect them from both reacting with light and decomposition.

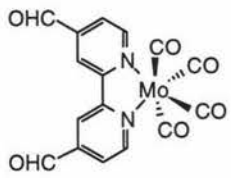

(21) 1,1'-Mo(CO)$_4$[4,4'-diformyl-2,2'-bipyridine]

Synthesised by Dr. A. Burrell from $Mo(CO)_4(piperidine)_2$ and 4,4'-diformyl-2,2'-bipyridine in these laboratories.

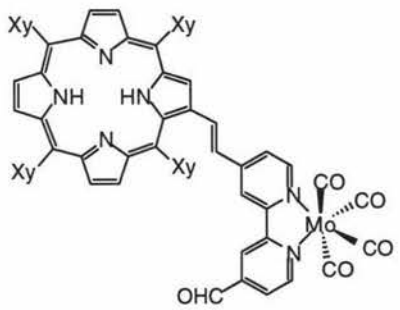

(22) 1,1'-Mo(CO)$_4$[4-(trans-2''-vinyl-TXPyl)-4'-formyl-2,2'-bipyridine]

A 25 mL 3-neck round bottomed flask was charged with TXP-CH_2PPh_3Cl, **13** (0.128 g, 0.123 mmol) and 1,1'-$Mo(CO)_4$[4,4'-diformyl-2,2'-bipyridine], **21** (0.050 g, 0.119 mmol), and fitted with two septa (one containing an argon source) and an oil bubbler. Dry, distilled CH_2Cl_2 (4 mL) was added *via* syringe and the stirring solution was purged with argon. The needle was removed from the solution and CH_2Cl_2 (3 mL) was added to rinse the walls of the flask and the needle. Triethylamine (149 μL) was added and the reaction was left stirring for 90 mins. Analysis by tlc showed some molybdenum starting material remaining, so a further amount of TXP phosphonium salt, **13** (0.050 g, 0.048 mmol) was added with CH_2Cl_2 (2 mL). After 30 mins no molybdenum starting material remained by tlc so the solvent was removed. The resultant residue was dissolved in 1:1 CH_2Cl_2:Hexane (5 mL) and loaded onto a long thin silica column. The column was run using a solvent gradient elution (from the 1:1 CH_2Cl_2:Hexane, to CH_2Cl_2, 4% MeOH in CH_2Cl_2, and finally 10% MeOH in CH_2Cl_2). The product was collected and the solvent removed. The residue was recrystallised slowly overnight from CH_2Cl_2 with MeOH. The precipitated crystals were collected by filtration and washed with a small volume of methanol. Drying under high vacuum yielded complex **22** (0.102 g, 75%) as purple crystals.

R_f = 0.35, 1:1 CH_2Cl_2:Hexane.

^{1}H NMR (270 MHz, $CDCl_3$): δ -2.57 (br s, 2H; N*H*), 2.57 (s, 6H; CH_3), 2.64 (s, 12H; CH_3), 2.69 (s, 6H; CH_3), 7.22 (d, ^3J = 4.9 Hz, 1H; $H_{5\text{-bpy}}$), 7.32 (s, 2H; $H_{p\text{Xy}}$), 7.44 (appt t, ^3J = 16.2 Hz, 2H; $H_{\text{trans-vinylic}}$), 7.46 (s, 1H, $H_{p\text{Xy}}$), 7.53 (s, 1H; $H_{p\text{Xy}}$), 7.75 (d, ^3J = 4.9 Hz, 1H; $H_{5'\text{-bpy}}$), 7.80-7.94 (m, 8H; $H_{o\text{Xy}}$), 8.39 (s, 1H; $H_{3\text{-bpy}}$), 8.68 (s,

1H; $H_{3'\text{-bpy}}$), 8.81 (d, ^3J = 4.9 Hz, 1H; $H_{6\text{-bpy}}$), 8.84-9.00 (m, 6H; $H_{\text{pyrrolics}}$), 9.03 (d, ^3J = 4.9 Hz, 1H; $H_{6'\text{-bpy}}$), 9.08 (s, 1H; $H_{\beta\text{-pyrrolic}}$), 10.20 (s, 1H; C*H*O).

UV/Vis (CH_2Cl_2): λ_{max} (log ε) = 309 (4.42), 429 (5.24), 525 (4.17), 566 (3.90), 599 (3.79), 655 (3.52) nm.

IR (Nujol): 1599 (m, CHO), 1838 (m, CO), 1874 (m, CO), 1898 (m, CO), 2018 (m, CO) cm^{-1}.

FAB MS: 1088.50 [M^+ -$(CO)_2$].

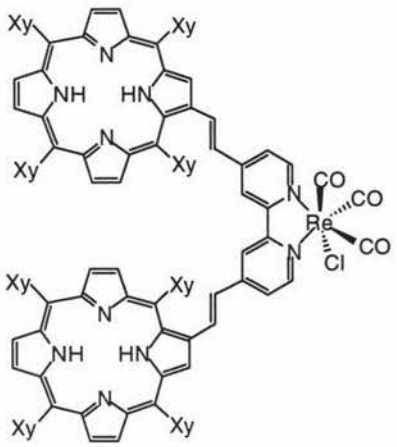

(23) 1,1'-Re(CO)$_3$Cl[4,4'-(trans-2''-vinyl-TXPyl)-2,2'-bipyridine]

Bipyridine-bisporphyrin conjugate **20** (0.032 g, 0.019 mmol) and rhenium pentacarbonyl chloride (0.009 g, 0.025 mmol) were placed in a 50 mL round bottomed flask. Dry, distilled benzene (5 mL) was added and the flask was flushed with argon. The reaction mixture was heated at reflux temperature for 90 mins. Tlc showed that the reaction had reached completion thus the heat source was removed and the flask allowed to cool. The reaction mixture was poured directly onto a silica column and elution was carried out using EtOAc, followed by 1:1 CH_2Cl_2:EtOAc to remove the large band containing the relatively non-polar product. This material was recrystallised slowly from CH_2Cl_2 with MeOH. The recrystallised product was collected by filtration and dried under high vacuum to yield the purple bisporphyrinyl rhenium bipyridyl complex **23** (0.028 g, 74%).

R_f = 0.50, EtOAc.

^{1}H NMR (270 MHz, $CDCl_3$): δ -2.51 (s, 4H; N*H*). 2.64 (s, 36H; CH_3), 2.66 (s, 12H; CH_3), 7.34 (d, ^3J = 5.8 Hz, 2H; $H_{5,5'\text{-bpy}}$), 7.40-7.49 (m, 10H; $6H_{p\text{Xy}}$ + $4H_{\text{trans-vinylic}}$), 7.61 (s, 2H; $H_{p\text{Xy}}$), 7.81-7.94 (m, 16H; $16H_{o\text{Xy}}$), 8.08 (s, 2H; $H_{3,3'\text{-bpy}}$), 8.84-8.93 (m, 12H; H_{pyrrolic}), 8.98 (d, ^3J = 5.8 Hz, 2H; $H_{6,6'\text{-bpy}}$), 9.20 (s, 2H; H_{β}-pyrrolic).

UV/Vis (CH_2Cl_2): λ_{max} (log ε) = 312 (4.72), 426 (5.44), 527 (4.62), 573 (4.37), 602 (4.30), 661 (3.96) nm.

IR (Nujol): 1896 (m, CO), 1918 (m, CO), 2018 (m, CO) cm^{-1}.

FAB HRMS: [M^+] calcd. for $ReC_{121}H_{100}N_{10}O_3Cl$ 1962.7255, obs. 1963.7373.

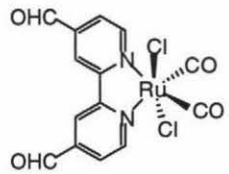

(24) 1,1'-Ru(CO)$_2$Cl$_2$[4,4'-diformyl-2,2'-bipyridine]

A 10 mL 2-neck round bottomed flask was charged with a solution of 4,4'-diformyl-2,2'-bipyridine (0.100 g, 0.471 mmol) in MeOH (2 mL) and fitted with a septum and a stopper. An argon source was introduced and the stirring suspension was purged with argon for 30 mins. $[Ru(CO)_2Cl_2]_n$ (0.107 g, 0.471 mmol) was added and the reaction mixture was heated at reflux temperature under an inert atmosphere for 40 mins (upon heating all solid material dissolved to give a clear orange coloured solution). The heat was removed and the reaction mixture allowed to cool slowly overnight. The precipitated solid was collected by filtration and dried under vacuum to yield product **24** as a light yellow powder (0.130 g, 63%).

^{1}H NMR (270 MHz, $CDCl_3$): δ 8.13 (dd, ^3J = 5.5 Hz, ^4J = 1.5 Hz, 2H; $H_{5,5'}$), 8.77 (d, ^4J = 1.5 Hz, 2H; $H_{3,3'}$), 9.49 (d, ^3J = 5.5 Hz, 2H; $H_{6,6'}$), 10.28 (s, 2H; C*H*O).

UV/Vis (CH_2Cl_2): λ_{max} (log ε) = 315 (3.79) nm.

IR (Nujol): 1562 (m, CHO), 1620 (m, CHO), 1997 (s, CO), 2073 (s, CO) cm^{-1}.

EI HRMS: [M$^+$] calcd. for $RuC_{14}H_8N_2O_4Cl_2$ 439.8902, obs. 439.8924.

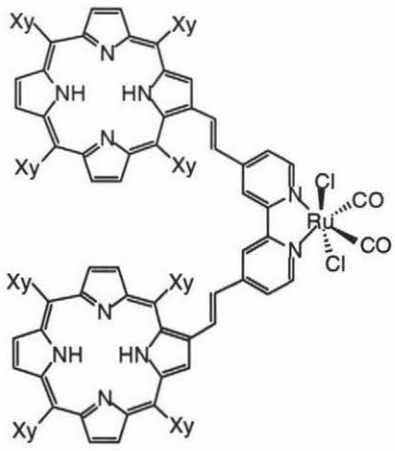

(25) 1,1'-Ru(CO)$_2$Cl$_2$[4,4'-(trans -2''-vinyl-TXPyl)-2,2'-bipyridine]

Complex **24** (0.010 g, 0.023 mmol) and TXP phosphonium salt **13** (0.047 g, 0.045 mmol) were placed in a 10 mL 2-neck round bottomed flask. The flask was flushed with argon, then dry distilled CH_2Cl_2 (13 mL) was added *via* syringe. The solution was stirred vigorously for 5 mins before adding DBU (0.034 mL). After 30 mins, analysis by tlc showed that the reaction had reached completion. The solvent was removed and the resultant residue dissolved in 1:1 CH_2Cl_2:Hexane (5 mL) and loaded onto the silica column. Elution

with the 1:1 CH_2Cl_2:Hexane removed a very small quantity of Me-TXP, followed by a large band containing the desired product. The solvent was removed and the residue recrystallised slowly overnight from CH_2Cl_2 with MeOH. The recrystallised product was filtered and dried under high vacuum to yield the ruthenium complex **25** (0.031 g, 55%) as a purple solid.

$R_f = 0.45$, CH_2Cl_2.

^1H NMR (270 MHz, $CDCl_3$): δ -2.52 (s, 4H; N*H*), 2.63 (s, 36H; CH_3), 2.66 (s, 12H; CH_3), 7.42-7.50 (m, 12H; $2H_{5,5'\text{-bpy}} + 4H_{\text{trans-vinylic}} + 6H_{p\text{Xy}}$), 7.60 (s, 2H; $H_{p\text{Xy}}$), 7.85-7.94 (m, 16H; $H_{o\text{Xy}}$), 8.11 (s, 2H; $H_{3,3'\text{-bpy}}$), 8.84-8.93 (m, 6H; H_{pyrrolic}), 9.10 (d, $^3J = 5.8$ Hz, 2H; $H_{6,6'\text{-bpy}}$), 9.19 (s, 2H; $H_{\beta\text{-pyrrolic}}$).

UV/Vis (CH_2Cl_2): λ_{max} (log ε) = 307 (4.79), 426 (5.52), 527 (4.68), 575 (4.42), 613 (4.18), 660 (3.96) nm.

IR (Nujol): 1994 (m, CO), 2055 (m, CO) cm^{-1}.

FAB HRMS: [M^+] calcd. for $RuC_{120}H_{100}N_{10}O_2Cl_2$ 1886.6422, obs. 1886.6525.

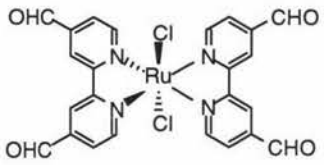

(26) 1,1'-RuCl$_2$[bis-4,4'-diformyl-2,2'-bipyridine]

Synthesised by Dr. A. Burrell from $RuCl_2(DMSO)_4$ and 4,4'-diformyl-2,2'-bipyridine, **4**, in these laboratories.

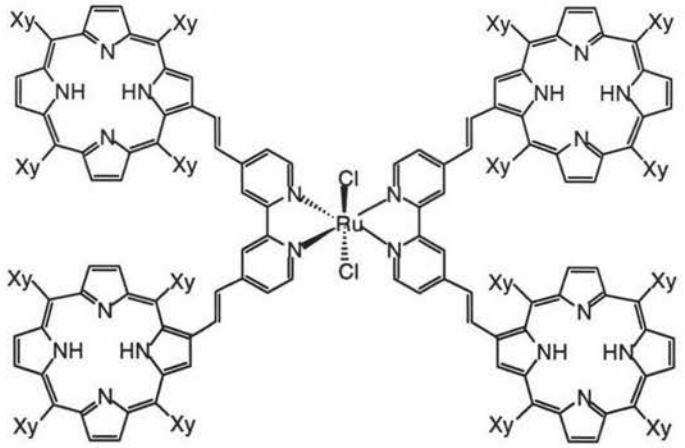

(27) 1,1'-RuCl$_2$[bis-4,4'-(trans-2''-vinyl-TXPyl)-2,2'-bipyridine]

Bipyridine-bisporphyrin conjugate **20** (0.054 g, 0.033 mmol) and $RuCl_2(DMSO)_4$ (0.0053 g, 0.011 mmol) were placed in a 25 mL round bottomed flask. Benzene (4 mL) was added and the reaction mixture was heated at reflux temperature for 20 h under an inert atmosphere. The mixture was allowed to cool and was then poured directly onto a silica column. The

column chromatography was run under a slow stream of argon and eluted with EtOAc, then 1:1 CH_2Cl_2:EtOAc, followed by 4% MeOH in CH_2Cl_2. Three bands were collected, filtered and dried under vacuum. The first fraction was identified as unreacted bipyridine-bisporphyrin conjugate **20** (0.034 g, 64% recovery of starting material). The second band was very weak and turned out to contain a mixture of the starting material, **20**, the mono-bipyridyl complex **25**, and a very small quantity of the bis-bipyridyl complex **27** (0.008g combined). The third band was isolated and characterised as the tetraporphyrinyl ruthenium(II)bisbipyridine complex **27** (0.0106 g, 28%) as a purple solid.

R_f = 0.4, 4% MeOH in CH_2Cl_2.

^{1}H NMR (270 MHz, $CDCl_3$): δ -2.54 (s, 8H; N*H*), 2.60 (s, 24H; CH_3), 2.63 (s, 72H; CH_3), 7.32 (d, ^3J = 6.2 Hz, 4H; $H_{5,5'\text{-bpy}}$), 7.40-7.50 (m, 24H; $8H_{\text{trans-vinylic}}$ + $16H_{p\text{Xy}}$), 7.58 (d, ^3J = 6.2 Hz, 4H; $H_{5,5'\text{-bpy}}$), 7.80-7.93 (m, 32H; $H_{o\text{Xy}}$), 8.02 (s, 2H; H_3), 8.08 (s, 2H; $H_{3'}$), 8.83-8.91 (m, 24H; H_{pyrrolic}), 9.16 (s, 2H; $H_{\beta\text{-pyrrolic}}$), 9.19 (s, 2H; $H_{\beta\text{-pyrrolic}}$), 9.66 (d, ^3J = 6.2 Hz, 4H; $H_{6,6'\text{-bpy}}$), 9.81 (d, ^3J = 6.2 Hz, 4H; $H_{6,6'\text{-bpy}}$).

UV/Vis (CH_2Cl_2): λ_{max} (log ε) = 312 (4.83), 431 (5.58), 526 (4.77), 572 (4.57), 608 (4.28), 661 (4.07) nm.

MALDI MS: [M^+] obs. 3488.81.

5.5 References

(1) Complex **21** was synthesised by Dr. A Burrell in these laboratories.

(2) Personal communications with research chemists and mass spectrometer operator.

(3) Rouschias, G.; Wilkinson, G. *Journal of the Chemical Society (Inorganic Physical Theory, A)* **1967**, 993-1000.

(4) Schoonover, J. R.; Strouse, G. F.; Dyer, R. B.; Bates, W. D.; Chen, P.; Meyer, T. J. *Inorg. Chem.* **1996**, *35*, 273-274.

(5) Herrmann, W. A.; Rauch, M. U.; Roesky, P. W. *J. Organomet. Chem.* **1996**, *511*, 299-302.

(6) Helberg, L. E.; Orth, S. D.; Sabat, M.; Harman, W. D. *Inorg. Chem.* **1996**, *35*, 5584-5594.

(7) Balzani, V.; Juris, A.; Venturi, M.; Campagna, S.; Serroni, S. *Chem. Rev.* **1996**, *96*, 759-833.

(8) Juris, A.; Balzani, V.; Barigelletti, F.; Campagna, S.; Belser, P.; Von Zelewsky, A. *Coord. Chem. Rev.* **1988**, *84*, 85-277.

(9) Durham, B.; Caspar, J. V.; Nagle, J. K.; Meyer, T. J. *J. Am. Chem. Soc.* **1982**, *104*, 4803-4810.

(10) Riesen, H.; Wallace, L.; Krausz, E. *J. Phys. Chem.* **1995**, *99*, 16807-16809.

(11) Zhang, X.; Rodgers, M. A. J. *J. Phys. Chem.* **1995**, *99*, 12797-12803.

(12) Noble, B.; Peacock, R. D. *Inorg. Chem.* **1996**, *35*, 1616-1620.

(13) Riesen, H.; Wallace, L.; Krausz, E. *Inorg. Chem.* **1996**, *35*, 6908-6909.

(14) Togano, T.; Nagao, N.; Tsuchida, M.; Kumakura, H.; Hisamatsu, K.; Howell, F. S.; Mukaida, M. *Inorg. Chim. Acta* **1992**, *195*, 221-225.

(15) Fabian, R. H.; Klassen, D. M.; Sonntag, R. W. *Inorg. Chem.* **1980**, *19*, 1977-1982.

(16) Anderson, P. A.; Deacon, G. B.; Haarmann, K. H.; Keene, F. R.; Meyer, T. J.; Reitsma, D. A.; Skelton, B. W.; Strouse, G. F.; Thomas, N. C.; Treadway, J. A.; White, A. H. *Inorg. Chem.* **1995**, *34*, 6145-6157.

Chapter Six

Conclusions and future work

The primary aim of this research was to formulate an efficient methodology for synthesising bipyridine-porphyrin conjugates containing vinylic linking groups. A second goal was to investigate the metal binding capabilities of the aforementioned compounds. Such complexes could be used to build-up multi-chromophore containing arrays which could potentially be capable of performing useful light-induced functions for energy generation.

Wittig chemistry was proposed as the methodology of choice for synthesising the bipyridine-porphyrin conjugates. The required precursors for the proposed Wittig chemistry, 4,4'-diformyl-2,2'-bipyridine, **4**, and two porphyrin phosphonium salts **5**, and **13** were successfully synthesised. Preliminary Wittig reactions were carried out using the *meso*-tetraphenylporphyrin phosphonium salt **5**, resulting in the synthesis of a monoporphyrinyl bipyridine ligand **14**, and the bisporphyrinyl bipyridine ligand **15**. Lack of solubility of the dimeric species, **15**, prevented any further reactions with this compound. Before continuing with the more soluble *meso*-tetraxylylporphyrin phosphonium salt **13**, a preliminary metallation study was carried out on the soluble monomeric ligand, **14**. Metallation of the porphyrin ring of ligand **14** with zinc(II) successfully formed complex **16**. Metallation using a rhenium(I) complex, at the bipyridyl moiety of ligand **14**, formed the resultant metal complex **17**. This monomeric porphyrinyl bipyridine complex was then reacted under Wittig conditions to form a bisporphyrinyl Re(I)bipyridine complex, **18**. This preliminary study demonstrated both the viability and the flexibility of this methodology, with the success of the synthesis of this range of target ligands and complexes.

The more soluble *meso*-tetraxylylporphyrin phosphonium salt, **13**, was then used to synthesise a soluble version of the target bisporphyrinyl bipyridine ligand. This ligand was synthesised both in two steps (*via* the monoporphyrinyl bipyridine ligand **19**), and in a single reaction from the two Wittig precursors. The single step methodology proved to be by far the more efficient synthesis, yielding the target compound **20** in 68% yield. Subsequent investigation into the metal binding capabilities of the soluble tetraxylylporphyrinyl bipyridine ligands was undertaken. A Wittig reaction between TXP phosphonium salt, **13**, and a molybdenum complex of 4,4'-diformyl-2,2'-bipyridine, **21**, produced the molybdenum-bipyridyl complex of porphyrinyl bipyridine **14**. The remaining metallation studies focused on the transition metals, rhenium and ruthenium. The bisporphyrinyl rhenium(I)bipyridine complex **23** was synthesised through coordination of

the rhenium complex $Re(CO)_5Cl$ to ligand **20**. The bisporphyrinyl ruthenium(II)bipyridine complex **25** however, was synthesised *via* a Wittig reaction of the ruthenium-bound dialdehyde, 1,1'-$Ru(CO)_2Cl_2$[4,4'-diformyl-2,2'-bipyridine], **24**, with phosphonium salt **13**. One final goal was set, to synthesise a tetraporphyrinyl bisbipyridine complex. Attempts at using a Wittig methodology were unsuccessful, however the reaction of excess bisporphyrinyl bipyridine **20**, with a $RuCl_2(DMSO)_4$ complex produced the desired ruthenium(II)bisbipyridine porphyrin tetramer, 1,1'-$RuCl_2$[bis-4,4'-(*trans*-2"-vinyl-TXPyl)-2,2'-bipyridine], **27**.

The development of the efficient methodology for the synthesis of the target bipyridine-bisporphyrin conjugate, **20**, and the success of the introductory investigation into the metal binding capabilities of these compounds, completes the research carried out for this thesis.

Future work to be carried out with the complexes synthesised for this thesis will involve extensive studies into their electrochemical, photoelectrochemical and physical properties. Now that the methodology has been developed, further studies into the metal coordination of both the bipyridyl moiety and at the porphyrin core can be undertaken. The metal ions of the complexes made herein can also be elaborated with further chemical modification. For example complex **27** of the form $Ru(bpy)_2Cl_2$, could be modified to produce a complex of the form $[Ru(bpy)_2(bpy')]^{2+}$. Consequently, study of coordination to the metal ions of such complexes, as well as further functionalisation of the bpy ligand will provide an abundance of further chemistry.